Roles for callose in plant development and intercellular communication

Linda C. Enns

A dissertation submitted in partial fulfillment of the requirements for the degree of

Doctor of Philosophy

University of Washington

2006

Program Authorized to Offer Degree: Biology

University of Washington
Graduate School

This is to certify that I have examined this copy of a doctoral dissertation by

Linda C. Enns

and have found that it is complete and satisfactory in all respects,
and that any and all revisions required by the final
examining committee have been made.

Chair of the Supervisory Committee:

Robert E. Cleland

Reading Committee:

Keiko U. Torii

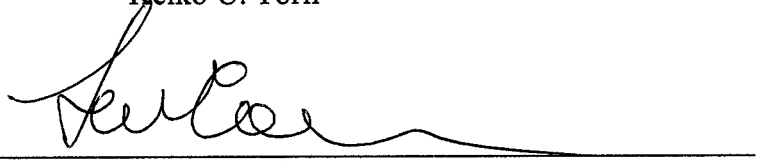

Luca Comai

Robert E. Cleland

Date: June 2, 2006

In presenting this dissertation in partial fulfillment of the requirements for the doctoral degree at the University of Washington, I agree that the Library shall make its copies freely available for inspection. I further agree that extensive copying of the dissertation is allowable only for scholarly purposes, consistent with "fair use" as prescribed in the U.S. Copyright Law. Requests for copying or reproduction of this dissertation may be referred to Proquest Information and Learning, 300 North Zeeb Road, Ann Arbor, MI 48106-1346, 1-800-521-0600, to whom the author has granted "the right to reproduce and sell (a) copies of the manuscript in microform and/or (b) printed copies of the manuscript made from microform."

Signature 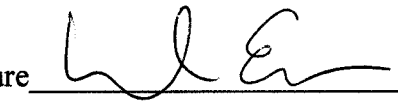

Date June 2/2006

University of Washington

Abstract

Roles for callose in plant development and intercellular communication

Linda C. Enns

Chair of the Supervisory Committee:
Professor Robert E. Cleland
Department of Biology

Cell-to-cell communication through plasmodesmata (PD) exists between most plant cells. The small fluorescent dye Lucifer Yellow CH (LYCH) has been used to determine that in the *Arabidopsis* root meristem there are tissues where PD occlude the movement of small molecules. A putative callose synthesis inhibitor chlorpromazine (CPZ) was tested and found to be effective. CPZ removed restrictions on LYCH movement in root tips, and impaired root gravitropism, supporting the idea that closure of PD in the root tip can be due to formation of callose at PDs, and that this is essential to maintain the normal circulation pattern for auxin. Other studies have used *Arabidopsis* expressing GFP under the control of a companion cell-specific promoter *AtSUC2* to conclude that GFP protein gets into all cells of the root meristem by moving through PD. We reexamined the movement of *AtSUC2::GFP* in an attempt to explain why GFP moves through PD where LYCH, a smaller molecule, cannot. We found that while GFP moves through the phloem

and out into all cells of the *Arabidopsis* root meristem, movement out of the stele is very slow. More importantly we found that GFP mRNA is able to move through all the PD. The newly assigned SEL of 27 kDa for cells of the *Arabidopsis* root meristem may thus be a gross overestimate. We speculate that there may be two types of PD in the *Arabidopsis* root meristem: one which allows the quicker diffusion of small molecules such as LYCH, the other which allows slower movement and has a higher SEL. Because chemical inhibitors are not specific, we then took a genetic approach towards looking at the importance of callose in plant intercellular communication. Callose is synthesized by callose synthase. *Arabidopsis* has 12 putative callose synthase genes (*GSL1-12*). We used TILLING and T-DNA insertion mutants to show that *GSL1* and *GSL5* are essential for normal sporophytic development in *Arabidopsis* and are also involved in pollen grain formation during cytokinesis, tetrad dissociation, cell expansion and mitosis. While we have not yet found which GSL makes PD callose, GSL3 is a candidate.

TABLE OF CONTENTS

LIST OF FIGURES

LIST OF TABLES

CHAPTER 1 - GENERAL INTRODUCTION

Callose and plasmodesmata

Callose is a linear ß-1,3-glucan that is widespread in plants (Stone and Clark, 1992). It is thought to have a variety of roles. It is found at the phragmoplast during cell division (Hong et al., 2001). It is believed to be involved in pollen grain formation and is a major part of pollen tubes (Li et al., 1999). Callose seals sieve elements after damage to phloem. It has a role in the defense of cells against pathogens (Benhamou, 1992). And callose is believed to play a significant role in the control of cell-to-cell communication through plasmodesmata (PD) (Overall and Blackman, 1996). However, up until recently, the importance of callose in these various aspects of plant development was inferred largely from its coincident presence at various developmental stages and with different subcellular components. Indeed, some scientists even argued that its presence, at PD at least, was more an artifact - a wound response due to histological preparation - than a reflection of its involvement in any developmental role (Radford and Overall, 1998; Radford and White, 2001).

When I first started work on this project, I was interested in the role callose was believed to play in plasmodesmatal (PD) regulation. PD are membrane-lined, cytoplasmic channels that traverse cell walls, linking cells together in a 'symplastic continuum' (Ding et al., 1992). PD allow the intercellular diffusion of molecules less than a certain size, known as the size exclusion limit (SEL). Observations on the intercellular movement of differently sized, fluorescently labeled dextrans have shown

that in many plant cells, the SEL is about 1 kDa. This SEL has been demonstrated for many tissues including leaf mesophyll (Wolf et al., 1989; Goodwin, 1983; Terry and Robards, 1987) and epidermis (Derrick et al., 1990) and staminal hairs (Tucker, 1982) and is consistent with the role of PD in the intercellular transport of sucrose.

A popular belief is that PD may be involved not only in photosynthate movement but in regulating plant development as well. The SEL for a PD is not a fixed value, but can increase or decrease in response to chemical or environmental signals (Schulz, 1999). It can be reduced, in order to restrict the movement of molecules into, or out of certain cells, and can vary between cell layers (Erwee and Goodwin, 1985). Closed PDs between two cell layers will result in symplastic domains: regions of the organ that are isolated from each other symplastically (Ehlers et al., 1999). PDs can be rapidly closed (gated) in response to increases in cytoplasmic calcium (Holdaway-Clark et al., 2000) or to differences in pressure across the PD (Oparka and Prior, 1992). SELs can also be decreased by wounding of tissues (Radford and White, 2001).

In addition to rapid closure, PD SEL can become gradually restricted during development. Duckett et al., 1994, demonstrated that while young epidermal cells of *Arabidopsis* roots are coupled to neighboring cells [i.e., carboxyfluorescein (CF) can move from cell to cell through the PD], as the cells mature, they become isolated from each other. Similar results have been obtained with wheat roots (Cleland, unpublished data). Likewise, the PD of developing cotton fibers are initially open, but close at day 10 during rapid cellular expansion, only to reopen at day 16 when the growth spurt is over

(Ruan et al., 2001). The symplastic domain in the shoot apical meristem changes during the conversion of a vegetative apex to a floral apex (Ormenese et al., 2002).

Macromolecules much larger than 1 kD have also been shown to move through PD. PD are now believed to be instrumental in determining and maintaining cell fate in the multicellular plant, by regulating the movement of RNA and proteins, believed to be signaling molecules. For example, the *Arabidopsis* root protein SHORTROOT (SHR) is expressed in the stele, but moves through PD into the endodermal cell layer where it is required to determine endodermal cell fate (Nakajima et al., 2001). DEFICIENS (DEF) is a MADS-box transcription factor in *Antirrhinum* that moves from inner to outer tissue layers in developing flowers - its movement is stage- and organ-dependent (Perbal et al., 1996).

How do such large molecules move through PD? Since PD SELs can be different depending on the tissue or stage of development, passive diffusion of large molecules could be governed by the endogenous SELs of certain PD. LEAFY is a floral identity protein that shows strong non-autonomous effects when expressed in the epidermis of the floral meristem (Sessions et al., 2000). GFP fusions show that the protein moves into underlying layers of the apex in a graded distribution consistent with passive diffusion (Wu et al., 2003). And GFP, when expressed under the control of the promoter for the companion-cell specific gene *AtSUC2* has been shown to move through the phloem and into sink tissues, where it moves from cell to cell, presumably through PD (Imlau et al, 1999).

Alternatively, specific interactions between transported macromolecules and PD components could lead to an increase in SELs. Initial studies on intercellular macromolecular trafficking showed that viral movement proteins (MPs) could increase the SEL of PD to facilitate the spreading of viral genomes (Waigman et al., 1994), and the discovery of a functionally related plant protein, CmPP16, led to the hypothesis that viral MPs hijack an endogenous trafficking system (Xoconostle-Cazares et al., 1999). KNOTTED (KN1), a maize protein that moves symplastically into the L1 layer of the shoot apical meristem (Jackson et al., 1994; Smith et al., 1992) has been shown to enable its intercellular transport by increasing the SEL of PD (Kragler et al., 2000). Very little is known about the mechanisms behind such targeted movement.

The mechanism by which PD are gated is not known (Schulz, 1999). There have been two main theories proposed. The first involves closure by actin microfilaments. The fact that the SEL of tobacco mesophyll cells can be greatly increased by depolymerization of actin (Ding et al., 1996) would support this idea. The second idea is that PDs are gated by the buildup of callose in the walls at the two ends of the PD (Olesen and Robards, 1990; Turner and Roberts, 1994). Such a deposition of callose at PD has been repeatedly demonstrated by both EM (Hughes and Gunning, 1980) and light microscopy (Radford and White, 2001). Schulz, 1999 has argued that callose is unlikely to be involved in the rapid reversible gating of PD, but it may be the main cause of developmental gating of PD. While it has been claimed that the callose associated with PD is artifactual (Radford and Overall, 1998; Radford and White, 2001), produced during the fixation of tissues for microscopy, there is considerable evidence to the contrary. For example, antibodies to a 65 kDa subunit of callose synthase have been prepared (Delmer

et al., 1993; McCormack et al., 1997) and localized to the PD (McCormack et al., 1997; Brown et al., 1998). Mutants for the β-1-3-glucanase in tobacco show a reduced SEL (Iglesias and Meins, 2000). And in birch apical meristems there is a loss of PD-localized callose and a change in symplastic domains during chilling-induced breakage of dormancy (Rinne et al., 2001).

Symplastic domains and gravitropism in the Arabidopsis root

I initially became interested in the interaction of callose with PD through studies on the mechanism of gravitropism in roots (funded by a grant from NASA). When plant roots and shoots are displaced from the vertical, they undergo a differential rate of cell elongation on the upper versus the lower side, resulting in a redirection of growth until the organ is vertical again. In the root, the direction of the gravity vector is detected primarily in the root cap. The hormone auxin, moving towards the tip in the stele, is displaced outwards to the cortex/epidermis and then away from the tip to the zone of cell elongation by polar auxin transport (Masson, 1995). There it slows down the rate of cell elongation. When roots are displaced from the vertical, the lateral movement of auxin at the tip becomes asymmetric, with more auxin moving to the lower side. When the asymmetric auxin concentration moves to the elongation zone, the higher auxin concentration on the lower side causes its growth to be more severely inhibited, resulting in a downwards curvature (Chen et al., 2002).

There may be non-auxin-mediated processes involved in root gravitropism as well (Chen et al., 2002; Ishikawa and Evans, 1993), but the asymmetric gradient of auxin across the root appears to be the main mechanism. For gravitropism to occur, then, a

gradient of auxin must be maintained across the root (Masson, 1995). Since the main auxin, indoleacetic acid (IAA) has a molecular weight of 175, it should freely move through PD between cell layers, and if this occurs it would be impossible to maintain the necessary asymmetric gradient of auxin across the root. There is evidence that the auxin involved in root gravitropism moves in the epidermal cells (Yang et al., 1990); if so, the PD between the cortex and epidermis must be closed in roots that undergo gravitropic curvature, separating the epidermis into a distinct symplastic domain. The epidermis may always be symplastically isolated; it is also possible that the PD in the longitudinal walls between epidermis and cortex are not gated when the root is vertical, but close in response to gravistimulation. Jaffe and Leopold, 1984 found that callose deposition in corn coleoptiles and pea shoots preceded gravity-induced curvature. The deposition was found to be asymmetric, with more callose deposited on the upper, more slowly growing side of the horizontally-placed organ. The shoot agravitropic pea mutant "*Ageotropum*", in contrast to its wild-type relative, showed no increase in callose deposition upon gravistimulation. In addition, inhibiting callose synthase in corn coleoptiles with 2-deoxy-D-glucose (DDG) resulted in a lessening of their gravitropism.

I initially decided to test the hypothesis that symplastic domains are necessary for root gravitropism by following the movement of low MW fluorescent dyes, loaded into the phloem of *Arabidopsis* seedlings at the cotyledons, as they move from the phloem into the root tip (Oparka et al., 1994). This allowed me to delineate the symplastic domains of the root tip. The *Arabidopsis* root presented an ideal model for my studies. It has a well-defined and predictable developmental pattern. It has defined symplastic domains and a gravitropic response that is well-characterized (Masson, 1995). Its small

size and general lack of autofluorescence makes it amenable to use in confocal microscopy, allowing facile visualization of intercellular tracer movement in-vivo, and in real-time, without dissection and physiological damage (Erwee and Goodwin, 1985).

My initial study, described in more detail in chapter 2, indicated that symplastic domains are indeed present in the *Arabidopsis* root. When my tracer of choice, Lucifer Yellow (LYCH), was loaded into the phloem at the cotyledons of *Arabidopsis* seedlings, it moved through the phloem to the root meristem. Its subsequent movement from the point of unloading showed restrictions into the epidermis, stele inner to the phloem, root cap and quiescent center. These results indicated that, at least for this molecule, these tissues are symplastically isolated.

At that time I started this project, the genes involved in callose synthesis had not yet been identified, and so I took an inhibitor approach to try and determine the role of callose in setting up these symplastic domains in *Arabidopsis* root tips. By giving the roots of seedlings a gravistimulation, with or without application of putative chemical inhibitors of callose synthase, I could get an indication as to whether the boundaries of the symplastic domains were altered by either gravistimulation or by an inhibition of callose synthesis. My chosen inhibitor, chlorpromazine (CPZ) (Harriman et al., 1992) inhibited callose synthesis, caused a loss of symplastic domains and rendered *Arabidopsis* roots agravitropic.

GFP movement in Arabidopsis roots

My work showing symplastic domains in *Arabidopsis* roots was contradictory to findings that GFP can move freely through all PD of *Arabidopsis* root meristems (Imlau et al., 1999; Stadler et al., 2005). LYCH is much smaller than the 27 kDa GFP, and thus should also be able to move through the same PD. I thus reexamined GFP movement in *Arabidopsis* root meristems to try and explain this inconsistency. This study, outlined in chapter 3, used grafting techniques to show that while GFP protein can move from companion cells of *AtSUC2::GFP* transgenic plants to phloem and thence into wild-type roots, GFP RNA moves as well. More importantly, GFP RNA also moves between all cells of the grafted wild-type root meristems. This study introduced the possibility that the GFP fluorescence seen in all cells of the root meristem in previous studies was due not to GFP protein movement between PD, but to GFP mRNA movement and subsequent translation. This would mean that the SEL of PD between cells of the root meristem could be much smaller than 27 kDa.

The callose synthases - genetic studies

My inhibitor work represented only preliminary data in support of our hypothesis that callose is important in setting up symplastic domains in the *Arabidopsis* root, and that these domains are essential for root gravitropism. The use of chemical inhibitors is not ideal because they are rarely specific for only one enzyme, and CPZ was no exception. Not only did it presumably inhibit all callose sythases, including those not involved in the synthesis of PD callose, but its general ability to inhibit calcium-activated enzymes probably caused additional physiological effects. When I started this project, it

was unknown what genes were involved in callose synthesis. Soon after I completed our inhibitor studies, a breakthrough occurred that allowed me to continue the project using a genetic approach.

In addition to callose, the cell wall contains other polyglucans, similar to callose except for differences in the type of linkage between glucose subunits. For example, a major component of the cell wall in all plants, cellulose, has a β-1,4-glucan backbone. Cellulose synthases are β-glycosyl transferases that are encoded by the *CesA* genes (Pear et al., 1996). In addition to cellulose, grass cell walls contain a β-1,3;1,4-glucan - this polysaccharide has been shown to be made by proteins encoded by the *Csl* or 'cellulose synthase-like' genes (Burton et al., 2006). As their name would suggest, these genes are related to the *CesA* genes, and are included with them in a larger superfamily. *Arabidopsis* and other dicotyledons also have *Csl* genes, some of which have been shown to encode (1,4)-β- D-mannases (Liepman et al., 2005).

For many years, the enzymatic mechanism of callose synthesis was a mystery. It was known that in most cases, callose synthesis requires calcium ions (Kauss, 1996), although callose synthesis in some pollen tubes is calcium insensitive (Doblin et al., 2001). Various attempts to isolate and purify callose synthase resulted in disagreement as to its identity, although there was general agreement that it is a multisubunit complex. It was thought that wounding could induce CESA complexes to switch from cellulose to callose synthesis (Dhugga, 2001), since attempts to obtain *in vitro* cellulose synthesis kept resulting in an isolated complex that only made callose (Delmer, 1999).

However, it is now known that the bulk of callose produced in plants is made by a different enzyme complex. It had been known for some time that the *FKS1* gene in yeast

codes for a β-1,3-glucan synthase (Douglas et al., 1994). The ca 200 kDa protein is the catalytic subunit of the callose synthase complex. Homologous genes have now been cloned from cotton (Cui et al., 2001), *Nicotiana* (Dobin et al., 2001) and *Arabidopsis* (Hong et al., 2001) and have been found to be unrelated to the *Csl* or *CesA* family. Hong's group called the *Arabidopsis* gene *CalS1* and showed that its polypeptide product catalyzed the synthesis of cell plate callose. They identified a family of 12 *CalS*-like genes in *Arabidopsis,* and named them *CalS1* through *CalS12*. Doblin's group called the genes from *Nicotiana NaGSL1* and *2*, gsl standing for 'glucan synthase like'. This terminology has also been used by the Stanford cell wall group (http://www.cellwall.stanford.edu). In this dissertation, and in accordance with the majority of recent publications on this gene family, I will use the *GSL* terminology.

During the course of this project, the cloning and verification of the first callose synthase, and the identification of its family members enabled me to take a genetic approach to my problem. Which of the GSL gene products are responsible for the synthesis of PD callose? And also of interest, if only some of these proteins are involved in PD callose synthesis, what do the rest of the *GSL* genes in *Arabidopsis* do? Are any redundant, or do each of them serve a different developmental function? I wished to answer these questions exclusively using the *Arabidopsis* root. In addition to the advantages of this model described above, focusing on the root allowed me to narrow down the number of genes of interest, thus limiting the amount of phenotyping as well as the number of mutant combinations I would have to make.

I took advantage of two facilities in order to acquire an extensive library of mutants for each of the root-expressed *GSL* genes: T-DNA insertions were available for

some of the genes from the Salk Institute Genomic Analysis Laboratory (SIGnAL; http://signal.salk.edu/cgi-bin/tdnaexpress), and a spectrum of point mutations for all the genes was isolated in cooperation with the Seattle TILLING Project (STP; (http://tilling.fhcrc.org:9366/). This library is described in Chapter 4.

I did not know which of the root-expressed *GSL* genes were involved in PD callose synthesis. Preliminary phenotyping at the gross morphological level did not pinpoint the identity of such a gene, although it did reveal a small number of interesting mutants.

Further work on these mutants revealed one promising candidate for a PD callose synthase: GSL3. A point mutation in the gene encoding for this protein may cause a loss of intercellular communication in roots. This work, described in Chapter 5, is ongoing.

Work has been completed on two of the other *GSL* genes. I found a role for *GSL1* and *GSL5* not in PD regulation, but in pollen development. Callose is highly conspicuous at two stages of pollen development and germination. It first surrounds the meiotic tetrad prior to the formation of the pollen grain wall (McCormick, 1993; Fei and Sawhney, 2001; Edlund and Preuss, 2004) and is also part of the pollen tube wall and plug within the tube, required for pollen tube growth (Ferguson *et al.*, 1998; Schlüpmann *et al.*, 1994). Its prominence at these stages suggested an essential role. At the time of my study, only limited genetic evidence supported this idea, although recent evidence has indicated that *GSL2* is involved in exine patterning (Dong et al., 2005; Nishikawa et al., 2005).

My work on *GSL1* and *GSL5*, described in Chapter 6, shows that these two genes are redundant, and are involved in multiple aspects of both plant and pollen development and fertility.

CHAPTER 2 - A ROLE FOR CALLOSE IN DELINEATING SYMPLASTIC DOMAINS IN THE *ARABIDOPSIS* ROOT TIP

(SUBMITTED TO PLANTA)

Introduction

Almost all plant cells are interconnected by protoplasmic bridges, the plasmodesmata (PD). If a molecule can diffuse from cell to cell through the PD, the cells are part of the same symplast. However, if the PD restricts the movement of the molecule, the cells on either side are isolated into separate symplastic domains. Symplastic domains can be as small as a single cell (e.g. mature root epidermal cells, Duckett et al., 1995) or as large as almost a whole organ (e.g. *Egeria* leaf, Erwee and Goodwin, 1985). The presence of such domains has been demonstrated in the shoot apex (Rinne and van der Schoot, 1998; Gisel et al., 1999; Kobayashi et al., 2005), but less is known about the root tip. Studies on the short-time movement of the small dye carboxyfluorescein (CF, m_r 376) from the phloem into root tip cells (Oparka et al., 1994; Zhu et al., 1998a) provide some indication that symplastic domains may exist in the root tip. On the other hand, HPTS (8-hydroxypyrene-1,3,6-trisulphonic acid, m_r 524) (Wright and Oparka, 1996), and the much larger green fluorescent protein (GFP, mw 27 kDa) (Roberts and Oparka, 2003), apparently move from the phloem into all cells in the root tip, raising doubts about symplastic domains in the root. One of the objectives of this research was to investigate more fully the existence of symplastic domains in the

Arabidopsis root tip. This was to be tested by examining the pattern of movement of the small fluorescent dye Lucifer Yellow (LYCH) from the phloem to the cells in the root.

The location and extent of symplastic domains depends on whether or not a molecule can pass through the PD. In general, PD permit the movement of molecules that are less than a critical size (shape). This cutoff is called the size exclusion limit (SEL). The SEL of many PD has been reported to be about 1 kDa (Lucas et al., 1993). However, the SEL is a dynamic property (Schulz, 1999), and changes in the SEL can be rapid. These include transitory decreases in the SEL in response to increases in cytoplasmic calcium (Holdaway-Clark et al., 2000), pressure differences across the PD (Oparka and Prior, 1992), or wounding (Radford and White, 2001). SEL increases occur in response to a decrease in ATP (Cleland et al., 1994) or can be induced by viral movement proteins (Nelson, 2005) or by certain endogenous proteins (Xoconostle-Cazares et al., 1999).

In addition to these rapid changes in the SEL, slower developmental changes in the SEL have also been documented. As young epidermal cells of *Arabidopsis* and wheat roots mature, they become isolated from each other (Duckett et al., 1994), as evidenced by the impeded intercellular movement of small fluorescent dyes. The PD of cotton fibers, initially open, close during rapid cellular expansion, only to reopen when the growth spurt is over (Ruan et al., 2001).

It is not known how PD are gated (Holdaway-Clark, 2005). One possibility is that the gating is due to a buildup of callose around the ends of the plasmodesma. Callose, a β-D-glucan containing mostly 1,3 links, is widespread in higher plants (Stone and Clarke,

1992). Its role in plant defense is well documented, as it forms and seals both phloem sieve plates and plasmodesmata in response to wounding (Benhamou, 1992). But callose also occurs in undamaged plants during cell plate formation (Hong et al., 2001), pollen grain development (Dong et al., 2005; Enns et al., 2005) and as a major component of both pollen tubes (Li et al., 1999) and other cell walls, where it is frequently found associated with plasmodesmata (Radford et al., 1998).

The conjunction between callose and PD (Radford et al., 1998; Olesen and Robards, 1990; Botha and Cross, 2000) has led to the hypothesis that callose buildup at the two ends of the PD may be involved in their slower closure during general plant development. Tobacco mutants for the β-1,3-glucanase show a reduced SEL (Iglesias and Meins, 2000), and in birch apical meristems there is a loss of PD-localized callose and a subsequent change in symplastic domains during chilling-induced breakage of dormancy (Rinne et al., 2001). The second objective of this research was to test the hypothesis that callose is involved in the maintenance of symplastic domains in the root. This was undertaken by chemical inhibition of callose synthesis and then examination of its effects on symplastic domains and on root development.

Materials and Methods

Plant materials and growth conditions

Arabidopsis thaliana, ecotype Columbia seeds were sterilized for 2 minutes in 70% ethanol, 10 minutes in 50% bleach, 0.1% Triton X-100 (Sigma, T-9284), and rinsed

7 times with sterile distilled water. Seeds were sown on petri dishes containing 1.2 % Phytagar (Gibco 10695-039), 1% sucrose, 0.5X Murashige & Skoog Salt Mix (Gibco, 11117-074) at a pH to 5.7 with KOH. Seedlings were grown by placing petri dishes vertically under an 18-h-light/6-h-dark cycle at 21°C. Seedlings used were 6 days old.

Fluorescent tracer dyes

Fluorescent tracer dyes tested were as follows: 5-(and-6)-carboxyfluorescein diacetate (CFDA) (Molecular Probes, C-195), 5-(and-6)-carboxyfluorescein (CF) (Molecular Probes, C-194), 1-acetoxypyrene-3,6,8-trisulfonic acid trisodium salt (HPTS-acetate) (Sigma, A-3332), 8-hydroxypyrene-1,3,6-trisulfonic acid trisodium salt (HPTS) (Molecular Probes, H-348), and lucifer yellow CH potassium salt (LYCH) (Molecular Probes L-1177).

Membrane permeability assays

To test whether or not fluorescent dyes could cross plasma membranes, intact seedlings were laid out on partially agar-coated microscope slides, such that the main root tip extended a couple of millimetres over the end of the agar. The bottom several millimetres of the root, including the root tip was then put into contact with an agar block (1.2% Phytagar) containing the requisite dye, such that the dye-containing block did not come into contact with the non-dye-containing agar on the slide. After a certain period of time, the plant was taken off the slide and rinsed in a petri dish containing 50 mL of distilled water, for one hour.

Loading concentrations and times were as follows: CFDA, 125 μM for 1 h; CF, 150 μM for 1, 5, 10 and 30 min; HPTS-acetate, 5 mg/mL for 7 min, 30 min, and 2.5 h; HPTS, 2.5 mg/mL for 1 h; Lucifer Yellow, 4.8 mM for 2 h and overnight.

The presence of dye inside the root of the intact, living plant was assessed by CLSM (BioRad MRC-600).

Symplastic domain assays

Assays were performed as described in Oparka et al. (1994). The seedlings were laid out on partially agar-coated microscope slides, such that the hypocotyl and shoot extended over the end of the agar. Under a dissection microscope, the tip of a cotyledon was excised. The cut cotyledon was then inserted into an agar block containing the fluorescent dye of choice, such that the dye-containing agar did not come into contact with the non dye-containing agar on which the roots rested. Tracer dyes tested were CFDA (125 μM), HPTS-acetate (5 mg/mL), HPTS (25 mg/mL) and Lucifer Yellow (4.8 mM).

The microscope slide was taped in a petri dish, which was sealed with micropore tape, and oriented vertically in a growth chamber under the previously described conditions. The presence of dye in the meristem was assessed half-hourly from 1 hour after the beginning of loading until 7 hours after loading, and after loading overnight.

Observations were made with both a Leica and a BioRad confocal microscope. When using the former microscope, prior to loading the dye, the main root tips of 6 day old seedlings were excised, and branch roots were allowed to develop for 2 more days. Following dye loading, branch root meristems were then observed (it was found that

branch roots were slightly thinner than main root meristems, and easier to observe with this microscope). When using the latter microscope, obervations were made on both branch root and main root meristems. Results obtained using either method were similar for both branch root and main root meristems. When using the Leica microscope, seedlings were immersed in a 0.01 mg/mL solution of propidium iodide (PI) (Molecular Probes, P-1304) for approximately one minute prior to mounting in distilled water. This allowed the visualization of cell wall fluorescence as well as tracer dye fluorescence, using dual excitation.

Callose inhibitor assays

Seedlings were grown on agar as previously described. To test the effectiveness of inhibitors on digitonin and aluminum-induced callose synthesis, 6 day seedlings were transferred to agar containing either 10 μM or 30 μM digitonin (Sigma, D5628) or 20 μM $AlCl_3$-$6H_20$ (Sigma, A3017). Either 5 X 10^{-5} M or 10^{-4} M 2-chloro-10-[3-dimethylamino-propyl]phenothiazine (CPZ) (Sigma, C-8138) or 10^{-4} M or 10^{-3} M 2-deoxy-D-glucose (DDG) (Sigma, D-3179) were also added to the agar. Callose synthesis was evaluated after three days under previously described growth conditions, by the following protocol. Intact plants were fixed in 96 % ETOH for 1 h. Roots were then excised approximately 1 cm from the tip, and stained with toluidine blue (Allied Chemical, 641) (0.1 % in 100 mM $P0_4$ buffer, pH 4.4) for 2 h in order to quench autofluorescence. They were then mounted in aniline blue (Allied Chemical, 707) (0.1% in 1M glycine, pH to 9.5 with NaOH) and observed with a BioRad confocal microscope.

Antibody labelling and inhibition of callose synthesis

The aniline blue staining protocol was not sufficiently sensitive to observe physiological levels of callose. I used antibody labeling to assess the effects of CPZ and DDG on normal callose levels, in situ.

Seedlings were grown on agar as previously described. 6 day seedlings were transferred to agar prepared as described and also containing either 6 X 10^{-5} M CPZ or 10^{-3} M 2-deoxy-D-glucose DDG. Callose synthesis was evaluated after four days under previously described growth conditions, by the following protocol.

In addition to non-CPZ-treated controls, prior to antibody labelling, some controls were treated for 10 minutes with 6 X 10^{-5} M CPZ to preclude the possibility that wound callose would be induced by fixation. This was done by placing seedlings on CPZ-containing agar. Antibody labelling of callose was then performed for all seedlings as described in Harper et al., 1996. Seedlings were fixed for 30 min in a 4% (w/v) paraformaldehyde (Sigma, P6148) solution in PME buffer (see below) containing 10% dimethylsulphoxide (DMSO) (Sigma, D5879). PME buffer consisted of 50 mM PIPES [piperazine N,N'-*bis*-(2-ethane sulphonic acid)] buffer containing 5 mM EGTA (ethyleneglycol-*bis*-[B-aminoehtyl ether] N,N,N',N'-tetraacetic acid), and 2 mM $MgSO_4$-$7H_20$. Seedlings were then washed three times for 10 min each in PME (without DMSO). Seedlings were enzymatically digested with 0.5% pectolyase (P3026), 1% bovine serum albumin (BSA, fraction V) (Sigma, A2153), 10% glycerol (Sigma , G5516) and 0.2% Triton-X 100 (Sigma, T9284) in PME for 30 min. Seedlings were again washed three times, 10 min each, this time in PME containing 0.2% Triton-X 100 and 10% glycerol. Seedlings were extracted at -20°C in methanol for 15 minutes, and then

rehydrated and rinsed twice (5 min each) with phosphate buffered saline (PBS; 3 mM KH_2PO_4, 150 mM NaCl, pH to 7.2 with KOH). Root excision was not required.

Primary antibodies to callose (anti-β-(1-3)-glucan; Biosupplies, Parkville, Victoria, Australia) and secondary antibodies (fluorescein isothiocyanate (FITC)-conjugated sheep-anti mouse; Sigma) were diluted in PBS containing 1% BSA with 0.02% sodium azide (Sigma, S2002). Root tips were labelled for 12 h at 37°C with the primary antibody, diluted 1/200. The roots were then rinsed three times (5 min each) in PBS. Roots were then incubated in the secondary antibody, diluted 1/30, for 3 h at 37°C, washed in PBS twice (5 min each), and mounted on slides in AF1 antifade mountant (Citifluor, Australia). Roots were observed with a Leica confocal microscope. Controls with secondary antibody only were also performed.

Antibody labelling of callose was also used to verify that digitonin was enhancing callose synthesis.

CPZ treatments and observations on root morphological effects

5-6 day seedlings were transferred to agar containing concentrations of CPZ ranging from 10^{-4} - 10^{-5} M. After 6 days under previously described growth conditions, they were assessed for the following: root symplastic domains using cotyledon-loaded LYCH as previously described, length of root growth, number of lateral roots, overall direction of root growth, and the maximal deviation of root growth from the gravity vector, which was set at 0 degrees. (For branch roots, the intial direction of protuberance, which typically occurs at an angle, was not counted in this last measurement.) To make sure that CPZ was not increasing membrane permeability to LYCH, external loading

experiments were also performed as already described, with 4.8 mM LYCH and a loading time of 2 hours.

Results

Delineation of symplastic domains in the Arabidopsis root, using Lucifer Yellow

One approach to delineating symplastic domains in the *Arabidopsis* root tip is to load a small molecular weight fluorescent dye into the phloem at a cut cotyledon. The dye is then transported to the root in the phloem, where it is unloaded through PD into root cells. If the dye is unable to move from one cell to the next, the two cells exist in separate symplastic domains. Previous studies on symplastic domains in roots have used carboxyfluorescein (CF, m_r 376) (Oparka et al., 1994; Zhu et al., 1998a), or 8-hydroxypyrene-1,3,6-trisulphonic acid (HPTS, m_r 524) (Wright and Oparka, 1996), both loaded in their ester form. Significant differences were obtained between these studies.

Three criteria were used to choose a PD tracer dye for this study: First, it must be possible to load the dye into the phloem at a cut cotyledon and have it unloaded into root cells. HPTS in its non-ester form could not be loaded in this way (data not shown). CFDA, HPTS-acetate and LYCH (m_r 457) all met this criterion. For example, CF (produced from CFDA in the phloem) moved through the phloem to the root meristem where it was sequestered by the young epidermis, cortex, endodermis and root cap cells. CF did not move into the central stele, however (**Fig. 2.1A**).

Second, the fluorescent dye must be incapable of crossing the plasma membrane of root cells. This provides assurance that any dye that appears in a cell remote from the phloem has reached the cell by a symplastic pathway. To test this, dye was applied externally to root tips for periods of up to 2h, and after washing, observed in the confocal microscope. As expected, HPTS-acetate and CFDA entered the cells; the non-fluorescent CFDA was converted to the fluorescent CF inside the cells. Contrary to previous reports (Oparka et al., 1988; Baluska et al., 2004), no LYCH could be detected within the root cells (**Fig. 2.1C**). This result was confirmed even after treating the roots externally with LYCH for 24h (data not shown). On the other hand, CF, at 150 μM was taken up into many root cells (**Fig. 2.1D**), if administered for longer than 5 min. The cell layer at which the CF entered could not be determined; for example, it might have been taken up only into epidermal cells and then moved through PD to the other cells, or it could have entered all of the cells. It is not possible to determine, therefore, whether all the CF found in the variety of root cells of cotyledon-loaded plants (**Fig. 2.1A**) arrived there through PD, or whether some was taken up from the apoplast.

The third criterion is for dyes which must be loaded in an ester form. The permeable ester form must not be fluorescent, so that one can distinguish symplastic movement of the non-permeable dye from apoplastic uptake of the permeable form. HPTS-acetate does not meet this criterion. It is thus not possible to determine whether the fluorescence in root tips after cotyledon-loading of HPTS-acetate is due to symplastic movement of HPTS, or apoplastic uptake of HPTS-acetate.

LYCH was shown to meet all three criteria. At high concentrations (4.8 mM) it loaded into the phloem of cut cotyledons. The transport of the dye in the phloem, and not

the xylem, was verified at shorter loading times (data not shown) and longer loading times of 24h (**Fig. 2.3A**). Both tissues could frequently be compared in the same optical section. Xylem vessels could be discerned from phloem both by the strong propidium iodide staining of its secondary walls (**Fig. 2.3A**), and by the presence of distinctive secondary wall thickenings (data not shown). LYCH was unable to enter root cells from the apoplast (**Figure 2.1C**). Since LYCH does not require a membrane-permeable form for phloem-loading, the third criteria is not of concern. LYCH was thus chosen as the most suitable phloem-loading PD tracer dye, since its appearance in root cells after loading in the cotyledon could only occur via symplastic movement of the dye from the phloem.

The dye moved down the phloem and into the root tip, where it showed up prominently after about 4 hours. LYCH, upon reaching the area just distal to the zone of root-hair production, moved laterally from the distal end of the phloem to adjacent files of cells, showing up most brightly in the cortex and endodermis (**Fig. 2.2**). During this initial phase of LYCH unloading, the pattern of fluorescence was similar to that of CF. Unlike CF, however, which then diffuses to most of the remaining cells of the root tip, the LYCH moved primarily towards the root tip and in the proximal direction in the cortical and endodermal layers. Ultimately, the fluorescent dye could be seen in all of the cortical and endodermal cells, from the point of unloading to the initials (**Fig. 2.2**). (The pericycle layer, and the cells between the phloem and pericycle, were difficult to resolve, but it appears that the dye was in these cells as well). Movement of the dye into the epidermis, quiescent center, columella cells and inner stele was restricted. I could find no evidence for a rapid, low-level movement of LYCH into all the cells of the root tip, such

as that reported by Zhu et al. (1998a) to occur with CF. Even after 24 hours, fluorescent dye was not detectable in the quiescent zone, the columella cells of the root cap or the stele inner to the phloem, and only at a very reduced level in the young epidermis (**Fig. 2.3B**). In the more mature regions of the epidermis, there was discernibly less dye than in the cortical layer (**Fig. 2.3C**).

Lucifer Yellow is taken up by vacuoles. This uptake is unlikely to be by fluid-phase endocytosis from the apoplast (Oparka et al., 1988), since as shown earlier (**Fig. 2.1C**), apoplastic LYCH does not get taken up into *Arabidopsis* root cells. In my studies, the dye can clearly be seen in the vacuoles of the cortical and endodermal cells. Epidermal cell vacuoles were shown to be as capable of sequestering LYCH as cortical cells if plants were allowed to load for over 24 h. The observed differences in fluorescence between these tissues are thus not due to differences in their ability to sequester dye in the vacuole, but to the amount of dye which has moved into them.

Chlorpromazine, but not 2-deoxy-D-glucose, is an effective inhibitor of callose synthesis in the Arabidopsis root

I wanted to test the hypothesis that closure of PD by callose (Schulz, 1999; Botha et al., 2000) might be responsible for creating the LYCH-delineated symplastic domains that exist in the *Arabidopsis* root tip. I thus looked for a callose synthesis inhibitor that would be effective on *Arabidopsis* roots. Two such inhibitors have been described in the literature: chlorpromazine (CPZ) (Harriman et al., 1992) and 2-deoxy-D-glucose (DDG) (Radford et al., 1998; Sivaguru et al., 2000). I first used aniline blue, a histochemical dye for callose, to test the ability of these inhibitors to decrease the amount of callose in the

Arabidopsis root. Aniline blue causes callose to fluoresce yellow. While this dye is excited optimally by UV light, if the fluorescence is strong enough it can be detected by our BioRad confocal microscope at an excitation of 488 nm. In untreated roots callose was not detectable using this method (data not shown). I used a callose synthesis enhancer, digitonin, to increase callose levels in the *Arabidopsis* root. Once roots were treated with digitonin, callose could readily be detected (**Fig. 2.4A**). The increase in callose was confirmed using ß-1,3-glucan antibodies (data not shown). The digitonin-induced callose occurred over the whole root, but was most prominent in the mature epidermal cells. As a result, I used this tissue for these initial callose inhibitor studies. When roots were treated with both digitonin and CPZ, callose synthesis was inhibited dramatically (**Fig. 2.4B**). On the other hand, when treated with digitonin and with DDG at concentrations which either partially or completely inhibited root growth, there was no effect of DDG on the ability of digitonin to stimulate callose synthesis (**Fig 2.4C**). As a further confirmation, *Arabidopsis* roots were treated with aluminum (20 μM $AlCl_3.6H_2O$), which Sivaguru et al. (2000) reported caused massive increases in callose synthesis in wheat roots. Al^{3+} has a similar effect on *Arabidopsis* roots (**Fig. 2.4D**), and this callose synthesis was inhibited by CPZ (**Fig. 2.4E**) but not DDG (**Fig. 2.4F**).

I also tested the ability of CPZ to cause the loss of callose in situ, using antibodies to ß-1,3-glucan to detect the callose. In untreated roots, callose appeared prominently in the cell plates of dividing cells (**Fig 2.5A**). At higher magnification, a punctate deposition of callose was also noticeable in the cell walls between cells (**Fig. 2.5B,C**); this is thought to be PD callose. PD callose was especially noticeable in the lateral walls both between the cortex and epidermis and between the epidermis and lateral root cap, as

well as in all walls of the root cap cells. This pattern of callose was observed even if roots were given a 10 minute treatment of CPZ prior to fixation in order to suppress wound callose. A treatment of CPZ for 5 days caused a loss of both types of callose (**Fig. 2.5D,E**). Presumedly, the loss of callose is due to a combination of the normal turnover of callose by ß-1,3-glucanase, coupled with inhibition of resynthesis of callose by CPZ.

CPZ disrupts symplastic domains in the Arabidopsis root

Arabidopsis seedlings were transplanted to CPZ-containing agar at the age of about 5 days. They were allowed to grow on 6 $x10^{-5}$ M CPZ for 7 days, after which time they were phloem-loaded with LYCH. Treatment of roots with CPZ frequently changed the pattern of dye movement in the root tip. Visible effects ranged from small increases in dye movement into the epidermis and stele (not shown) to diffuse movement of the dye in all tissues (**Fig. 2.6B**). Often LYCH was no longer restricted to the phloem in the mature regions of the root (**Fig. 2.6C**). To make sure that CPZ was not just making the plasma membranes of cells more permeable to Lucifer Yellow, I externally applied LYCH to CPZ-treated roots, as described above. The dye was still unable to cross plasma membranes (data not shown).

CPZ affects root development and alters root gravitropism

CPZ had multiple effects on root growth (**Fig. 2.7**). At $5x10^{-5}$ M CPZ, the main root length was reduced by 50%, although branch root length was not affected. CPZ also increased the number of lateral roots. CPZ had little effect on the average direction of

root growth, but at increasing CPZ concentrations the variation in the direction of the root growth became more random (**Fig. 2.7**). This suggests that CPZ has not interfered with the perception of the gravity vector, but has disrupted, to a varying degree, the gravitropic growth reaction. This is consistent with the epidermis no longer existing as a different symplastic domain from the internal cells of the root.

Discussion

Symplastic domains in the Arabidopsis root tip.

Plant development requires that morphogenetic molecules be restricted to groups of cells, called symplastic domains (SDs), and not be free to affect all cells (Kobayashi et al., 2005). Since virtually all plant cells are interconnected by the protoplasmic bridges called plasmodesmata (PD), it is thus essential that the PD be able to limit which molecules can freely diffuse from cell-to-cell. SDs occur whenever a molecule is unable to move from cell to cell through the PD; the cells on either side of the blocked PD form separate symplastic domains for that molecule.

Symplastic domains are both molecule and developmental stage specific. PD can differ greatly in both the type and the size of the molecules that they exclude. For most PD, there is a maximum size of molecule, called the size exclusion limit (SEL), that can diffuse through them (Goodwin, 1983). Although it is the Stokes radius rather than the molecular weight that determines whether a molecule can diffuse through a PD (Fischer and Oparka, 1996), SEL values are usually given as molecular weights. In many tissues,

this SEL is about 1 kDa; however, it can vary from between near zero and >80 kDa (Lucas et al., 1993). The SEL can undergo rapid decreases in response to agents such as cytoplasmic calcium (Holdaway-Clarke, 2000) or rapid increases in response to a lack of ATP (Cleland et al., 1994). PD can also discriminate between different molecules of similar size (Goodwin and Cantril, 1999). For example, in *Egeria densa* leaves, small fluorescein isothiocynate-amino acid conjugates containing aliphatic amino acids freely diffuse through the PD, while conjugates containing aromatic amino acids cause closure of the PD (Erwee and Goodwin, 1984). Small proteins such as GFP (mw 27 kDa) are thought to diffuse through many PD (Imlau et al., 1999; Itaya et al., 2000), while larger proteins are excluded unless either the PD is dilated by some factor such as a viral movement protein (Ghoshroy et al., 1997), or the protein is moved across the PD by a targeted process (Lucas and Lee, 2004).

During development there are often significant changes in the SEL of plasmodesmata. For example, CF moves freely between young epidermal cells of the *Arabidopsis* root, but cannot move out of epidermal cells when they begin to form root hairs (Duckett et al., 1994). In growing tobacco leaves, sink leaves have PD that permit the movement of GFP, but as the cells age and they are converted to source leaves, this capacity for GFP diffusion is lost (Oparka et al., 1999). Both HPTS (m_r 524) and FITC (F)-dextran (10 kDa) can move freely between all cells in heart stage *Arabidopsis* embryos, but by the mid-torpedo stage, the SEL has decreased so that while HPTS can still move between cells, the F-dextran can no longer move (Kim et al., 2002). In vegetative *Arabidopsis* shoots HPTS, introduced into cut leaf petioles, moves into a ring comprising the peripheral cells of the SAM. However, when the transition to flowering is

induced, HPTS is no longer able to move into these cells (Gisel et al., 2002). This capacity for HPTS movement is restored later during inflorescence development. In *Sinapis* alba the central symplastic field of the shoot apical meristem expands during the transition to flowering (Ormenese et al., 2002). In each of these cases, the decrease in the SEL resulted in the formation of symplastic domains where such SDs had not previously existed.

What symplastic domains exist in the root? Mature phloem is in a different SD than the adjacent cells of the mature root (Oparka et al., 1994; Schulz, 2005), indicating that export of sugars from the phloem to the neighboring cells must involve a release of the sugars into the apoplast surrounding the phloem. This symplastic isolation can change, however. When nodules are induced by *Sinorhizobium* in mature alfalfa roots, a symplastic connection for the dye CF is established between the phloem and the developing nodule (Complainville et al., 2003). The situation regarding SDs at the root tip is far less clear. Studies in which fluorescent molecules were loaded into the phloem at cut cotyledons or synthesized in companion cells have given conflicting results. Both HPTS (Wright and Oparka, 1996) and GFP (Roberts and Oparka, 2003) have been found to move equally into all cells in the *Arabidopsis* root tip. Zhu et al. (1998a) reported that low levels of CF moved rapidly and equally into all of the root tip cells. On the other hand, Oparka et al. (1994), Zhu et al. (1998a) and Complainville et al. (2003) have all shown that when CF is unloaded from the end of the phloem into the pericycle/endodermal cells, it then moves preferentially towards the tip in just these cell files.

I elected to reexamine this problem using LYCH as the fluorescent dye. It has the advantage that in my system, unlike CF, it will not cross from the apoplast into *Arabidopsis* root cells (**Fig. 2.1C**). Also, since both CFDA and HPTS-acetate can be taken up from the apoplast, the presence of fluorescence in root tip cells after addition of either of these ester dyes may not always be by a symplastic route. Contrary to the report of Oparka et al. (1994), I found that LYCH would load into the phloem of *Arabidopsis* through a cut cotyledon. The ability of LYCH to cross the plasma membrane of some plant cells has been previously demonstrated (O'Driscoll et al., 1991); however, the mode of entry of LYCH into the cut *Arabidopsis* cotyledon is unknown. I have shown that in the *Arabidopsis* root meristem, at least, LYCH cannot cross plasma membranes, making it an appropriate tracer for root symplastic domains in this organism. My LYCH concentration is higher and my exposure times to LYCH are longer than those employed previously with CFDA, in part to assure that the symplastic domains are fully delineated, and in part because LYCH loads more slowly than CFDA into the phloem. One disadvantage of LYCH, in contrast to HPTS, is that it accumulates in vacuoles. But since the LYCH cannot be taken up from the apoplast of the root, the LYCH in vacuoles must have first moved to those cells in the symplast.

My results confirm that the phloem is a distinct symplastic domain from the other mature root cells; there is little or no movement of LYCH from the phloem to these mature cells. When the LYCH reaches the distal end of the phloem, it moves outwards into the cells external to the phloem. The dye becomes especially concentrated in the cortical and endodermal cells, where it moves distally to the initial cells in the meristem. Little dye moves into the central stele, the quiescent cells or the root cap. These cells

form symplastic domains that are distinct from the cortical/endodermal cells. There is a limited movement of LYCH into the epidermal cells, indicating that either the conductance through the PDs into this cell layer must be reduced, or that this cell layer has fewer PD. It is apparent that the barriers that delineate symplastic domains are not always complete, i.e. PD are not always completely absent or closed, since with prolonged LYCH treatment the epidermal cells do accumulate considerable LYCH in their vacuoles.

The data for LYCH movement are consistent with the information about the frequency and types of plasmodesmata in the *Arabidopsis* root tip (Zhu et al., 1998a). PD are more abundant in the transverse walls within cell files than they are on the longitudinal walls between cell files. The highest density of PD is in the transverse walls of the cortical cells. The PD in transverse walls are all primary PD, while those in the longitudinal walls are mostly secondary PD, and some are branched PD as well. Since the SEL of primary PD tends to be greater than that of secondary PD (Oparka et al., 1999), it is to be expected that boundaries of SDs would occur at the longitudinal walls rather than the transverse walls. The density of the transverse PD declines sharply as the cells mature (Zhu et al., 1998b). This probably accounts for the fact that LYCH, after unloading from the phloem, mores rapidly towards the apex in the cortical cells, while it moves poorly in the basipetal direction in this cell file.

An apparent contradiction to the idea of symplastic domains in the *Arabidopsis* root is the finding that GFP, which is much larger than LYCH, seems to move symplastically between all cells of the root tip (Imlau et al., 1999; Roberts and Oparka,

2003). In the next chapter, I will try to explain the discrepancies between those studies done with GFP and my work with LYCH.

The role of callose in the establishment of symplastic domains in the root tip.

The SEL of PDs can change dramatically from 376 to 80,000 Da, depending on circumstances (Lucas et al., 1993). Increases in cytoplasmic Ca^{2+} or reductions in turgor can cause rapid but transitory closure of PD (Schulz, 1999). These rapid changes in SEL may be controlled by actin, myosin or centrin (Holdaway-Clarke, 2005). Significant increases in the SEL occur in response to viral movement proteins or to a selected group of endogenous plant proteins (Lucas and Lee, 2004). The mechanism of these increases in SEL is still unknown. Developmental changes in the SEL, as evidenced by opening or closure of PD to movement of the small dyes CF or LYCH, are slower and persist for extended periods of time (Schulz, 1999).

It would appear that callose may be responsible for at least some of the developmental changes in the SEL. Callose is formed in cells at sieve plates (Stone and Clarke, 1992) and at PD in response to wounding (Benhamou, 1992) or to viral movement proteins (Rinne et al., 2005). Callose constricts the opening of PD by forming rings outside the ends of the PD (Olesen and Robards, 1990; Bayer et al., 2004) or within the sphincters of the PD (Rinne et al., 2005). Questions have been raised as to whether callose exists at PD in the absence of wounding (Radford and White, 2001). However, a coincidence of callose and PD has been repeatedly reported (e.g., Bayer et al., 2004; Sagi et al., 2005). In addition, it is clear that callose is closely correlated with PD closure in birch shoot apical meristems (Rinne et al., 2001), cotton fibers (Ruan et al., 2001), and

source leaves of tobacco expressing a viral movement protein (Rinne et al., 2005). Enhanced callose deposition in a β-1,3-glucanase-deficient mutant is correlated with a decline in the SEL (Iglesias and Meins, 2000).

If callose is responsible for the closure of PD that mark the boundaries of symplastic domains in the *Arabidopsis* root tip, inhibition of callose synthesis should result in an opening of the PD as the in situ callose is degraded by ß-1,3-glucanases, and this should lead to a loss of defined symplastic domains. The most commonly employed inhibitor of callose synthesis is 2-deoxy-D-glucose (DDG) (Radford et al., 1998). In my hands, DDG was unable to prevent synthesis of normal, digitonin-induced or Al-induced callose, whether applied at concentrations that still permitted, or at higher levels that completely inhibited root growth. A second inhibitor is chlorpromazine (CPZ) (Harriman et al., 1992). In contrast to DDG, a concentration of CPZ was found that effectively inhibited normal, Al^{3+}- or digitonin-induced callose synthesis, while only partly inhibiting root growth. The CPZ treatment resulted in the loss of defined symplastic domains. In this case, LYCH was found to spread to all the cells of the root tip, including the epidermis, root cap and central region of the stele. This movement of LYCH was still symplastic, as shown by the fact that externally applied LYCH failed to enter any of the cells in the tips of CPZ-treated roots (data not shown).

CPZ, however, is not a specific inhibitor for callose synthesis. It is commonly used to inhibit calmodulin-mediated responses (Hosey and Luzdunski, 1988). The loss of the symplastic domains might be due to some action of CPZ other than inhibition of callose synthesis. Synthesis of callose is carried out by the enzyme callose synthase (GSL) (Li et al., 2003). In *Arabidopsis* there are 12 *GSL* genes (Hong et al., 2001).

Chapter 4 describes the genetic approach I undertook to try and determine which of these genes is responsible for callose synthesis in non-damaged *Arabidopsis* root tips, and my attempts at selective inhibition of either their expression or function of their encoded proteins.

Are symplastic domains for LYCH movement in the root tip significant?

While many proteins are cell-autonomous, a number of morphogenetic proteins use plasmodesmata as their pathway to gain access to neighboring cells (Jackson, 2005). In some cases, such as the LEAFY protein, the movement is simply by diffusion (Wu et al., 2003). More commonly the movement is targeted, and requires specific transport signals and receptors (Lucas and Lee, 2004; Jackson, 2005). For small molecules, movement through PD is by diffusion (Lucas et al., 1993). Free movement of small molecules through PD has several important consequences for cells. First, the neighboring cells must have identical or nearly identical membrane potentials (van Bel and Ehlers, 2005). In tomato stems, differences in membrane potential between adjacent cells was well correlated with the presence of SD, as measured by dye movement (van der Schoot and van Bel, 1990). Secondly, if different concentrations of small molecules exist between cells, diffusion should drive the movement of the molecules towards equilibrium. Finally, if hormones (e.g. auxin, gibberellin and cytokinin) are free to diffuse through PD, asymmetric gradients will be difficult to maintain.

It is tempting to believe that the pattern of symplastic domains for LYCH also hold true for other small molecules. If so, the symplastic domain consisting of the cortex/endodermis would appear to be an efficient pathway for the movement of sugars

from the phloem to the root meristem. This pathway has been a matter of some dispute (Bret-Harte and Silk, 1994; Fischer and Oparka, 1996).

The SDs described here may be of particular importance in the circulation of auxin in the root tip. IAA moves apoplastically from cell to cell in the polar auxin transport system (Morris et al., 2004). In the root, IAA moves towards the tip in cells within the stele, and concentrates in the quiescent center cells and columella initials. It then moves outwards to the epidermal cells and basipetally to the epidermal cells in the elongation zone (Billou et al., 2005) (**Fig. 2.8**). If the cells in the stele were in the same SD as the epidermal cells, it would be difficult to maintain IAA flows in the stele and the epidermis moving in opposite directions.

During a gravitropic response, there is an asymmetric movement of auxin in the root cap towards the lower side of the root, which results in a higher concentration of auxin in the epidermis on that side (Ottenschläger et al., 2003). If the cells in the stele were in the same SD as the epidermal cells, it would be difficult to establish and maintain any significant auxin gradient across the root. One would predict that PD must be blocked towards IAA movement at the stele/cortex and cortex/epidermis boundaries, the very places where LYCH movement through PD is restricted (**Fig. 2.8**). The loss of these SD boundaries in the presence of CPZ would therefore be expected to interfere with gravitropism, since the maintenance of asymmetric auxin concentrations across the root would be difficult. As shown in **Fig. 2.7**, a concentration of CPZ that causes a severe depletion of callose in the root also disrupts gravitropism, without completely inhibiting root growth.

Figure 2.1. Permeability of *Arabidopsis* root membranes to different fluorescent dyes. Confocal (BioRad) optical longitudinal sections through center of the root. **A.** CF movement into the root meristem after cotyledon loading of 188 μM CFDA for 4 h. **B.** Autofluorescence, no dye. (The autofluorescence in the young cortical layers is only observed when using the BioRad confocal microscope at maximum gain.) **C,D.** Direct application of (**C**) 4.8 mM LYCH and (**D**) 150 μM CF to root tip for 2h. (LYCH observed at maximum gain.) Root meristem cells were not permeable to LYCH, but some were permeable to CF.

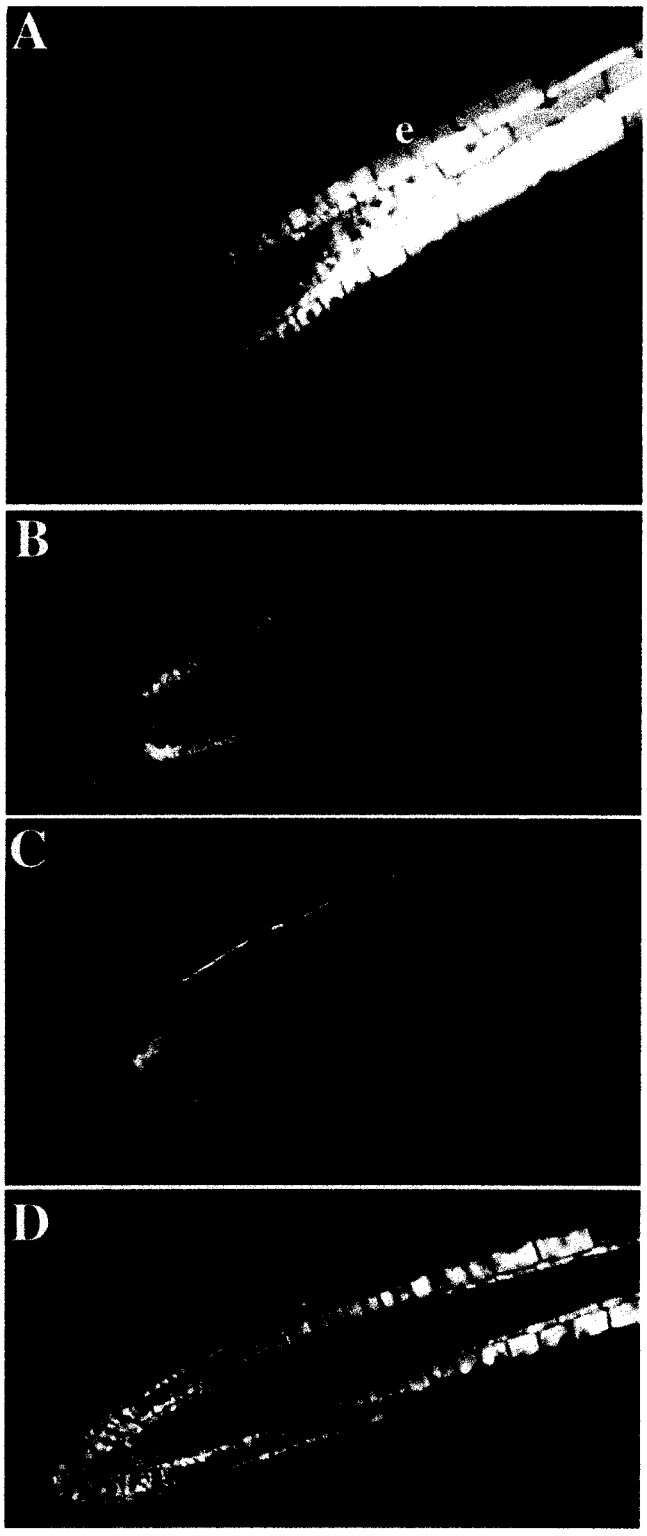
A
e
B
C
D

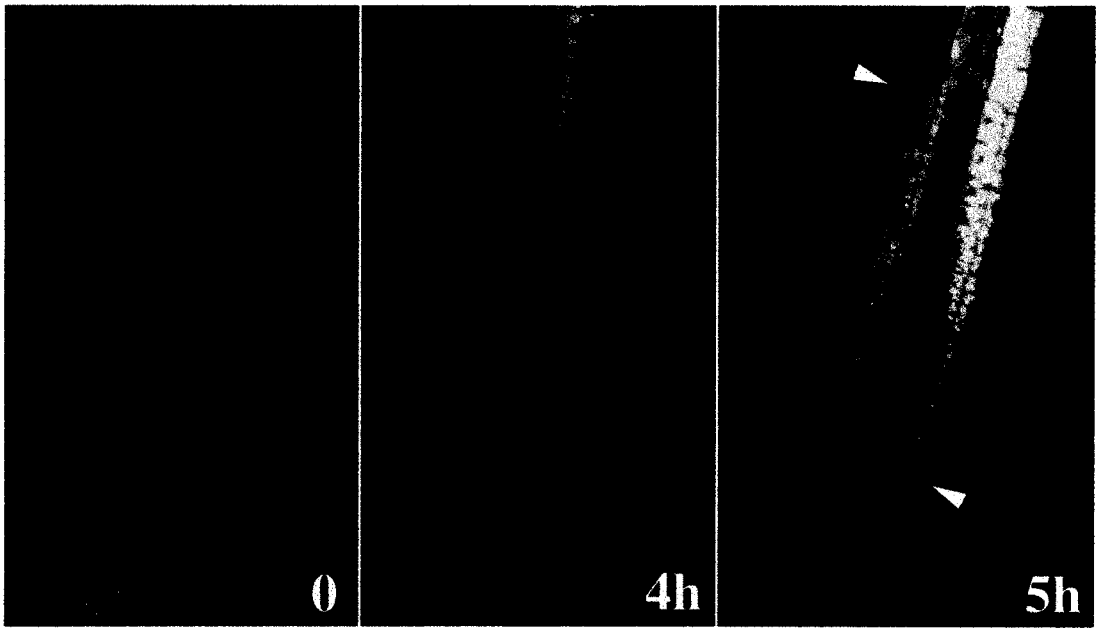

Figure 2.2. LYCH movement after cotyledon loading, 4.8 mM. Confocal (Leica) optical longitudinal sections through center of the root. Autofluorescence (no dye), 4h and 5h after loading. LYCH moved from the phloem and into the cortex and endodermis. Its movement into the epidermis, quiescent center, central stele and root cap was largely restricted. Significant fluorescence beyond the background was not observed prior to the appearance of these symplastic domains.

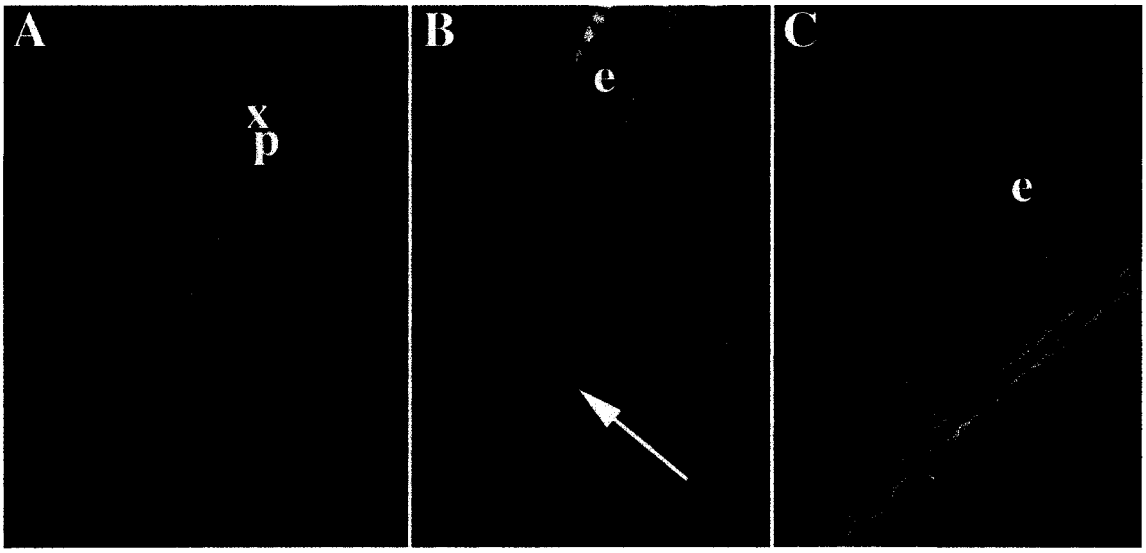

Figure 2.3. LYCH movement after cotyledon loading for 24 h (4.8 mM). Confocal (Leica) optical longitudinal sections through center of root, dual excitation of LYCH and propidium iodide. LYCH appears green; propidium iodide, red. **A.** Mature section of root. Xylem (X) fluoresces red; phloem strand (P) shows accumulation of LYCH. LYCH is clearly moving in the phloem, and not in the xylem. **B.** Even after 24 hours, while some movement of the dye into restricted areas was observed, they still contained much less dye than the cortex and endodermis. **C.** Even in mature regions of the root, there was a clear difference between the amount of LYCH in the cortex and in the epidermis. The regions of the root tip shown in (**B**) and (**C**) are denoted with white arrowheads in Figure 2.2. The white arrow in (**B**) points to quiescent center cells. e=epidermis; c=cortex.

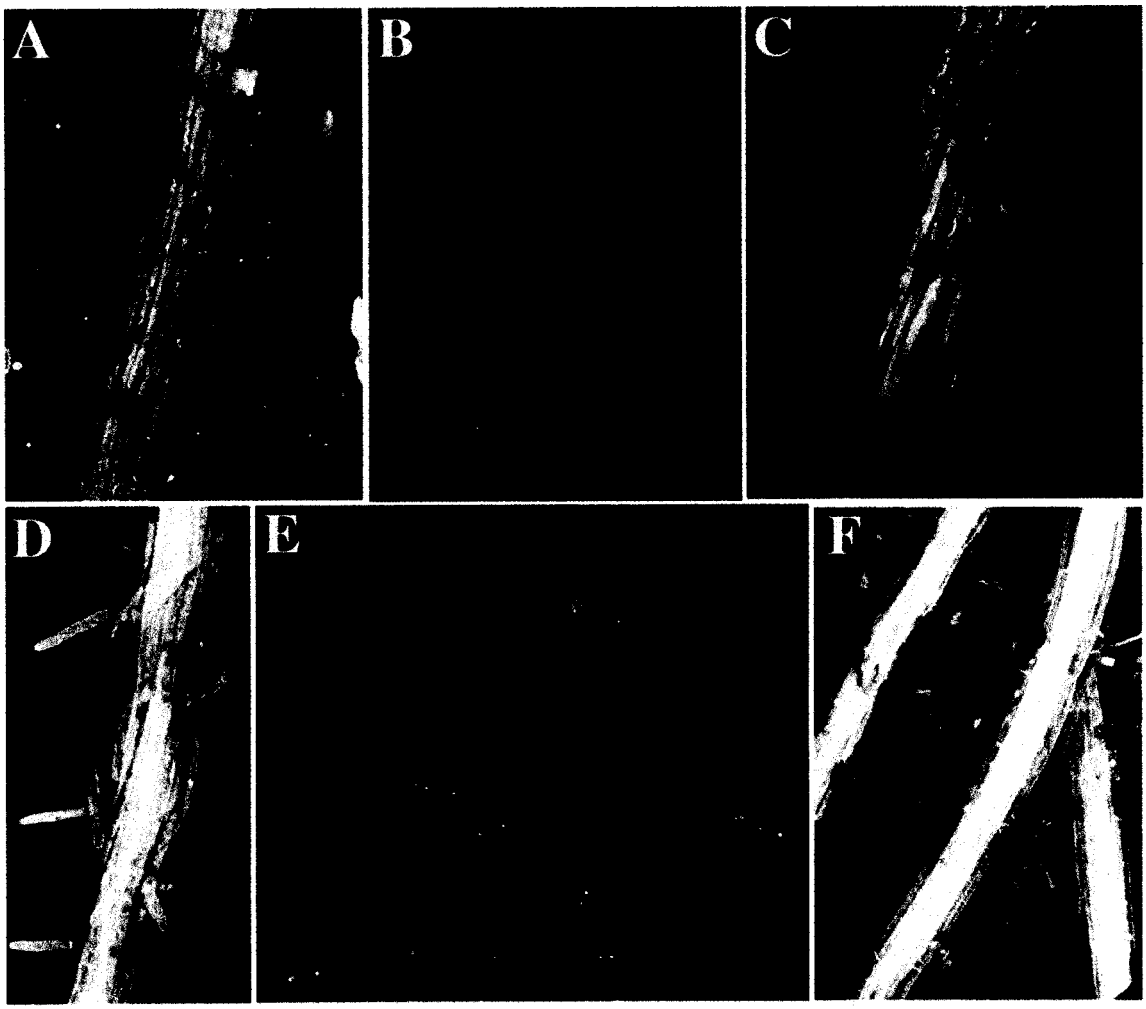

Figure 2.4. Effectiveness of putative callose synthesis inhibitors on stress-induced callose synthesis. Confocal (BioRad) images. Aniline blue labeling of callose. Optical longitudinal sections through epidermis of mature roots treated with: **A)** 30 μM digitonin; **B)** 30 μM digitonin + 10^{-4} M CPZ; **C)** 30 μM digitonin + 10^{-3} M DDG; **D)** 20 μM $AlCl_3$; **E)** $AlCl_3$ + 10^{-4} M CPZ; **F)** $AlCl_3$ + 10^{-3} M DDG. CPZ, but not DDG, was an effective inhibitor of stress-induced callose synthesis in the *Arabidopsis* root meristem. Controls for aniline blue staining (toluidine blue only) showed little background fluorescence (data not shown).

Figure 2.5. Reduced physiological levels of callose in the root meristem by CPZ. Antibody labeling of callose. Confocal (Leica) optical longitudinal sections through center of root. **A.** Low magnification of control root showing root meristem. White box indicates region magnified in **(B)**. **B.** White arrowhead shows phragmoplast callose; white arrow points to punctate fluorescence indicative of plasmodesmatal callose. **C.** Higher magnification of root tip from **(A)**. **D.** Low magnification of CPZ-treated root (6 X 10^{-5} M for 5 days). White box indicates region magnified in **(E)**. Treatment with CPZ resulted in a dramatic reduction of phragmoplast callose, and a complete loss of PD callose.

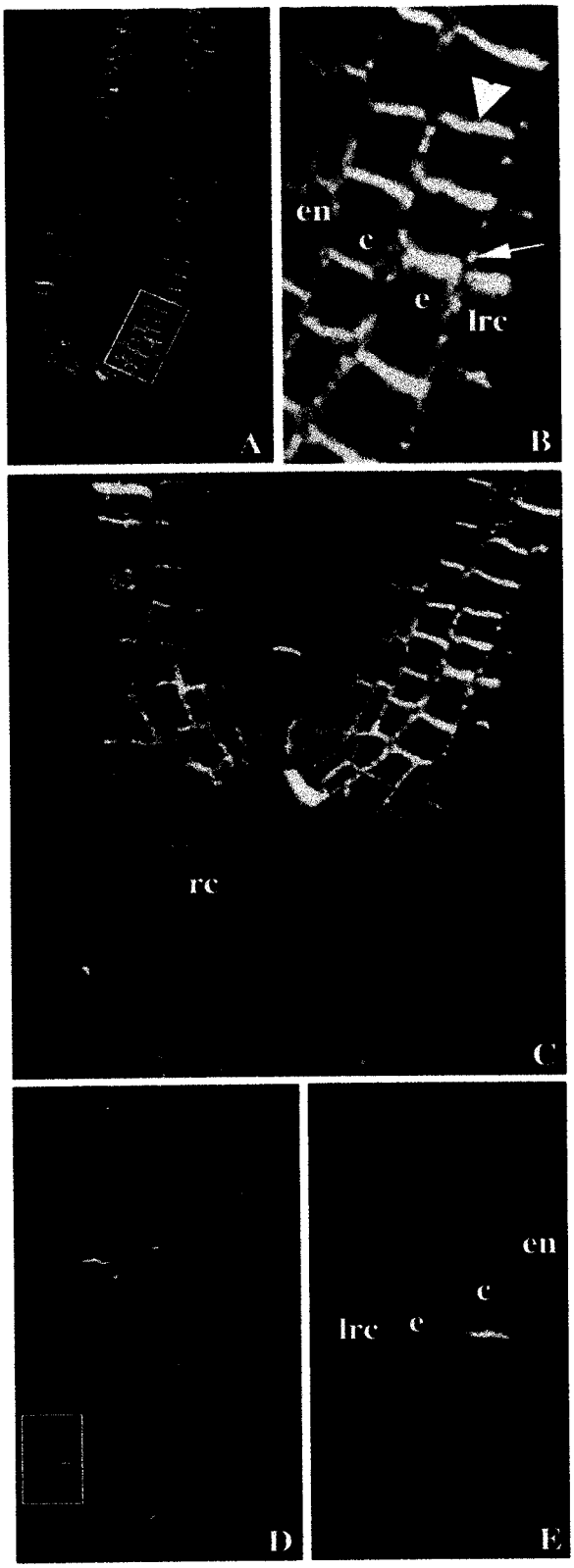
A
en
c
e
lrc
B
rc
C
D
en
c
lrc
e
E

Figure 2.6. Effects of CPZ on LYCH movement. Confocal (BioRad) optical longitudinal sections through center of root tip, 24 hr after cotyledon-loading with 1.2 mM LYCH. **A.** Control. **B,C.** 7 day pretreatment/continued treatment with $6x10^{-5}$ M CPZ. CPZ removed restrictions on LYCH movement in the root meristem.

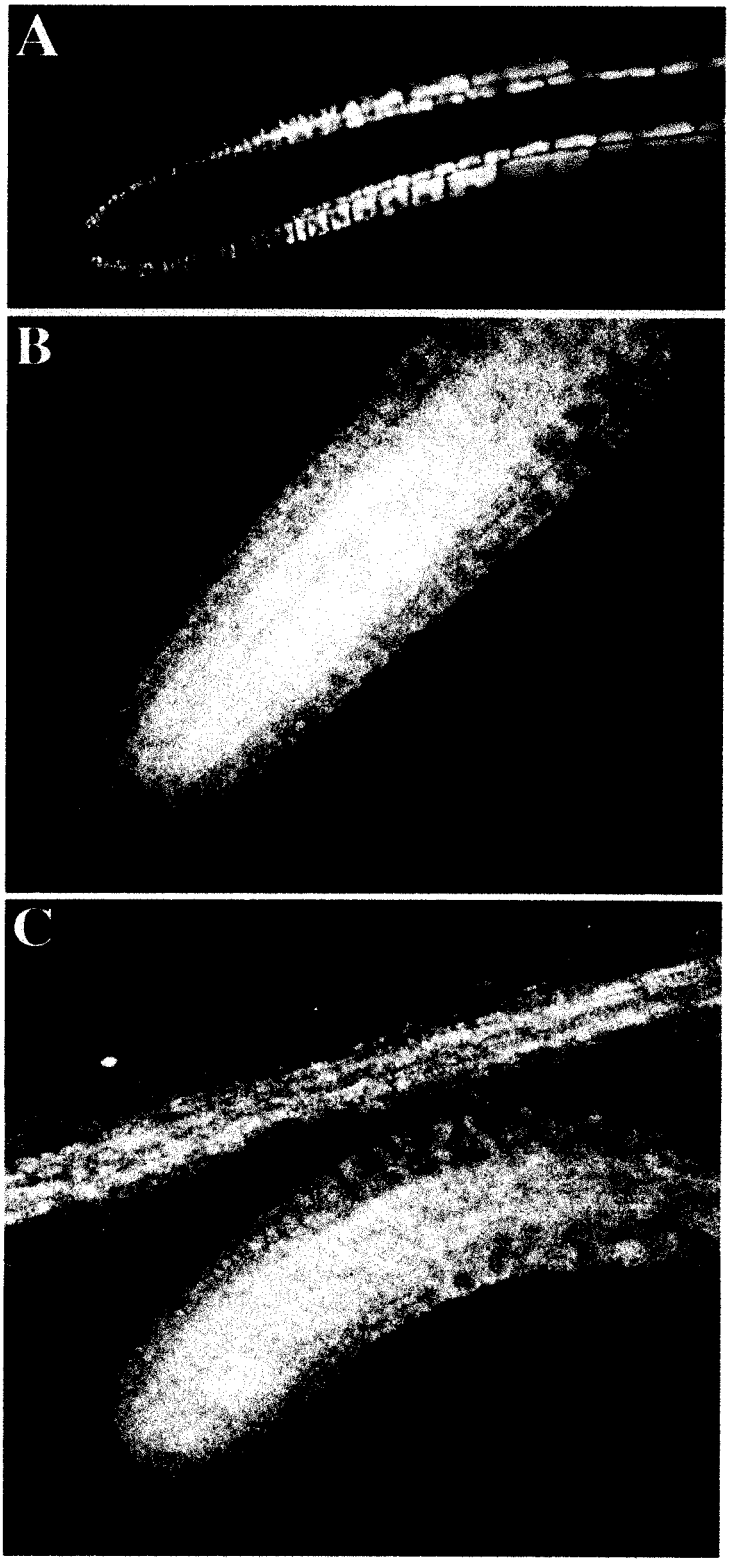
A
B
C

Figure 2.7. Effects of CPZ on root growth, branch root formation, and gravitropism. Seedlings were incubated for 7 days in from 0 up to 10^{-4} M CPZ. **A.** Length of main root and combined lengths of the lateral roots. **B.** Number of lateral roots. **C, D.** Average direction of the main root **(C)** and branch roots **(D)** from the vertical direction, and maximal deviation of the roots from the vertical.

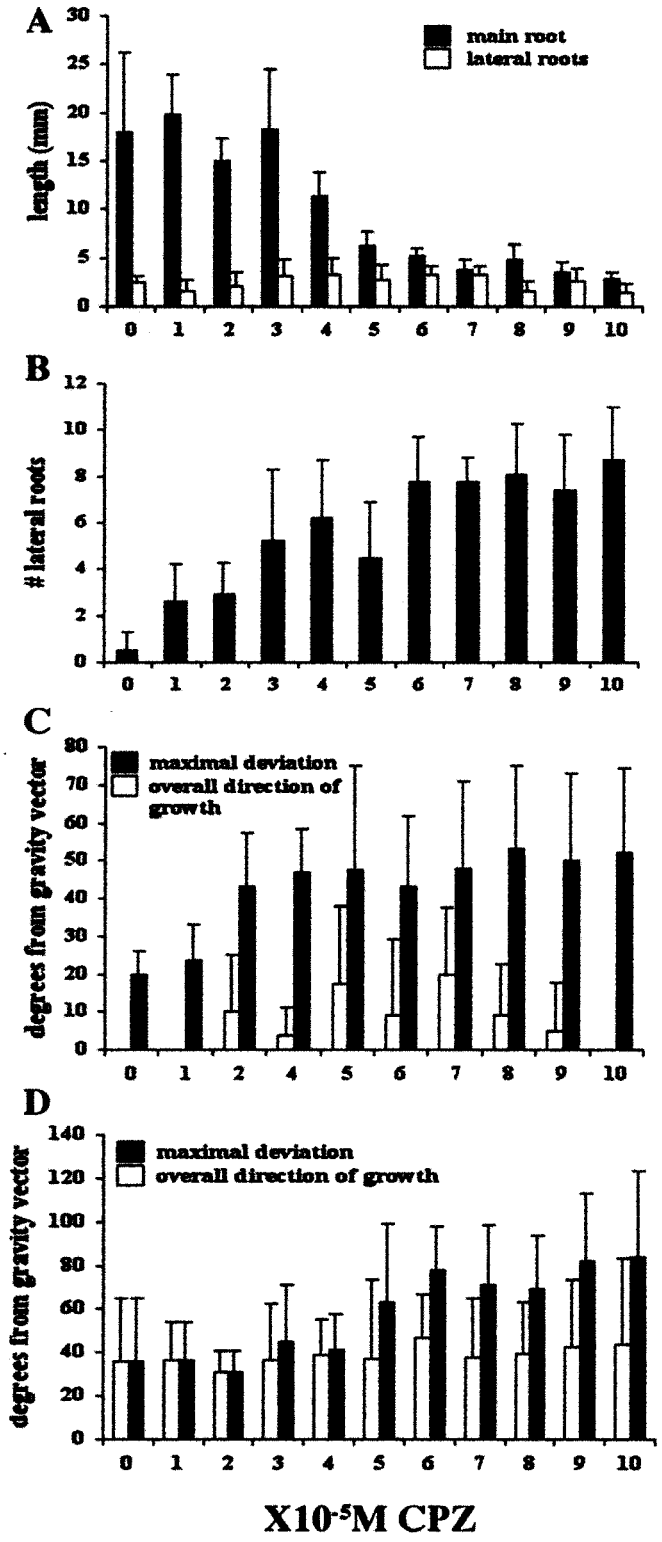
A
main root
lateral roots
length (mm)
B
lateral roots
C
maximal deviation
overall direction of growth
degrees from gravity vector
D
maximal deviation
overall direction of growth
degrees from gravity vector
X10-5M CPZ

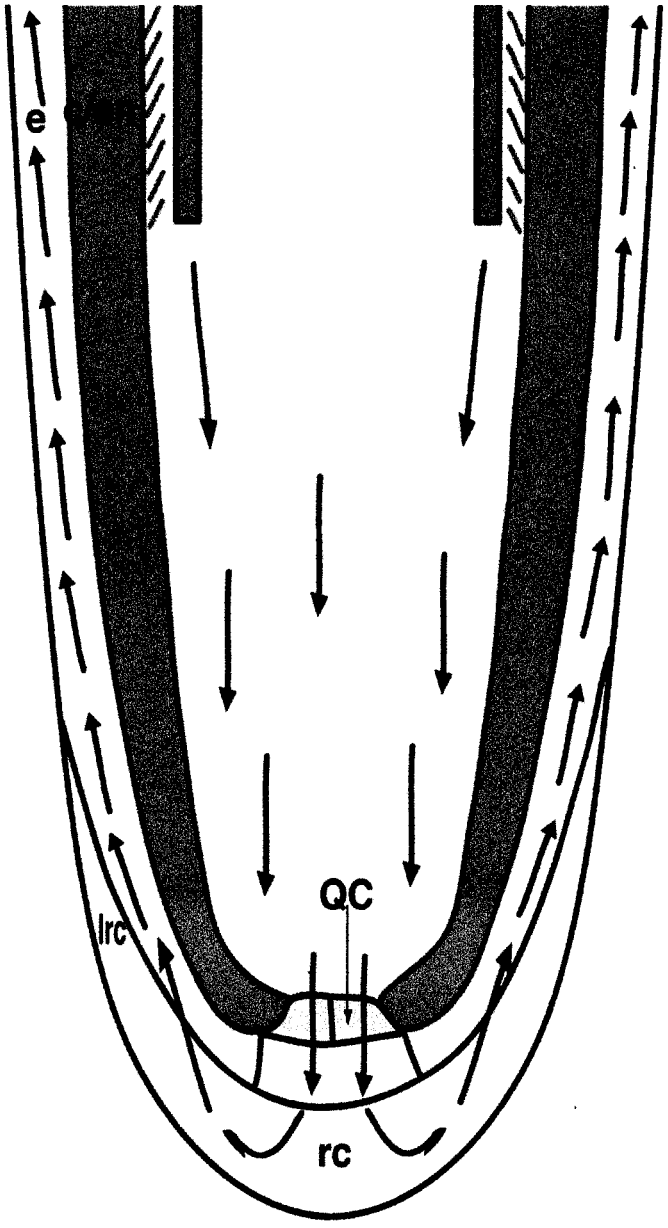

Figure 2.8. Importance of symplasmic domain boundaries for the movement of IAA in the root tip. IAA moves by polar auxin transport towards the root tip in the stele. It concentrates in the quiescent center (QC) and root cap (rc), then moves laterally to the lateral root cap (lrc) and epidermis (e) where it moves away from the tip. The boundaries of the cortical domains between the cortex and epidermis, and between the endodermis and the stele, keep the opposing auxin flows separate. c/en = cortex and endodermis.

CHAPTER 3 - INTERCELLULAR MOVEMENT OF GFP IN *ARABIDOPSIS* ROOTS - A REEXAMINATION.

Introduction

In the previous chapter, I used cotyledon-loaded Lucifer Yellow (LYCH) to demonstrate the existence of symplastic domains in the *Arabidopsis* root tip. When *Arabidopsis* seedlings were phloem-loaded with LYCH through a cut in their cotyledons, LYCH moved down through the phloem and into the roots. Upon reaching a certain distance from the root meristem corresponding to the zone of root hair formation, the dye unloaded from the phloem and moved symplastically in a predominantly apical direction, from cell to cell. This movement was mostly restricted to the cortical and endodermal cell layers. The dye showed a restricted ability to move into the epidermis, the interior of the stele, the quiescent zone and the root cap. Its ability to move faster in certain tissues, and its tendency to be restricted from other tissues, showed that the cortex and endodermis constituted a single symplastic domain.

Symplastic restrictions to movement of LYCH in the *Arabidopsis* root tip are in apparent contradiction to the finding that GFP, under control of the *AtSUC2* promoter, move between all cells of this region (Imlau et al., 1999; Roberts and Oparka, 2003). *AtSUC2* is a companion cell-specific AtSUC2 sucrose H+ symporter gene. GUS, under control of its promoter, is produced specifically in the vascular system of *Arabidopsis* (Imlau et al., 1999).

The observation that GFP is present in all cells of the *Arabidopsis* root meristem of *AtSUC2::GFP*-expressing plants has been used to conclude that symplastic domains for GFP do not exist in this organ. The presence of GFP in the phloem strands throughout the plant has led to the conclusion that the GFP protein moves from companion cells of leaves into the phloem, where it is translocated to the root meristem and other sink tissues. The movement of GFP from companion cells to phloem in source tissues is not surprising, since the SEL of PD of the phloem sieve-element-companion-cell (SE-CC) complex is believed to be quite large. But GFP movement out of the SE-CC complex and into and between cells of surrounding tissues in sinks is quite surprising. It is believed that in root meristems, the protein is unloaded from the phloem and thence diffuses freely from cell to cell, through all the plasmodesmata of the root tip. Since GFP is a 27 kDa protein, previous estimates for plasmodesmatal size exclusion limits, set at about 1 kDa (Lucas et al, 1993), have been drastically adjusted for the *Arabidopsis* root meristem. According to these conclusions, LYCH, with a molecular weight of only 453 Da, should not encounter restrictions to its symplastic movement in the *Arabidopsis* root tip.

In this chapter I describe the examination of four alternate hypotheses for the presence of GFP throughout the *Arabidopsis* root meristem: 1) the *AtSUC2* promoter is not companion cell-specific (ie. it promotes expression of GFP throughout the root tip); 2) GFP, which has a life span of 4 days, is partioned between dividing cells of developing root meristems; 3) GFP does not move symplastically between cells of the root tip, but is exocytosed into the apoplasm and subsequently endocytosed into those cells; 4) it is not the GFP protein itself that is moving, but its mRNA - in this case, the SELs between cells

of the root tip could be much lower than 27 kDa. For both hypothesis 1 and 4, the assumption is that the specific presence of GUS in the companion cells of *AtSUC2::GUS* transgenic plants is not a reliable indicator of the *AtSUC2* promoter's activity - ie. *AtSUC2::GUS* is a less sensitive reporter than *AtSUC2::GFP*.

To address the first two hypotheses, I grafted *AtSUC2::GFP*-expressing shoots onto wild-type roots and observed the real-time movement of GFP into living and fully developed root meristems using confocal microscopy. To address the third hypothesis, I isolated the GFP protein and applied it to roots externally, then used confocal miscoscopy to see it it had been taken up by root meristem cells. Finally, to address the last hypothesis, I tested for the presence of *GFP* mRNA in the root meristem cells of wild-type root systems that had been grafted on to *AtSUC2::GFP*-expressing shoots.

Materials and Methods

Plant materials and growth conditions

Wild-type: Wild-type seedlings used were *Arabidopsis thaliana*, ecotype Columbia. *AtSUC2::GFP* transgenic plants: Transgenic seedlings expressing *AtSUC2::GFP* were provided by Dr. Norbert Sauer of the University of Erlangen-Nürnberg, Germany. The production of these transgenic seedlings is described in Imlau et al., 1999. Briefly, their genetic background is *Arabidopsis thaliana C24*. They were transformed with a construct containing 2159 bp of the *AtSUC2* promoter, followed by 730 bp of the GFP coding sequence taken from pGFP-TYGpA-K (Chiu et al., 1996) and the nopaline synthase terminator.

Seeds were sterilized and sown on petri dishes as described in the previous chapter. Seedlings were also grown under the same conditions described previously.

Isolation of GFP protein and exo/endocytosis experiment

Two different types of GFP were isolated. The plasmid pGLO carries the 'cycle 3' variant of GFP described in Crameri et al., 1996. The plasmid PGREEN harbors a modified GFP variant called mGFP4, described in Haseloff, 1997. Neither of these GFP variants carries additional peptide targeting sequences, ie. they are not targeted to the endoplasmic reticulum like some other variants. For this reason, they are called 'soluble GFPs', and can move freely through the cytoplasm without being sequestered.

E. coli (DH10ß) was transformed with either the plasmid pGREEN (Carolina Biological, 21-1449) or pGLO (Bio-Rad, 166-0405). GFP was isolated using a GFP Chromatography Kit (Bio-Rad, 166-0005EDU). 6-day-old *Col-0* seedlings were treated with extracted GFP as follows: depression slides were coated with 1.2% phytagar, except for the depression, which was filled with the solution containing the extracted GFP. Seedlings were laid on the agar such that the root tips extended into the GFP solution. After 3 h, the depression was refilled with distilled water, and the root tips were left to rinse for 1 h. The root tips of the intact seedlings were examined using the confocal microscope.

Micrografting

Grafting was adopted from techniques described in Turnbull et al., 2002. 6 day-old seedlings for both wild-type *Col-0* and the transgenic line expressing *AtSUC2::GFP*

were laid out on petri plates containing 1.2% phytagar. The shoots of the seedlings (in this paper referred to as scions) were excised from their root systems by making a straight, clean cut across the middle of the hypocotyl. Using forceps, the cut surfaces of the excised shoots of the transgenic seedlings were positioned above the cut surfaces of the excised roots of the wild-type seedlings (in this paper referred to as stocks), and the two were gently but firmly pressed together. After 3-4 days, success of the graft was determined by gently trying to pull the shoots and roots apart; if the graft held, the root system of the seedling was then examined.

Confocal Microscopy

The confocal microscope used was a Leica SP1/MP. For the exo/endocytosis experiment, the microscope was set at an excitation of 488 nm for GFP. For observations of GFP fluorescence in micrografted roots, it was set at a dual excitation of 488 nm and 561 nm for propidium iodide. In this case, seedlings were immersed in a 0.01 mg/mL solution of propidium iodide (PI) (Molecular Probes, P-1304) for approximately one minute prior to mounting in distilled water. The dual excitation allowed for the visualization of both cell wall fluorescence and GFP fluorescence in separate channels.

RT-PCR analysis

RNA was isolated from the roots of *Arabidopsis Col-0*, from the roots of *AtSUC2::GFP*shoot/wild-type root grafts, and from the leaves of *AtSUC2::GFP* transgenic plants. RNA was isolated using the RNeasy Plant Mini Kit (Qiagen, Valencia, CA) and treated with DNaseI Amp grade (Gibco BRL). First-strand cDNA was

synthesized from 2 μg of RNA with random hexamer primers using the ThermoScript reverse transcriptase–mediated PCR system (Gibco BRL) according to the manufacturer's instructions. The GFP variant used in these experiments, also known as sGFP, is from plasmid blue-sGFP-TYG-nos KS. PCR was performed with 2 μL of the first-strand reaction using gene-specific primers to sGFP (5'-TCAGCCGCTACCCCGACCAC-3'; 5'-CGCTGCCGTCCTCGATGTTG-3'). As a control, gene-specific primers were also used to amplify endogenous *ACT2* (5'-GCCATCCAAGCTGTTCTCTC-3'; 5'-GCTCGTAGTCAACAGCAACAA-3'). The PCR program used was as follows: 95^{0}C for 2 min; (94^{0}C for 20s, 73^{0}C - 1^{0}C per cycle for 30s, 72^{0}C for 1 min) X 8 cycles; (94^{0}C for 20 s, 65^{0}C for 30s, 72^{0}C for 1 min) X 45 cycles; 72^{0}C for 5 min.

Probe Synthesis for In Situ Hybridization

Probe to GFP was made by amplifying 315 bp from the genomic DNA of an *AtSUC2::GFP* expressing plant that had been isolated using a FastDNA kit (Q-Biogene) and treated with RNase A (Gibco BRL). The GFP gene-specific primers and PCR program used were the same as described above for RT-PCR analysis. The PCR product was inserted into a TOPO TA vector with a dual promoter (Invitrogen 45-0640). Insertion and subsequent transformation of *E. coli*, recovery and plating were performed as per the kit's instructions. Plasmids were isolated using a Qiagen miniprep kit (27104).

Plasmids were digested with either BamHI or Xho1. Linearized plasmids were purified again using the Qiagen miniprep kit. Probes were synthesized in 25 μL reactions at 37°C for 2 h using either T7 or Sp6 RNA polymerase for the antisense probe and the sense control, respectively (a Promega P1440 kit was used with digoxigenin RNA

labeling mix from Roche). Probes were then treated with 2 μL RQ1 RNase-free DNase, and incubated at 37°C for 15 min. The reaction was stopped with 1 μL 0.5 M EDTA, and the probe was precipitated by adding 2 μL yeast tRNA (10 μg/μL), 40 μL 5 M NH_4OAc, 33 μL DEPC water and 250 μL ethanol for 1 h. Probe was stored at -20°C.

Paraffin Embedment/Preparation for In Situ Hybridization

AtSUC2::GFP shoot/wild-type root grafts were allowed to develop for 1 week following the establishment of the graft. Care was taken to excise any adventitious roots developing from the scion. Both grafts and 10 day-old *Col-0* wild-type seedlings were then fixed for 1 h, whole in FAA (10% formalin/50% ethanol/5% acetic acid). The tissue was then put through a dehydration series at room temperature, using the following percentages of ethanol and treatments of 1 h each: 50, 60, 70, 85, 95 + 0.1% eosin Y (Sigma E4009). They were then treated with 100% ethanol for 30 min (2X) and for 60 min (2X), and then the following ratios of histoclear II (National Diagnostics HS-202)/ethanol for 1h each: 1:3, 1:1, 3:1, 1:0 (2X).

Seedlings were embedded in paraplast (Fisher 23-021-401) by putting in falcon tubes containing 1/4 volume histoclear and 3/4 volume paraplast chips at 60°C until the chips were melted; the solution was then replaced with pure melted paraplast at 60°C overnight, and changed twice daily with pure melted paraplast for 4 more days. Paraplast was then allowed to solidify at room temperature. 0.5 μm sections were cut on a microtome (Leica RM2165) and put into DEPC water on slides (ProbeON PLUS, Fisher Scientific 15-188-52). The slides were baked at 50°C overnight.

Slides were dewaxed using 2 treatments of histoclear for 10 min each. They were hydrated by treating with 100% ethanol for 1 min (2X), 95% ethanol for 30 s, and then the following percentages of ethanol in 0.85% NaCl for 30 s each: 85, 70, 50, 30. They were then put in 0.85% NaCl for 2 min, 0.2M HCl for 20 min, DEPC water for 5 min, and PBS for 2 min.

Slides were put through a protease digestion by incubating in a solution of proteinase K (Invitrogen 25530-049) (10 μL in 50 mM Tris, 5 mM EDTA, pH 7.5) for 30 min at 37°C. They were then put through the following series: PBS/0.2% glycine for 2 min, PBS for 2 min, 3.7% formaldehyde in PBS for 10 min, PBS for 2 min (2X), 0.85% NaCl for 2 min.

Slides were then put through a dehydration series using the following pecentages of ethanol in 0.85% NaCl for 30 s each: 30, 50, 70ethanol, 85, 95. They were then treated with 100% ethanol for 1 min (2X). After drying, they were immediately used for in situ hybridization.

In situ hybridization

The probe was centrifuged for 30 min at 11,200 rpm at 4°C, washed in cold 75% ethanol and centrifuged for 15 min at 9,900 rpm at 4°C. After air-drying, it was suspended in 50 μL DEPC water.

Probes were heated to 80°C for 2 min, and then were diluted 1/50 in a solution of 6X SSC, 3% SDS, 50% formamide, 100μg/mL tRNA. The probe was then kept at 50°C.

Labeling was done 2 slides at a time by adding 250 μL of diluted probe to one slide on a 50°C slide warmer and lowering a second slide, face down, on top.

Slides were put in a prewarmed (53°C) humidified container lined on the bottom with Kimwipes saturated in 2X SSC and 50% formamide. They were kept at 53°C overnight. The next day, they were separated in prewarmed 50% formamide/2X SSC and then washed in 50% formamide/2X SSC at 50°C (2X 90 min each).

After 5 min in TBS, they were put in blocking buffer [TBS/0.5% block reagent (Roche)] for 1 h, antibody (Ab) buffer (TBS/1% BSA/ 0.3% triton X-100) for 30 min, anti-DIG AP-conjugated Ab (diluted 1:3000 with Ab buffer) for 90 min and then washed 3 times with Ab buffer for 20 min each. They were then treated with detection buffer (0.1 M Tris, 0.1 M NaCl, 0.05 M $MgCl_2$) for 5 min and then put into 1% NBT + BCIP (Roche) in detection buffer, in the dark, for 5 days. (Detection buffer and NBT/BCIP was replaced once during this time.)

Before photographing, slides were washed three times with water (30 s each). They were viewed with a light microscope (Olympus BX51) and photographed with a Kodak MDS 290 camera.

Results

External application of GFP

When observed under the confocal microscope, no fluorescence above background was seen in the GFP-treated roots, for either of the GFP variants tested (data

not shown). GFP is thus not capable of being endocytosed into root meristems through the epidermis.

GFP fluorescence in micrografted roots

Grafts between shoots expressing *AtSUC2::GFP* and wild-type roots took 3-4 days to develop (**Fig.3.1A**). The success of the graft was assessed by gently pulling on the hypocotyl - successful grafts remained intact. Care was taken to make sure that the stock and scion were not merely being held together by adventitious root growth from the scion. Any additional roots growing from the *AtSUC2::GFP*-expressing scion were excised. As soon as the graft had developed, the roots were observed using confocal microscopy. A strong fluorescent signal for GFP was detected in the phloem of the root stock, as reported in previous studies (**Fig. 3.1B**). This GFP must have moved from the scion into the stock. GFP was found in all cells of the stock root meristems. If observed at 3-4 days after the graft attempt, ie. soon after the graft took hold, root meristems showed a strong signal in all the cells of the stele; however, the signal detected in cells exterior to the pericycle was much less than for roots from *AtSUC2::GFP* transgenic plants (**Fig. 3.1C,D**). In many cases, the signal in such cells was so faint as to barely be visible. If observed a couple of days later, grafted wild-type roots more closely resembled those of the wild-type plants (data not shown). This indicates that in the root meristem, the apparent movement of GFP out of the stele and into surrounding tissues is slow.

GFP mRNA movement in micrografted roots

Using RT-PCR, I looked for the presence of GFP mRNA in wild-type roots which had been grafted onto *AtSUC2::GFP*-expressing shoots. Grafts were allowed to grow for several days; care was taken to excise any adventitious roots developing from the *AtSUC2::GFP*-expressing scion. Wild-type roots showed the presence of GFP mRNA (**Fig. 3.2**).

I fixed and embedded some of these grafted wild-type roots, and performed in situ hybridization using a probe for GFP mRNA. As a control for the probe, I also looked at the *AtSUC2::GFP*-expressing scions. As expected, in the scions of the grafts, a strong signal for GFP mRNA was found exclusively in the companion cells (data not shown). Surprisingly, a very strong signal for GFP mRNA was also found in all cells of the wild-type root meristems (**Fig. 3.3**). GFP mRNA must thus be moving between PD of the root meristem cells. While I cannot discount the possibility that both GFP protein and GFP mRNA are moving through PD of these cells, it is possible that only the mRNA is moving out of the phloem-companion cell complex and into and between other cells of the root meristem. This mRNA movement, and not the movement of the GFP protein itself, may be the explanation for the fluorescent GFP signal seen throughout the root meristem in this and in previous studies.

I am currently replicating this experiment with the inclusion of two other controls: wild-type shoots and roots in which we would expect to find no GFP mRNA, and roots from *AtSUC2::GFP* plants, which I would expect to show a similar GFP mRNA distribution to the grafted wild-type roots. Future experiments should also be done to look at GFP mRNA movement in wild-type roots grafted to plants expressing GFP

fusions such as *AtSUC2::GFP-Ubi*. GFP-Ubi is a fusion protein that combines GFP with ubiquitin, increasing its mass from 27 to 36 kDa. GFP fluorescence in the roots of such plants has been found to be limited to the phloem in roots (Stadler et al., 2005). I would hypothesize that *GFP-Ubi* mRNA is too large to move through root meristem PD in these plants.

Discussion

In chapter 2, I showed the existence of symplastic domains in the *Arabidopsis* root meristem using a small fluorescent tracer dye, Lucifer Yellow (LYCH). LYCH, a molecule of 453 Da, could not move through PD into the epidermis, root cap, quiescent center and stele inner to the phloem. Findings in the literature show the apparent unrestricted symplastic movement of the 27 kDa GFP protein between cells of these same tissues. The Stokes radius, and not the molecular mass of a molecule or macromolecule is really the ideal measurement to work with when trying to assess the SEL of PD. GFP is a very compact, barrel-shaped protein, with a Stokes radius of only 2.82 nm (Terry et al., 1995). It can thus cross PD that will not allow a 5 kDa dextran, with a larger diameter, to cross (Wyner et al., 2001). However the Stokes radius for LYCH is estimated to be around 0.75 nm (Waigmann et al., 1994) - smaller than that of GFP. My findings that LYCH could not move through the PD of tissues where GFP had been shown to have free intercellular movement, thus presented a conundrum.

Previous conclusions that PD in the root meristem do not exclude the GFP protein have been made from the observation that while GUS is found exclusively in the

companion cells of *AtSUC2::GUS* plants, GFP fluorescence is found throughout the *Arabidopsis* root meristem when its gene is expressed under the control of the same promoter. I reexamined the symplastic movement of GFP in the *Arabidopsis* root organism by addressing four alternative possibilities for this observation: 1) GFP may be crossing plasma membranes in the root meristem; 2) GFP may be expressed in all cells of the root meristem; 3) GFP may be partitioned between cells during root meristem formation; 4) GFP mRNA may be moving between cells of the root meristem.

I discounted the possibility that GFP was crossing plasma membranes, ie. moving out of and into cells by exocytosis and endocytosis, by purifying two different variants of soluble GFP, and externally applying the protein to *Arabidopsis* root tips. I found that unlike symplastic tracer dyes such as carboxyfluorescein and HPTS-acetate, the isolated GFP protein was not capable of entering *Arabidopsis* root meristems when applied in this manner. It was not surprising that GFP was not endocytosed into root meristem cells at any detectable level. It has been shown in the past that while HeLa cells take up a small amount of externally applied GFP, detectable by flow cytometry, they do not take up so much that it can be detected with either Western blot analysis or confocal microscopy (Ryu et al., 2003).

GFP is an extremely stable and long-lived protein. It has been reported to be as stable as proteins which persist in mammalian cell culture for up to 50 h (Sheen et al., 1995). This is more than enough time for a root meristem to develop and elongate by several centimeters. The possibility existed that the GFP observed in the root meristem of *AtSUC2::GFP* transgenic plants did not move from cell to cell through PD, but was partitioned between dividing cells during root meristem formation.

Another uncertainty about the movement of GFP through PD was raised from conflicting results in the literature about its ability to move between cells of the *Arabidopsis* root tip. Restrictions in GFP movement have been shown for soluble GFP under the control of a different promoter other than that for *AtSUC2*. When expressed under the control of the *Sultr1;1* promoter, GFP is detectable in the lateral root cap of root tips, but is reported to be absent from the endodermis and central cylinder of all root sections examined (Takahashi et al., 2000). While studies looking at GFP movement have used promoter driven GUS expression as controls to show cell-specific gene expression, this control assumes that GUS under the control of the *AtSUC2* promoter is as sensitive a reporter as GFP. Taken with the conflicting results from Takahashi et al., 2000, the possibility did thus exist that when under the control of the *AtSUC2* promoter but not the *Sultr1;1* promoter, the gene for GFP was being expressed in all cells of the *Arabidopsis* root tip. If so, *AtSUC2::GUS* may simply too weak a reporter to accurately reflect the expression pattern for this promoter.

Both possibilities were examined by grafting shoots from *AtSUC2::GFP* transgenic plants onto wild-type roots, and observing the subsequent movement into the root meristems. Since the root meristems were fully developed at the time of grafting, GFP could not be partitioned between dividing cells. Also, since the roots were genetically wild-type, they would not show any additional GFP as a result of gene expression. I found GFP in all cells of the root meristem, discounting both of these alternative hypotheses.

I did notice, however, that while there was a very strong GFP signal in the stele of the grafted roots, in comparison to the roots of *AtSUC2::GFP* transgenic plants, there

was much less GFP in cells outside of the stele. The implication is that the movement of GFP protein or its mRNA moves much more quickly between cells of the stele than it moves out of the stele. A similar slow rate of GFP movement has been shown in *Nicotiana benth.* by Liarzi and Epel (2005). A possibility then exists that all cells in the root tip contain PD that have a much larger SEL than the bulk of the PD. These PD are either very low in number, or by some other nature permit only extremely slow movement of GFP from cell to cell. This would be consistent with the very low coupling ratios that have been found for membrane potentials between adjacent cells (Holdaway-Clarke, 2005). It would also explain the discrepancies between my results for LYCH and those found using GFP as a symplastic tracer.

One last possibility I wanted to examine was that GFP mRNA, and not the GFP protein was moving through the PD. If it was the mRNA and not the 27 kDa protein moving, this would mean that the SEL of cells in the root meristem could be much smaller than previously thought. RT-PCR showed that GFP mRNA was indeed present in the wild-type root stocks when grafted to AtSUC2::GFP-expressing scions. This is not necessarily surprising. If we assume that sieve elements lack the ability to translate mRNA, then GFP protein must be able to move between companion cells and sieve elements, because strong GFP fluorescence is present in the phloem. If the protein can move through these PD, the much smaller mRNA should also be able to move into the sieve elements, and be translocated into the wild-type roots.

The important question is, what is moving out of the SE-CC complex? In situ hybridization reveals that GFP mRNA is moving out of this complex, into and between all cells of the root meristem. It is quite possible that the mRNA is then translated into

GFP protein inside these cells. It must be pointed out that I have not discerned whether or not both GFP protein and its mRNA are moving between the PD of root meristems of *AtSUC2::GFP* plants, or whether it is only the mRNA. If the GFP protein is also moving, it would not be surprising that the smaller GFP mRNA can move between the PD. But importantly, these studies introduce the possibility that only GFP mRNA is moving through PD of the root meristem, in which case their newly adopted SEL of 27 kDa may be a gross overestimate.

It has been shown that when ER-targeted GFP is expressed in root meristems under the control of tissue-specific promoters, its signal retains specificity - ie. the GFP or its mRNA does appear not move from cell to cell. Why can GFP mRNA, but not GFP-ER mRNA move? There are a number of possible explanations. Perhaps the GFP-ER mRNA does move, but the GFP signal for this variant is too weak to see in other tissues. Perhaps the retention signal (an additional 78 base pairs) makes the GFP mRNA larger than a certain cut-off point for free movement through PD, or signals the PD to actively preclude passage of the mRNA.

These studies shed new light onto previous conclusions drawn from the observations of GFP fluorescence in root meristems. It is possible that the SEL of PD in the root meristem, newly adjusted to 27 kDa for that of GFP protein, is in fact smaller, of the size which would allow the passage of GFP mRNA. It is possible that this movement of mRNA is quite slow out of the stele, and that this movement occurs through a second type of PD that occurs at a very low frequency and that has an SEL larger than that which allows the free passage of LYCH. Because this type of PD does not appear to permit the

passage of LYCH, it is also possible that by some unknown mechanism, they are mRNA specific.

Our studies indicate that two types of PD exist in the *Arabidopsis* root meristem. The first type has an SEL that allows for the rapid diffusion of the small fluorescent dye LYCH. These PD are either not present, are present at a low density, or are present but constricted in the epidermal, root cap and stelar tissues. They are likely the PD through which sucrose moves following phloem unloading. In order to explain the observations that GFP mRNA can move into and throughout the stele where LYCH cannot, a second type of PD must exist in tissues of the root meristem that allows for the movement of mRNA but not other small molecules. Possibly, these PD are normally selective for different endogenous mRNAs, but GFP mRNA is so small that it can successfully navigate the system. Since GFP moves quickly throughout the stele, but very slowly throughout extra-stelar tissues, such PD must also differ in nature depending on their localization in the root meristem.

The mechanism by which macromolecules traffick from cell to cell through PD is still largely unknown. While transcription factors such as the floral identity protein LEAFY have been shown to move from the L1 layer of the shoot meristem to underlying layers by simple, non-regulated diffusion (Wu et al., 2003), in some tissues, proteins and mRNA seem to require special domains for trafficking, implying an active mechanism. For example, the KNOX homeodomain is necessary for the trafficking of the KNOTTED protein and its mRNA. Fusing this domain to the cell autonomous protein GLABROUS1 confers it the ability to move through PD (Kim et al., 2006).

It has been proposed that the large SEL found in the PD between cells of meristematic tissues is important because these tissues are undergoing rapid growth (Imlau et al., 1999) - increased cellular connectivity may thus be necessary to permit the rapid symplastic movement of sucrose, necessary for energy. But growth is only one of two important phenomena that occur in meristems - differentiation is also a key function of this specialized complex tissue. Perhaps the large SEL in sink tissues indicated by GFP studies is in fact indicative of a specialized type of PD necessary for the selective symplastic movement of RNA. This regulated intercellular movement of specific RNAs may be important for cellular identity.

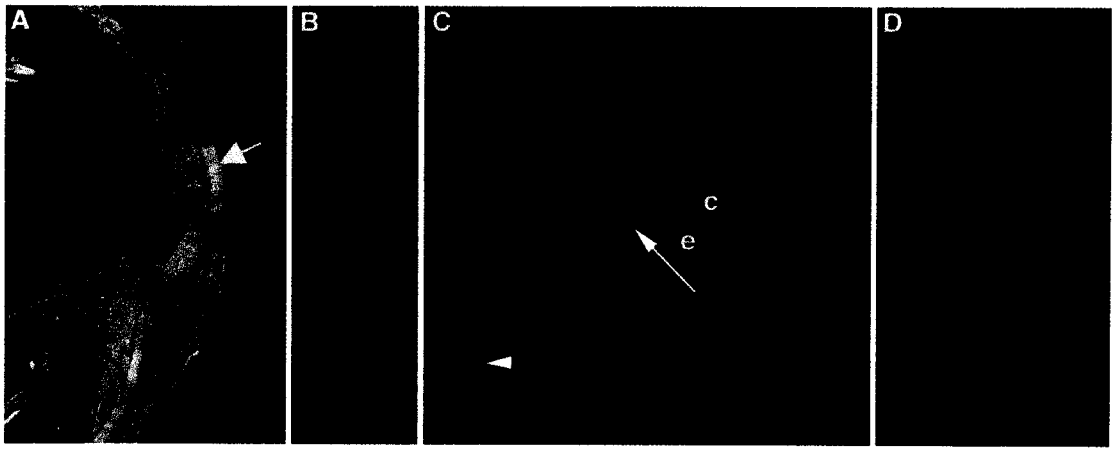

Figure 3.1. GFP movement in *Col-0* roots of grafts, compared to *AtSUC2:GFP* roots. **A.** Graft of *AtSUC2:GFP* shoot onto *Col-0* root. Black arrowhead indicates location of graft. White arrow points to an adventitious root growing out of the *AtSUC2:GFP* shoot; such roots were excised. **B-D.** Confocal optical longitudinal sections through **(B,C)** wild-type *Col-0* roots grafted onto *AtSUC2:GFP* shoots and **(D)** an *AtSUC2:GFP* root. **B.** GFP moves in the twin phloem strands of the root. **C.** GFP movement out of the stele and into the cortex (c) and epidermis (e) is slow. This restriction in movement is not apparent if observing *AtSUC2:GFP* roots **(D)**. White arrow in **(C)** indicates estimated location of end of mature phloem. White arrowhead indicates location of quiescent center.

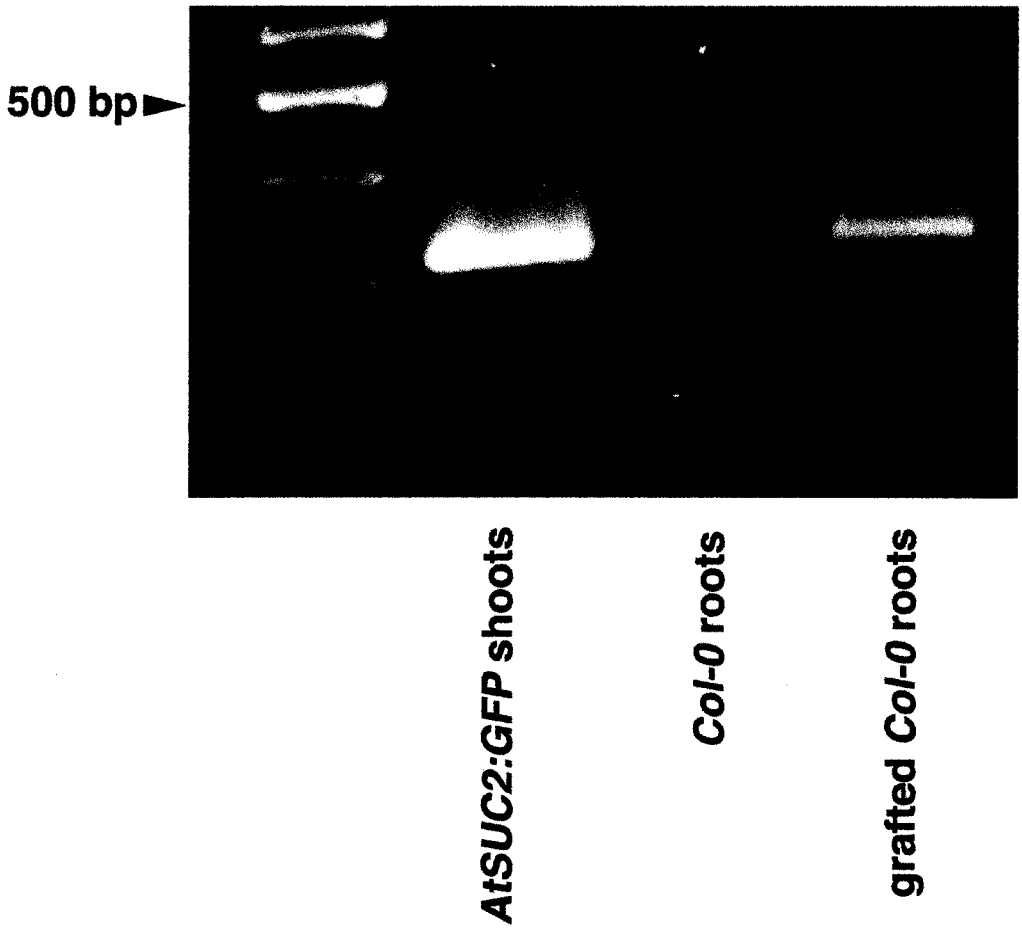

Figure 3.2. RT-PCR analysis of *GFP* expression in *AtSUC2:GFP* and *Col-0* plants, and in *Col-0* roots grafted onto *AtSUC2:GFP* shoots. Actin controls were also performed on RNA, in separate reactions (data not shown). The *GFP* transcript, absent in wild-type Col-0 roots, was found to be present in both *AtSUC2:GFP* shoots as well as *Col-0* roots that had been grafted to *AtSUC2:GFP* shoots.

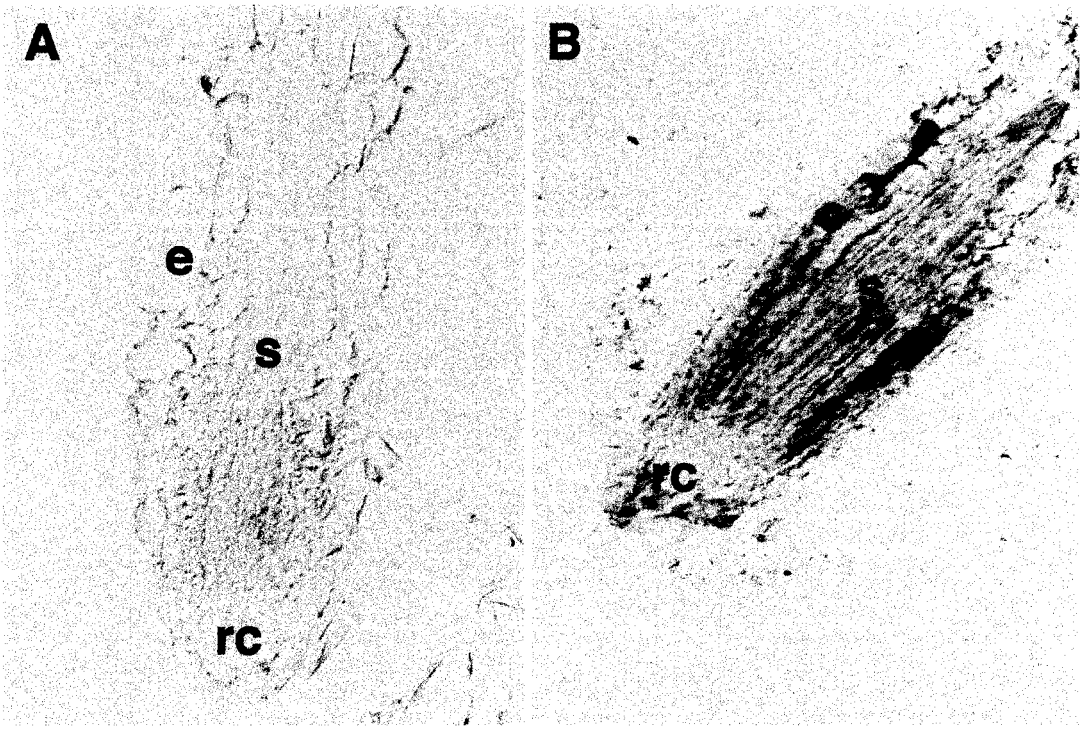

Figure 3.3. In situ hybridization analysis for GFP mRNA. Root meristems from wild-type roots grafted onto *AtSUC2:GFP* transgenic shoots. **A)** sense control. **B)** anti-sense probe. GFP mRNA is found throughout the grafted wild-type root meristems.

CHAPTER 4 - CONSTRUCTION AND PRELIMINARY SCREENING OF A CALLOSE SYNTHASE MUTANT LIBRARY

Introduction

The β-1,3-glucan in the fungal cell wall is synthesized by a complex in which *FKS1* or *FKS2* encodes the catalytic subunit (Douglas *et al.*, 1994; Schimoler-O'Rourke *et al.*, 2003). A homologous gene in barley, *HvGSL1*, has been shown to encode a protein linked to callose production (Li *et al.*, 2003). A putative callose synthase cDNA, *CFL1*, was cloned from cotton and found to be expressed in seed epidermal cells (Cui *et al.*, 2001). Two tobacco callose synthase genes, *NaGSL1* and *NaGSL2,* have been shown to be expressed in pollen tubes and in immature floral organs, respectively (Doblin *et al.*, 2001). A callose synthase gene, *GSL6*, was recently cloned in *Arabidopsis*, and its corresponding protein shown to localize to forming cell plates in dividing transgenic tobacco cells (Hong *et al.*, 2001). Through sequence similarity, 12 putative callose synthases (GSL1-12) have been identified in *Arabidopsis* (Hong *et al*, 2001); the genes for these proteins were also annotated independently by a group in Stanford (http://cellwall.stanford.edu/php/structure.php?family=gsl) (**Fig. 4.1**). The phylogenetic relationship between the genes has shown that many are closely related (**Fig. 4.2**). Since then, *AtGSL5* has been shown to be expressed abundantly in flowers (Østergaard, 2002) and to be involved in wounding and powdery mildew resistance (Nishimua *et al.*, 2003; Jacobs *et al.*, 2003). *GSL2* is involved in the synthesis of the callose that surrounds the microspore mother cells in the anthers, and is essential for pollen wall patterning (Dong

et al., 2005; Nishikawa et al., 2005). The role of the remaining callose synthases in *Arabidopsis*, and the role of callose in the development of plants remains uncertain.

Because of the uncertainties associated with the use of chemical inhibitors, I continued our studies using a genetic approach. Such a scheme confers the added advantage that the specific role of each of the *GSL* genes can be examined independently of one another, while chemical inhibitors can only inhibit all of the callose synthases at once.

During the course of this dissertation, a significant effort was made to develop a library of mutants for the *GSL* genes. Because the *Arabidopsis* root meristem was my main model of study, I focussed on only those *GSL* genes expressed in roots.

Two types of mutants were obtained: T-DNA insertions were available for some of the genes from the Salk Institute Genomic Analysis Laboratory (SIGnAL; http://signal.salk.edu/cgi-bin/tdnaexpress), and a spectrum of point mutations for all the genes was isolated in cooperation with the Seattle TILLING Project (STP; (http://tilling.fhcrc.org:9366/). Since TILLING produces many unwanted mutations in addition to the mutation in the *GSL* gene, it is necessary to clean up these lines by outcrossing. This was completed for many of the TILLING lines.

Initially, and in order to focus my efforts, I did very broad phenotyping on various homozygous T-DNA and TILLING mutant lines. For the TILLING mutant lines, those harbouring mutations predicted to have the most serious phenotypic effects were looked at first.

Materials and Methods

Nomenclature of putative callose synthase genes

Two different nomenclatures have been proposed for the 12 putative callose synthase genes in *Arabidopsis*. Verma and Hong (2001) have used *CalS1-CalS12* to designate these genes. The Stanford group (http://cellwall.stanford.edu/php/structure.php?family=gsl) have used *GSL1-GSL12* instead. The relationship between the two nomenclatures is shown in **Fig. 4.1**. I have used the *GSL* nomenclature because it has been more widely used up to this time (eg. Doblin *et al.*, 2001; Li *et al*, 2003; Nishimura *et al.*, 2003).

RT-PCR analysis

RNA was isolated from *Arabidopsis* Col-0 roots using the RNeasy Plant Mini Kit (Qiagen, Valencia, CA) and treated with DNaseI Amp grade (Gibco BRL). First-strand cDNA was synthesized from 2 μg of RNA with random hexamer primers using the ThermoScript reverse transcriptase–mediated PCR system (Gibco BRL) according to the manufacturer's instructions. PCR was performed with 2 μL of the first-strand reaction using gene-specific primers to identify each of the *GSL* genes: *GSL1* (5'-ACTTGGTTTGCCCTGATTTG-3'; 5'-GTGATCAGGAGCGTCACAGA-3'); *GSL3* (5'-GGTGACTTGGCTCTTTGCTC-3'; 5'-AGGATGATACCCCGTTTTCC-3'); *GSL4* (5'-TCGTACTCAGTGGGTTGCAG-3'; 5'-AGCAAGCTGTAGCTGCATGA-3'); *GSL5* (5'-TGATCGCACAGACTCAAAGG-3'; 5'-ATGATGCGAAGTCCTCTGCT-3'); *GSL6* (5'-TTCCTCGCACTTCCTCTGAT-3'; 5'-AACGCAACTGGTGTGAACAG-3'); *GSL7* (5'-

AGCTCTTCAAGCCCACAAGA-3'; 5'-CCGATAGGGAGCCATATGAA-3'); *GSL8* (5'-GCAAAGCATCCCGTGTTATT-3'; 5'-AAGTCAAACAGCTGCCCAAT-3'); *GSL9* (5'-TTTGCTAAATGCTGGTGCTG-3'; 5'-TATCAGGATCGAGGGGAAGA-3'); *GSL10* (5'-GGCTCTAGCTGGCATAATCG-3'; 5'-AGCATTCCCATTAACGCATC-3'); *GSL11* (5'-CCGATGGTAATGGAGATTGG-3'; 5'-TTGGCATGGAAAACAACAAA-3'); and *GSL12* (5'-TTTGCTCCCTTCCTCTTCAA-3'; 5'-TCACCAGCCATGATACTCCA-3'). As a control, gene-specific primers were also used to amplify endogenous *ACT2* (5'-GCCATCCAAGCTGTTCTCTC-3'; 5'- GCTCGTAGTCAACAGCAACAA-3'). PCR was also performed on 1.2 ng of Col-0 genomic DNA (0.12 ng/μL) using all of the above primer sets. Genomic DNA was isolated using a FastDNA kit (Q-Biogene) and treated with RNase A (Gibco BRL). The PCR program used was as follows: 95^0C for 2 min; (94^0C for 20s, 63^0C - 1^0C per cycle for 30s, 72^0C for 1 min) X 8 cycles; (94^0C for 20 s, 55^0C for 30s, 72^0C for 1 min) X 45 cycles; 72^0C for 5 min.

Construction of mutant library

Tilling mutants: The tilled lines are derived from a single *Col er105* plant (Big Mama), which provided seed for EMS mutagenesis. Big Mama was from the third backcross generation to Col of the original *er105* neutron-induced mutant (Torii *et al.*, 1996). For further information on how the TILLING lines were created, see Till *et al.*, 2003a. I backcrossed my mutant lines, obtained from the STP, into *Col-0* three times in order to eliminate as many of the background mutations, including *er105*, as possible. T-DNA mutants: T-DNA insertion lines from SIGnAL are in a *Col-0* background. For details on how these lines were generated, see Alonso *et al.*, 2003. Wild-type plants:

Arabidopsis thaliana ecotype *Columbia* (*Col-0*) was used. I also used the background plants from the mutant lines (plants from the same mutant lines obtained from TILLING and SIGnAL, which did not harbour the respective mutations, and which had undergone the same backcrosses to *Col-0* in the case of the TILLING mutants).

Genotyping

Genomic DNA was isolated as described above. TILLING mutants were either identified by restriction enzyme analysis, or, if the mutation did not cause a loss or gain of a novel restriction site, by the TILLING method for identifying induced point mutations (Till et al., 2003b). TDNA mutants were identified with PCR (Østergaard and Yanofsky, 2004).

Results and Discussion

GSL genes expressed in roots

The following *GSL* genes were found to be expressed in *Arabidopsis Col-0* wild-type roots: *GSL6, 3, 11* (at an extremely low level), *4, 10, 8, 1* and *5* (**Fig. 4.3**). All of my results were confirmed by Birnbaum et al., 2003, using an alternative method of expression analysis, except for *GSL12*, which they found to be expressed in all root tissues at high levels.. I neglected to do an RT-PCR analysis for *GSL2*, but Birbaum et al. found this gene to be unexpressed in root tissue.

Callose synthase library

I developed a mutant library for 8 of the 9 expressed genes (including *GSL12*), as well as for *GSL7*. In addition to the T-DNA insertion mutants from SIGnAL (**Fig. 4.4**), it contains 40 TILLING mutants (**Fig. 4.5**). Most of these TILLING mutations are clustered in the C-terminal conserved region of the gene.

I cleaned up mutant lines through outcrossing with *Col-O*. Genotypes of all mutants were always verified. Genotyping for TILLING mutants was done by both restriction digest analysis of PCR products and in cases where point mutations have not caused changes in restriction sites, by the TILLING protocol. Genotyping for T-DNA insertion lines was done by PCR (Østergaard and Yanofsky, 2004).

All mutant lines have been made available to the community on request, with the hope that this resource will prove of great value in future studies on callose synthase. I have already provided mutants to two laboratories.

Screening for mutants of interest - preliminary phenotyping

I have now completed preliminary phenotypic analyses for 35 of the single mutants in 8 of the *GSL* genes (**Table 4.1**). These analyses involve looking for gross morphological defects that are visible to the naked eye, at either the seedling stage or in the mature plants.

Most of the homozygous mutants were found to have no discernable mutant phenotype. There were notable exceptions. One TILLING mutant, *gsl10-1*, showed gametophytic lethality (double homozygotes for the mutation could not be generated). A T-DNA insertion in *GSL7* (*gsl7-1*) segregated with a weak floral phenotype (**Fig. 4.6**).

Another TILLING mutant, *gsl3-2*, behaved as a dosage-dependent, gain-of-function mutation. This mutant is described in the next chapter.

That mutations in many of the *GSL* genes lacked obvious phenotypes supports the idea that some of these genes might have overlapping functions. Examination of the phylogenetic map for the *GSL* gene family suggests that several of the genes might be so closely related as to be redundant. Pairs or even triplets of potentially redundant genes include *GSL1* and *GSL5*, *GSL8* and *GSL10, GSL7* and *GSL11* and *GSL3, GSL6* and *GSL12*. A double mutant homozygous for alleles conferring loss of function in *GSL1* and *GSL5* was found to be lethal, demonstrating just such a redundancy. Work on this double mutant is described in chapter 6.

Figure 4.1. Gene models for *Arabidopsis GSL1-12*. (Gene models were built from NCBI statements, annotated from complete chromosome sequence. Models were drawn with Gene Structure Draw (http://warta.bio.psu.edu/cgi-bin/Tools/StrDraw.pl).)

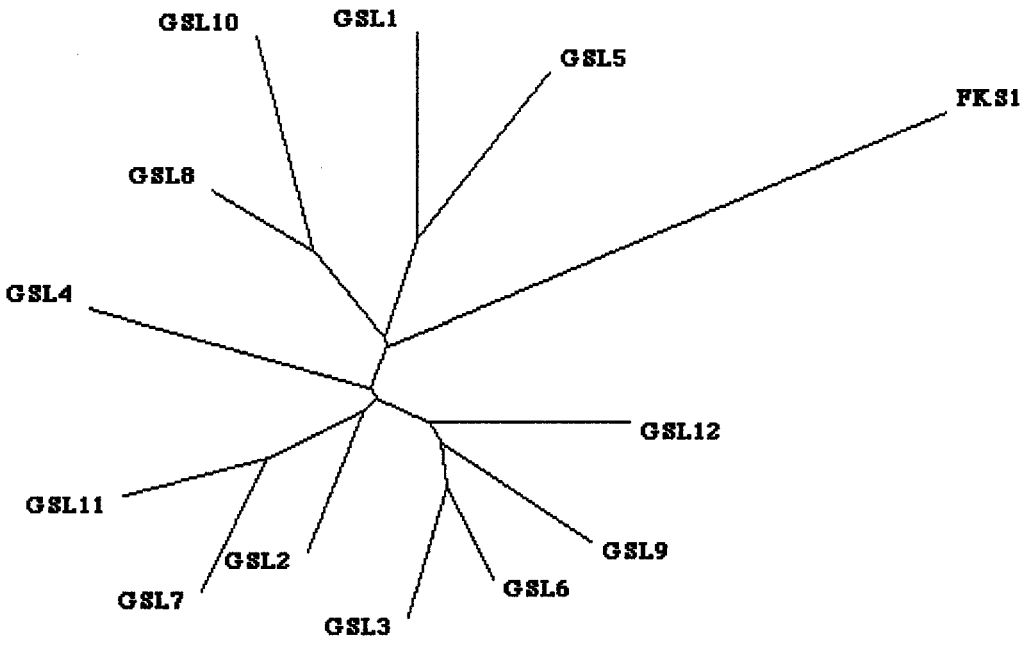

Figure 4.2. Phylogenetic analysis of GSL1-12, including FKS1, a callose synthase from *S. cerevisisae*. Analysis was done on amino acid sequences from TIGR (the Institute for Genomic Research; http://www.tigr.org/), using ClustalX alignment and bootstrap neighbour-joining tree analysis. Tree was drawn with TreeView (1998, Roderic D.M. Page, http://taxonomy.zoology.gla.ac.uk/rod/treeview.html).

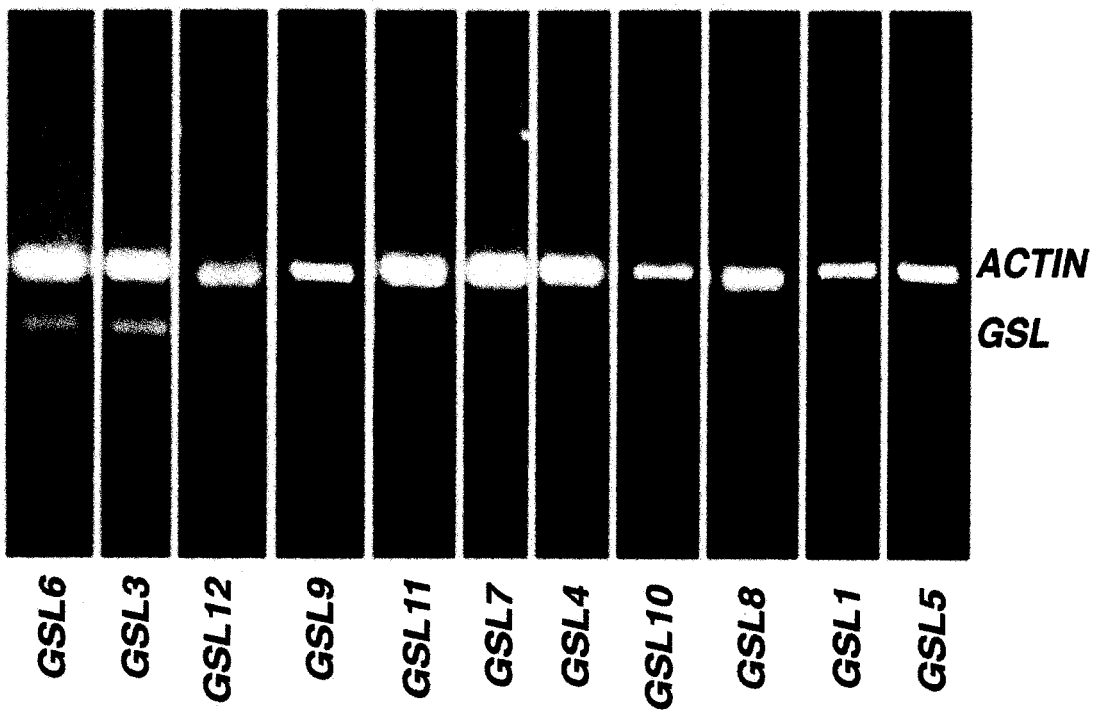

Figure 4.3. *GSL* expression in unwounded roots of *Arabidopsis*. RT-PCR analysis. Expression of actin is included as a control.

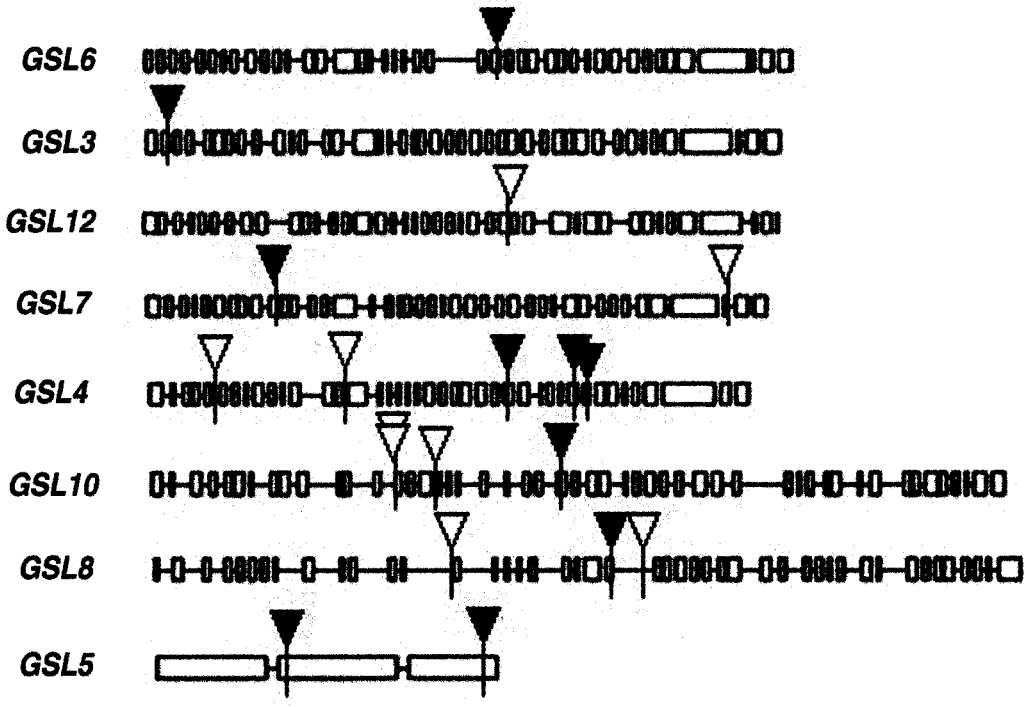

Figure 4.4. Library of *GSL* T-DNA insertion lines from SIGnAL (the Salk Insitute Genomic Analysis Laboratory; http://signal.salk.edu/cgi-bin/tdnaexpress). Red triangles are T-DNA insertions in exons. White triangles are intronic insertions.

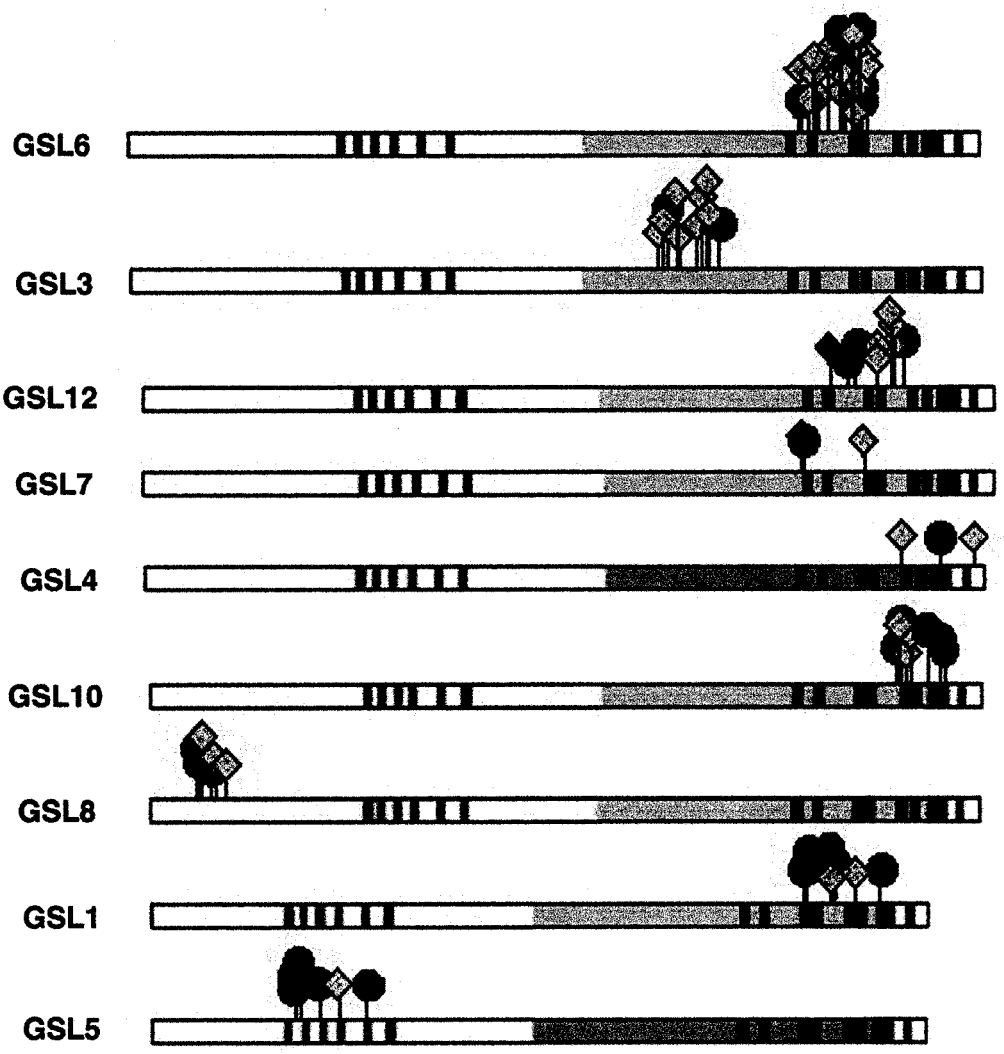

Figure 4.5. Library of *GSL* TILLING mutant alleles acquired from the Seattle TILLING Project (http://tilling.fhcrc.org:9366/). Protein models: the light grey region represents a conserved motif shared between callose synthases, and dark grey regions represent trans-membrane regions. Darkest grey are where these two types of regions overlap (Rost, 1996a; Rost et al., 1996b; Falquet et al., 2002) (http://www.predictprotein.org; http://myhits.isb-sib.ch/cig-bin/motif_scan)Protein models indicate transmembrane sequences (dark grey) and the putative ß-1,3-glucan synthase component shared by all callose synthases (light grey). Yellow diamonds are point mutations predicted to be deleterious by SIFT. Green circles are point mutations predicted to be non-deleterious. Red octagons are truncations. Red diamonds represent a loss of intron splicing.

Table 4.1. Mutant alleles in library, and outcrossings and phenotyping completed. TILLING mutants: amino acid change is shown. Asterisks denote truncations, diamonds denote a loss of intron splicing. Alleles predicted to be deleterious by SIFT are in bold. T-DNA insertion lines: those with insertions in exons are in bold. Black boxes indicate alleles of interest.

Gene	TILLING mutant	# out-crosses	pheno-typed?	TILLING mutant	# out-crosses	pheno-typed?	T-DNA mutant	p-typed?
GSL6	**V1525M**	**3X**	√	**Q1528***	**3X**	√	007820	√
	G1548E			**G1560E**				
	T1614I	**4X**	√	**P1628S**	**3X**	√		
	P1662L			**E1667K**				
	R1559K			**R1581H**				
	L1593F			**W1624***				
	L1630F	**2X**		**D1647N**				
	L1630F			P1661L				
	W1666*			**G1656R**				
	G1681E							
GSL3	**V1199M**	**3X**	√	M1223I			**11560** ***(gsl3-1)***	√
	E1206K			**V1253M**				
	T1246I	**3X**	√	**E1299K**				
	G1291D ***(gsl3-2)***	**5X**	√	**L1309F**				
	T1340I	**3X**	√	**G1313R**				
	L1363F							
GSL12	M1613I	**1X**		R1727K	**1X**		068418	
	G1709R	**1X**		P1608S	**1X**			
	G1677D	**1X**		**1573◊**	**2X**			
	V1718M			**V1707M**	**1X**			
	G1676D	**2X**						
GSL7	V1507M	**3X**		**1505◊**	**3X**		040051	
	G1641E	**3X**	√				**048921** ***(gsl7-1)***	√
GSL4	T1829I	**3X**	√				**000507**	√
	P1729S	**3X**					**015030**	√
	A1898T	**3X**					033590	
							037603	
							047978	
GSL10	**G1743E**	**3X**	√	**G1720D**			031800	√
	E1747K	**3X**	√	G1723E			**143945**	
	W1781* ***(gsl10-1)***	**2X**	√	S1815F			000283	
	A1826T			G1723R			000475	
GSL8	S105N	**3X**		S100F	**1X**		015454	√
	S112F	**3X**	√	E136K	**3X**		**039791**	
	D142N	**3X**	√	**R169Q**	**3X**		057120	
GSL1	A1489V	**3X**	√	D1561N	**3X**	√		
	V1494I	**3X**	√	**L1604F**	**3X**	√		
	W1549* ***(gsl1-1)***	**4X**	√	V1663I	**4X**	√		
	G1554D	**3X**	√					
GSL5	D328N	**3X**	√	M386I	**3X**	√	**002911** ***(gsl5-3)***	√
	D328N			**V432M**	**3X**	√	**090026**	
	D344N	**3X**	√	**Q509*** ***(gsl5-2)***	**4X**	√		

Figure 4.6. Weak floral phenotype of *gsl7-1*. Flowers on the left are from three different *Col-0* wild-type plants. Flowers on the right are from three different plants homozygous for the mutation. Plants homozygous for the mutant allele have smaller, rounder flowers.

CHAPTER 5: PRELIMINARY WORK WITH PUTATIVE PLASMODESMATAL CALLOSE SYNTHASE MUTANT

Introduction

Preliminary screening of single TILLING mutants revealed a mutant line with an interesting root phenotype. While not agravitropic, roots of this mutant were very short and showed excessive lateral root development.

Proper auxin distribution is important to lateral root formation (Malamy and Benfey, 1997). Chemicals that inhibit polar auxin transport inhibit the formation of lateral roots (Ruegger et al., 1997), and auxin-resistant mutants such as *axr1*, *axr4* and *aux1* have reduced numbers of lateral roots (Hobbie and Estelle, 1995; Timpte et al., 1995). Plants that overexpress auxin biosynthesis genes produce lateral roots in excess (Klee, 1987).

I originally hypothesized that symplastic domains in roots are essential for proper auxin distribution during plant development. Since auxin distribution is known to be important for lateral root positioning, I investigated this mutant for possible defects in PD connectivity.

Results and Discussion

Callose synthase and intercellular communication – GSL3

This study used two mutant alleles for *GSL3*: *gsl3-1*, a T-DNA insertion line and putative genetic knock-out (SALK_011560), and *gsl3-2*, a TILLING mutant with a point mutation (**Fig. 5.1**) causing an amino acid change in a conserved region of the protein (**Fig. 5.2**) predicted to have a deleterious effect, according to SIFT (Sorting Intolerant From Tolerant: Ng and Henikoff (Ng and Henikoff, 2003).

While the *gsl3-1* homozygote had no mutant phenotype, the *gsl3-2* homozygote was dwarfed. However, TILLING mutants are produced in an *er105* background, where a mutation in the *ERECTA* gene is known to cause dwarfism (Torii et al., 1996). Since *ERECTA* is linked with *GSL3* on chromosome 2 (within 4 centimorgans) I outcrossed the *gsl3-2* line five times with *Arabidopsis* ecotype *Col-0* to eliminate the *er105* and other mutations. The *gsl3-2* homozygote frequently segregated with a short, branchy root and small leaf phenotype (**Fig. 5.3; Fig. 5.4A,B**). Interestingly, the rosette leaves were no larger than when the *er105* mutation was present, indicating a potential epistasis between *GSL3* and *ERECTA* (data not shown). Both *GSL6*, the closest relative of *GSL3*, and *ERECTA* have been shown to be involved in cell division (Hong et al., 2001; Shpak et al., 2004). Early on in development, the *gsl3-2* heterozygous mutant had an average rosette diameter and root length between that of the wild-type and the *gsl3-2* homozygote, indicating a semi-dominant nature to the mutation (**Fig. 5.3**). Semi dominance is indicative of a gain-of-function mutation. Later in development, the rosettes of the *gsl3-1/gsl3-2* trans-heterozygotes were found to be much scrawnier than those of the *gsl3-2/+*

plants (data not shown), providing genetic evidence that there is a shoot phenotype that is at least in part the result of the *gsl3-2* mutation. The trans-heterozygotes never showed a more severe root phenotype than the *gsl3-2/+* plants, however. Taken together, these results indicate that the effects of the *gsl3-2* allele in both the root and shoot may be both gain-of-function and dosage dependent, and that a higher ratio of mutant to wild-type*GSL3* is required for the observed root phenotype.

The segregation of the *gsl3-2* allele with the small rosette phenotype was nearly perfect (about 50 plants in total were looked at from 3 different selfed heterozygous lines). However, while segregation of the *gsl3-2* allele with the root phenotype was frequent, it was not completely consistent. Infrequently, a *gsl3-2* homozygote was found that lacked the mutant root phenotype. While an explanation for this could be incomplete penetrance of the mutant phenotype, more worrisome was the occasional appearance of short, branchy roots in the progeny of selfed heterozygous *gsl3-2* lines that were found to be genetically wild-type for *GSL3*. There exists the possibility that even after 5 outcrosses with wild-type *Col-0*, the *gsl3-2* allele is still linked to one or more mutations causing the root mutant phenotype.

I investigated intercellular communication in the root meristem of the *gsl3-2* mutants by grafting roots showing the branchy/short phenotype onto *AtSUC2*:GFP-expressing shoots (methods are described in chapter 3). Confocal microscopy revealed the movement of GFP in the mutant root meristems to be dramatically restricted in comparison to wild-type (**Fig. 5.4 C,D**). Assuming that the mutation in *GSL3* is what is causing the loss of intercellular connectivity, there are two hypotheses that need to be tested: 1) the *gsl3-2* mutation leads to increased callose, and reduced SELs; 2) the *gsl3-2*

mutation causes disrupted callose synthesis, and the presence of callose at the phragmoplast in dividing cells is important for the construction of PDs; ie. *gsl3-2* mutants may have less PD between cells. If this second hypothesis is true, it would provide a whole new insight into a role for callose in PD development.

This mutant may also provide new information about the role of intercellular communication in plant development. In addition to short, branchy roots, there appeared to be occasional differentiation problems in the root meristem, internal tissue layers sometimes absent (data not shown). The intercellular movement of certain transcription factors has been shown to be important for cell identity (Nakajima et al., 2001). Mutants for one such transcription factor, SHORT-ROOT (SHR) have impaired intercellular SHR movement, short, branchy roots, and loss of tissue layers in the root meristem (Benfey et al., 1993). My mutant may have problems with the intercellular trafficking of signaling molecules such as SHR.

Alternatively, in addition to lateral root development, auxin has been shown to be involved in cell patterning. Interference with auxin transport in embryos causes patterning defects (Liu et al., 1993; Hadfi et al., 1998). Mutants lacking MONOPTEROS (MP), a protein very similar to the auxin-responsive transcription factor AUXIN RESPONSE FACTOR 1 (ARF 1), have problems with embryonic patterning and cellular differentiation (Berleth and Jürgens, 1993). Most pertinent to my work, mutants defective in auxin transport have been found to have patterning problems in the root meristem (Sabatini et al., 1999). If proper intercellular communication in the root meristem is essential for proper auxin distribution, it then stands to reason that the *gsl3-2* mutants would have defects in their root meristem patterning.

As already mentioned, I have concerns about the possibility of other linked mutations to *gsl3-2* that may be causing these effects on the root. Without a genetic rescue, I cannot be sure that the mutant phenotypes observed are due to the *gsl3-2* mutation. I attempted to rescue the *gsl3-2* homozygous mutant using pGREEN (http://www.pgreen.ac.uk/), into which I had inserted 23 kB from the F22D22 BAC insert, obtained from the *Arabidopsis* Information Resource (TAIR). The tail 23kB from the 100kB insert of this BAC, containing the entirety of the wild-type *GSL3* allele and lacking the entire coding region for any other gene, was removed using Not1 and BamH1, and ligated into the cloning site of pGREEN 0029. This kanamycin-resistant plasmid, when co-electroporated into *Agrobacterium* with the helper plasmid pSOUP, should have been able to rescue the mutant using *Agrobacterium*-mediated plant transformation. I verified the identity of our construct with PCR, Contour-clamped Homogeneous Electric Field (CHEF) gel analysis (Chu et al., 1986) and sequencing; however, I was unable to successfully transform *Agrobacterium* with my construct. Work on this mutant should not be continued until the branchy root/loss of intercellular communication phenotype is shown to be rescuable by insertion of a wild-type *GSL3* allele.

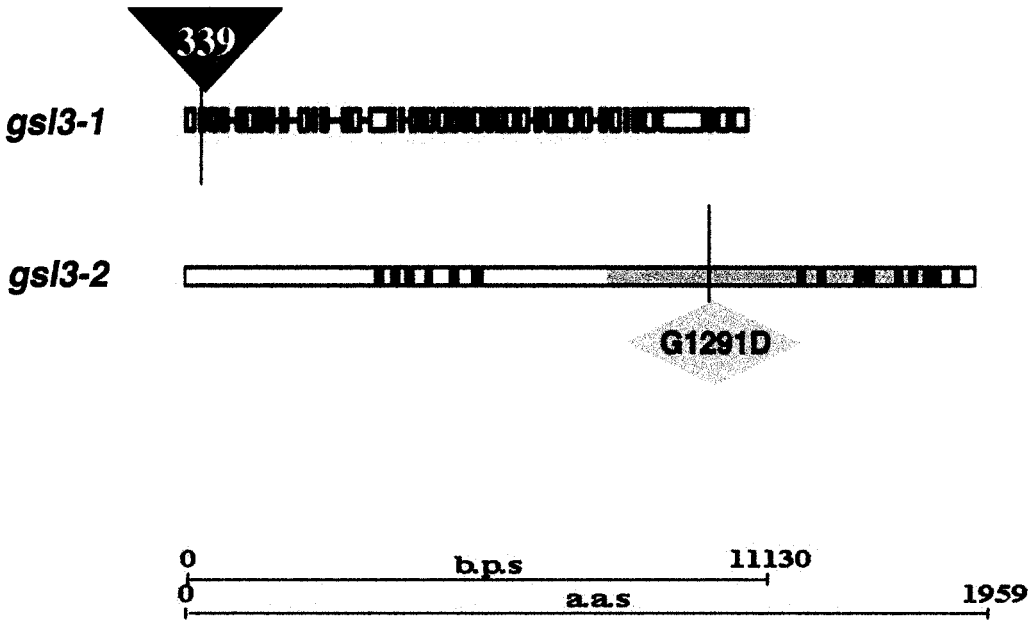

Figure 5.1. Mutant alleles for *GSL3*. *gsl3-1* carries and exonic T-DNA insertion, 339 base pairs into the gene. *gsl3-2* has a point mutation that causes amino acid 1291 to be converted from a glycine to an aspartic acid. The significance of the shaded areas in the protein model are explained in chapter 4.

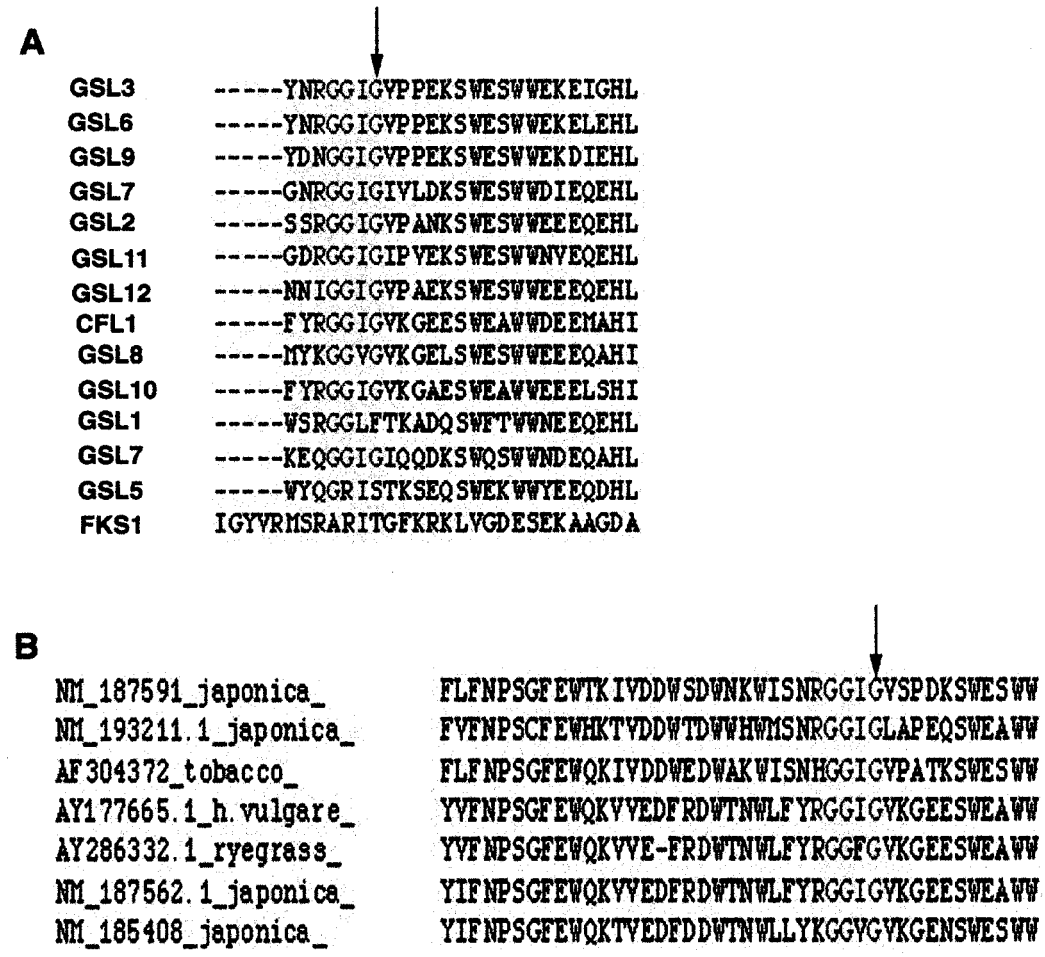

Figure 5.2. Conserved region of *GSL3* in which *gsl3-2* point mutation resides, compared with other callose synthases from **(A)** *Arabidopsis* (GSL), cotton (CFL1), yeast (FKS1) and **(B)** rice, tobacco, *Helianthimum* and ryegrass. The black arrow indicates the glycine that is mutated in *gsl3-2*.

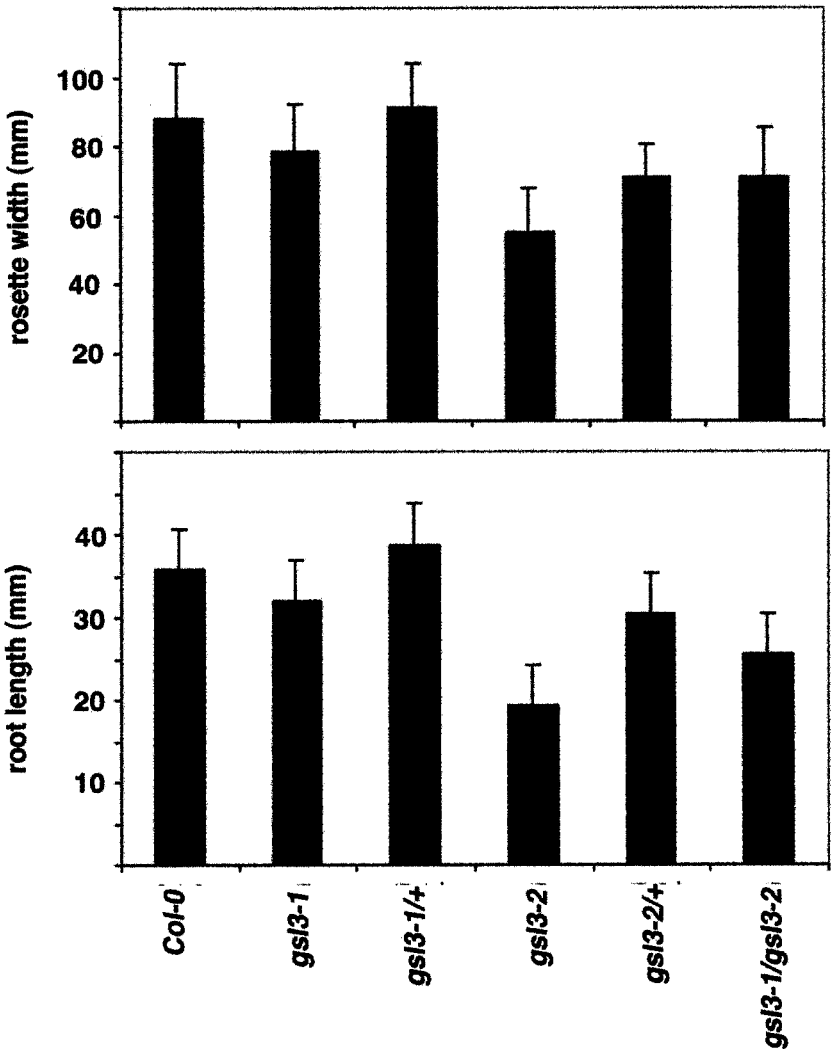

Figure 5.3. Phenotypes of *gsl3* mutants. Upper graph, rosette diameter of plants just after bolting. Lower graph, root length of 6 day-old seedlings.

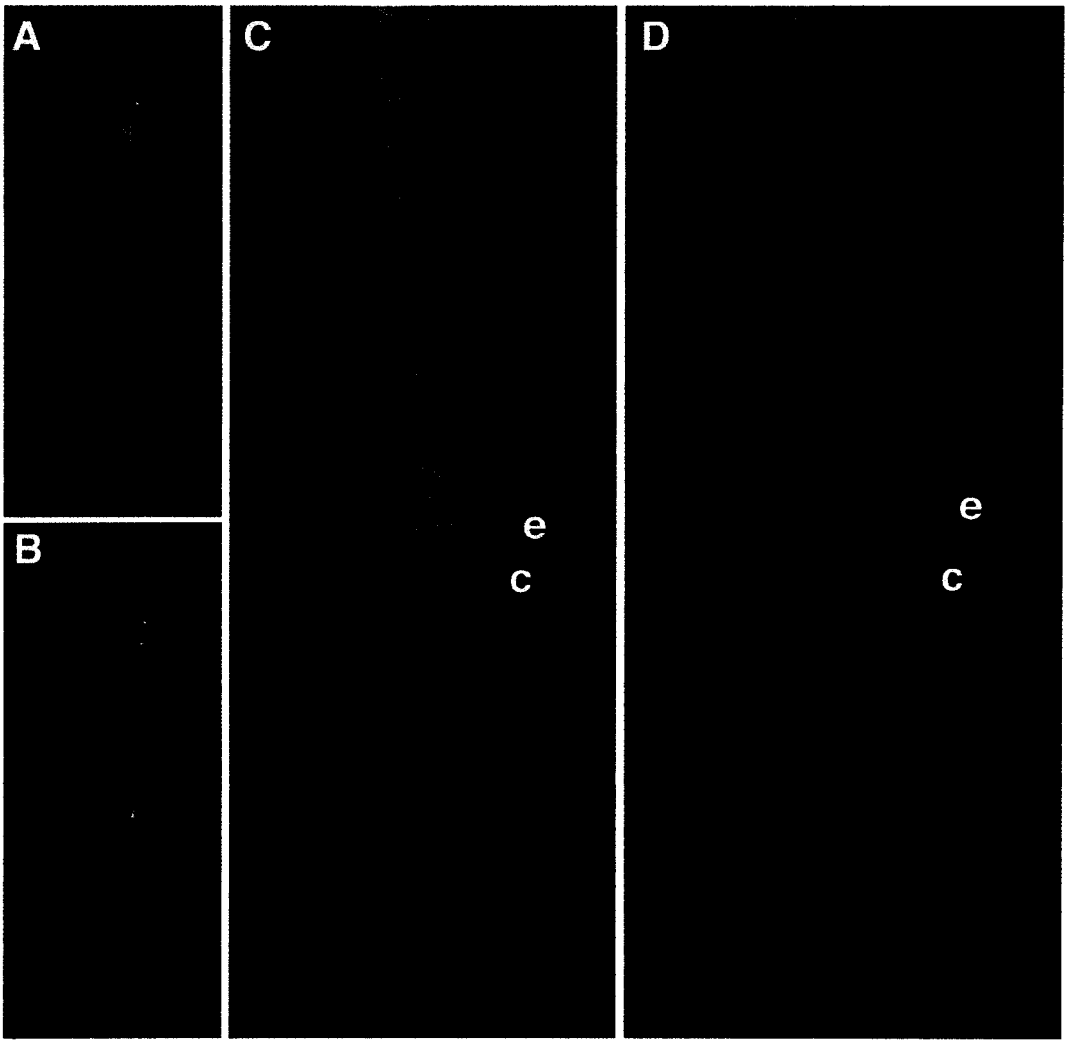

Figure 5.4. Root phenotype of *gsl3-2*. **A.** Wild-type Col-0 and **(B)** *gsl3-2* root. The mutant roots are short and branchy in comparison to wild-type. **C.** Wild-type *Col-0* root and **(D)** *gsl3-2* root several days after being grafted onto an *AtSUC2:GFP* shoot. GFP fluorescence is eventually seen throughout the meristem of the wild-type root, but GFP movement is highly restricted from moving out of the stele in the mutant. e=epidermis; c=cortex.

CHAPTER 6 - TWO CALLOSE SYNTHASES, GSL1 AND GSL5, PLAY AN ESSENTIAL AND REDUNDANT ROLE IN PLANT AND POLLEN DEVELOPMENT AND IN FERTILITY

(PUBLISHED IN PLANT MOLECULAR BIOLOGY (2005) 58:333-349)

Introduction

Callose is thought to play an important role in pollen grain formation and in pollen tube growth. It is highly conspicuous at two stages of pollen development. It first surrounds the meiotic tetrad prior to the formation of the pollen grain wall (McCormick, 1993; Fei and Sawhney, 2001; Edlund and Preuss, 2004). It is is also part of the pollen tube wall and plug within the tube, required for pollen tube growth (Ferguson *et al.*, 1998; Schlüpmann *et al.*, 1994). These results suggest that callose plays an essential role in the development of intact plants, but as yet there is only limited genetic evidence to support this idea.

In this chapter I focus on two closely related genes, *AtGSL1* and *AtGSL5*, using T-DNA and TILLING mutants that harbour genetic and putative functional knockouts. I demonstrate here that these two genes play a redundant but essential role in sporophyte development, and in pollen development, where they are involved in the synthesis of the callose that separates the microspores after meiosis as well as in pollen grain maturation.

Materials and Methods

RT-PCR analysis

RNA was isolated from *Arabidopsis Col-0* and treated with DNase as described in Chapter 4. First-strand cDNA was synthesized also as previously described. PCR was performed with 2 μL of the first-strand reaction using gene-specific primers to identify endogenous *GSL5* (5'-TGAAGAAATCAAGCCTGTGC-3'; 5'-TCTTGGTCAGCGTGTTCTTG-3') and *GSL1* (5'-GGGAAGACAGGATTTGTGGA-3'; 5'-CGAACACAACCTTGAGAAACG-3'). As a control, gene-specific primers were also used to amplify endogenous *ACT2* (5'-GCCATCCAAGCTGTTCTCTC-3'; 5'-GCTCGTAGTCAACAGCAACAA-3'). PCR was also performed on 1.2 ng of *Col-0* genomic DNA (0.12 ng/μL) using all of the above primer sets. Genomic DNA was isolated using a FastDNA kit (Q-Biogene) and treated with RNase A (Gibco BRL). The PCR program used was as follows: 95^{0}C for 2 min; (94^{0}C for 20s, 63^{0}C - 1^{0}C per cycle for 30s, 72^{0}C for 1 min) X 8 cycles; (94^{0}C for 20 s, 55^{0}C for 30s, 72^{0}C for 1 min) X 45 cycles; 72^{0}C for 5 min.

Plant materials and growth conditions

The tilling mutants selected from our library for this study were designated as *gsl1-1* and *gsl5-2*. The T-DNA insertion line used from my library is designated as SALK_002911 by SIGnAL; I have renamed the allele *gsl5-3*. For details on how all these lines were generated, see Chapter 4. Regardless of whether wild-type plants used

were *Col-0*, or plants obtained by crossing out the mutant allele from the mutant line, there were no differences in results. I thus grouped them all together as 'wild-type'.

Plants were grown on soil mixture (Sunshine Mix4:vermiculite:perlite, 2:1:1, Sun Gro Horticulture Canada, Seba Beach, Canada) supplemented with 0.85 mg/cm3 Osmocoat 14-14-14 (Scotts, Maysville, OH) under an 18-h-light/6-h-dark cycle at 21°C.

Genotyping

Genomic DNA was isolated as described in chapter 4. *gsl1-1* was genotyped using the TILLING method for identifying induced point mutations This protocol is described in Till *et al.*, 2003b. The gene-specific primers used were 5'-TCTCTCGAGCGTGGGTTTCTTCCA-3' and 5'-TTCTGAAAACCGGGCAACCATGAA-3'. For each genotyped plant, the protocol was performed on both its DNA, and its DNA combined 1:1 with DNA from a wild-type plant. *gsl5-2* mutants were identified by PstI digestion of the PCR product created using the gene-specific primers 5'-TGCCTTCTCTCTCAGGCGAAAACG-3' and 5'-TGGCAACCATAACAATGCGACAGA-3'. The point mutation in *gsl5-2* removes a PstI restriction site from this region. *gsl5-3* mutants were identified with PCR. Two sets of gene-specific primers were designed: one in which both primers flanked the insertion site (5'-GAACATTCACCACCCGCCCACT-3'; 5'-TGGGGGAGATCAGGGACATGG-3'); the other in which the right primer hybridized within the insert itself (5'-CCACCCGCCCACCTGTTTCC-3'; 5'-TGGTTCACGTAGTGGGCCATCG-3'). For an example of this method, see Østergaard and Yanofsky, 2004. It should be noted here that the direction of the T-DNA insertion in this line was found to be the reverse of what was

reported in the SIGnAL database at the time of primer design. For all genotyping, the concentration of DNA used was 0.12 ng/μL, for a total of 1.2 ng of DNA. For genotyping of *gsl5-2* and *gsl5-3*, the PCR program used was as follows: 95^{0}C for 2 min; (94^{0}C for 20s, 73^{0}C - 1^{0}C per cycle for 30s, 72^{0}C for 1 min) X 8 cycles; (94^{0}C for 20 s, 65^{0}C for 30s, 72^{0}C for 1 min) X 45 cycles; 72^{0}C for 5 min.

Microscopy

Confocal microscopy: Whole, mature flowers were prepared as described in Braselton *et al.*, 1996. The whole flower was squashed under a coverslip prior to resin polymerization. Following polymerization, the coverslip was removed, and the specimen was observed under oil. Anthers were observed using a BioRad MRC-600 confocal microscope with an excitation filter of 488 and a BHS emission filter block containing a dichroic and emission barrier filter.

Light/fluorescence microscopy: Aniline blue staining for pollen germination assays: Mature flowers were stained for 30 minutes with 0.1% toluidine blue o (Allied Chemical, New York, N.Y.) in 0.1 M KPO_4 buffer, pH adjusted to 4.4 with KOH, rinsed with distilled water and then mounted in 0.1% aniline blue (Allied Chemical, New York, N.Y.) in 1 M glycine, pH adjusted to 9.8 with NaOH. Flowers were squashed under a coverslip prior to observation. Pollen grains were whole-mounted by flicking mature anthers over slides which had been coated in germination medium (20% sucrose, 0.01% boric acid, 1 mM $MgS0_4$, 0.08% $CaCl_2$, 0.7% phytagar, 3% PEG M.W. 3350, pH adjusted to 7 with KOH). Prior to observation, slides were placed in a humid chamber at 30°C for 12 hours, and then aniline blue and a coverslip were applied. Alexander

staining: Pollen grains were whole-mounted as described above, but on a bare slide. Two drops of Alexander stain (Alexander, 1969) was added. A coverslip was applied, and sealed with clear nail polish. The slide was warmed on a slide warmer at 50°C for 2 hours, and then observed with light microscopy. Toluidine blue o/aniline blue staining at different stages of pollen development: Whole inflorescences were fixed in FAA (63% EtOH, 5% acetic acid and 5% formaldehyde) overnight. After dehydration through a graded EtOH series, samples were embedded in Technovit 7100 (Kulzer, Germany) as described by the manufacturer. Samples were cut into 5μm sections using a microtome, and stained with toluidine blue o (0.1% toluidine blue o in 0.1M phosphate buffer pH 7.0) for 45 seconds. For the observation of callose, the same sections were stained with 0.1% aniline blue (CHROMA-GESELLSCHAFT SCHMID GMBH&CO., Germany) in 0.1% K3PO4 for 15 minutes. Figure 6C-E and Figure 8: Sections were observed using an Axiophot2 microscope (Zeiss, Germany) mounted with an AxioCam HRc digital camera (Zeiss, Germany). Figure 6F-K: Specimens were observed using a Nikon Eclipse E600 upright microscope mounted with a Retiga EX camera (QImaging, Burnaby, BC). Scanning electron microscopy: Pollen grains were applied by flicking the anthers of mature flowers over mounting tape on a stub. The pollen grains were allowed to air-dry for about 30 minutes, sputter coated with gold, and observed with a JEOL 840A scanning electron microscope.

Results

Relationship between GSL1 and GSL5, and gene expression in Arabidopsis plants

There are 12 *GSL* genes in *Arabidopsis* (**Fig. 4.1**) (Verma and Hong, 2001; http://cellwall.stanford.edu/php/structure.php?family=gsl). *GSL1* and *GSL5* are linked, intron-poor genes that differ in structure from the other 10 *GSL* genes, but which are very similar in structure to each other. Phylogenetic analysis of GSL1-12 shows GSL1 and GSL5 to be more closely related to each other than to any of the other proteins in this family (**Fig. 4.2**). Østergaard *et al.* (2002) reported that *GSL5* is expressed abundantly in flowers. I used RT-PCR analysis (**Fig. 6.1**) to show that both *GSL1* and *GSL5* are expressed in all parts of the unwounded *Arabidopsis* plant.

Phenotypic analysis of gsl1 and gsl5 mutants

I obtained mutant lines for *GSL1* and *GSL5* from the Seattle Tilling Project (STP; http://tilling.fhcrc.org:9366/) and a mutant line for *GSL5* from the Salk Institute Genomic Analysis Laboratory (SIGnAL; http://signal.salk.edu/cgi-bin/tdnaexpress) (**Fig. 6.2A**). *gsl1-1* and *gsl5-2*, obtained from the STP, are alleles with a single point mutation that encodes a premature stop codon. The products, which lack or have an interrupted motif conserved in β-1,3-glucan synthases, are predicted to be non-functional. *gsl5-3*, obtained from SIGnAL, has a T-DNA insertion in its second exon, and is a genetic knock-out (**Fig. 6.2B**). As expected, the point mutations in *gsl1-1* and *gsl5-2* did not cause loss of transcript (data not shown for *gsl1-1*).

Plants homozygous for the *gsl1-1* mutation showed no phenotype when observed with the naked eye (**Fig. 6.3A**). This was confirmed upon quantification of various phenotypic characters (**Table 6.1**). On the other hand, both *gsl5-2* and *gsl5-3* homozygous mutants were smaller plants, with a rosette diameter that was 25-35% smaller than the wild-type. This was not due to a reduced leaf number, but rather to a smaller maximum leaf size. I analyzed 24 offspring from a selfed *gsl5-2* heterozygous plant: only homozygotes for the mutation showed this phenotype (data not shown). When I crossed the two homozygous *gsl5-2* and *gsl5-3* mutant lines, the resultant trans-heterozygote for both *gsl5* mutant alleles confirmed the mutant phenotype. Other quantified sporophytic mutant phenotypes were not apparent in the single *gsl5* mutants, but their bolts, and those of the trans-hetrozygotes were much sparser and spindlier (data not shown).

GSL1 and *GSL5* are linked, within 8 centimorgans of each other. Through recombination, I generated the following mutant lines: *gsl1-1/gsl1-1 gsl5-2/+, gsl1-1/gsl1-1 gsl5-3/+, gsl1-1/+ gsl5-2/gsl5-2* and *gsl1-1/+ gsl5-2/gsl-5-3*. Both the *gsl1-1/gsl1-1 gsl5/+* mutant lines had a normal phenotype (**Fig. 6.3A; Table 6.1**), but the *gsl1-1/+ gsl5/gsl5* mutant lines had extremely small rosette leaves and small, sparse, spindly bolts (**Fig. 6.3A,B**), shorter primary roots (**Fig. 6.3C**) and smaller floral organs, most notably the anthers (**Fig. 6.3D**). The *gsl1-1* and both *gsl5* single mutant lines were fertile, producing viable seeds. This suggests that *GSL5* and *GSL1*, by themselves, are not required for sexual reproduction. However both the *gsl1-1/+ gsl5/gsl5* mutant lines produced very few viable seeds when selfed, in contrast to both the *gsl1-1/gsl1-1 gsl5/+* lines which when selfed, produced fertile offspring. These data suggest that in a *gsl1-1*

homozygous background one *GSL5* allele results in nearly normal sporophytic development and fertile plants. When *GSL5* is lacking, however, two *GSL1* alleles are required for fairly normal development and fertile plants, while a single *GSL1* allele permits only limited plant development and fertility. The *gsl1-1/gsl1-1 gsl5/+* mutant lines, when selfed, produced no offspring homozygous for both mutations (**Fig. 6.4A**). The ratio of offspring bearing two wild-type *GSL5* alleles to one wild-type and one *gsl5* mutant allele (about 1:1), pointed to a gametophytic lethality. When *Col-0* wild-type plants were fertilized with pollen from these mutant plants, none of the offspring contained the *gsl1 gsl5* chromosome (**Fig. 6.4B**), indicating that either *GSL1* or *GSL5* in the male gamete is essential for its development into a functional pollen grain. A chromosome bearing *gsl1-1 gsl5* can be passed via the female however, since the *gsl5* alleles were not lost when either of the *gsl1-1/gsl1-1 gsl5/+* mutant lines were selfed; the genotypic ratios of the offspring indicate no reduction in a *gsl1 gsl5* female gametoyphyte's fertility. In addition, *gsl1-1/+ gsl5/gsl5* plants could be produced in genetic crosses.

The haplo-insufficiency of *GSL1* in the absence of *GSL5*, and the haplo-sufficiency of *GSL5* in the *gsl1-1* background indicates that while there is redundancy between *GSL1* and *GSL5*, at least in the sporophyte *GSL5* may be the more important of the two genes.

Effects of gsl1 and gsl5 mutations on pollen morphology

The pollen from the *gsl1-1/gsl1-1 gsl5-3/+* plants looked normal up to and including the bicellular stage (data not shown). But using multiple microscopic

techniques, I observed that the *gsl1-1/gsl1-1 gsl5/+* and *gsl1-1/+ gsl5/gsl5* mutant lines produced, in addition to phenotypically normal pollen grains, many small, collapsed pollen grains. Under the confocal microscope, these mutant pollen appeared as trichotomous stars (**Fig. 6.5A,B**). The *gsl1-1/+ gsl5/gsl5* mutant lines produced, in addition to small, collapsed pollen, many abnormally large pollen grains (**Fig. 6.5C,D**). These large pollen grains had varying and increased numbers of pores compared to the wild-type, which always had three. In *gsl1-1/+ gsl5-2/gsl5-3* plants, large and multinucleate microspores were sometimes observed (**Fig. 6.5E**) (microspore analysis was not done on *gsl1-1/+ gsl5-2/gsl5-2*). A mature pollen grain has three cells, due to mitotic divisions of the haploid microspore. Unlike normal pollen, under high transmitted light, collapsed pollen appeared to lack cellularization (**Fig. 6.5F**). Staining for cytoplasmic integrity (Alexander staining) showed reduced but present cytoplasm in the collapsed pollen (**Fig. 6.5G**). On occasion, collapsed pollen grains failed to disassociate from the tetrad (**Fig. 6.5H** and **I**, white arrow). Collapsed pollen grains fluoresced differently from normal pollen grains (**Fig. 6.5I, nos. 1,2**). A pollen tube growth analysis showed that all mutant lines produced some fraction of wild-type pollen grains, which were capable of germination (**Fig. 6.5I, no. 1**). But collapsed pollen grains were incapable of forming pollen tubes or plugs (**Fig. 6.5I-K**). Some pollen grains had only slight aberrations at one end, appearing under the fluorescent microscope as bulges that stained positive for callose (**Fig. 6.5I, no. 3**) (I hypothesize that this is wound callose, and is not directly related to the mutations in *GSL1* or *GSL5*). These slightly aberrant pollen grains also did not show normal pollen tube growth.

From this pollen tube growth analysis, I scored percentages of collapsed pollen grains for all the mutant lines (**Table 6.2**). The collapsed pollen grains were identified based on their small size, opaque appearance under the light microscope, and their different fluorescent signature. I found that *gsl5-2* and *gsl5-3* mutants produced a small percentage of collapsed pollen grains. However both the *gsl1-1/gsl1-1 gls5/+* mutant lines, and the *gsl1-1/+ gsl5-2/gsl5-3* mutants produced at least twice as many collapsed pollen grains as the *gsl5* single mutants, while the *gsl1-1* homozygous plants produced no collapsed pollen grains. Since pollen in *gsl5* and *gsl1-1/gsl1-1 gsl5/+* mutants looks normal up until the bicellular stage (data not shown) I conclude that *GSL1* and *GSL5* are involved in the late maturation of the male gametophyte, and are at least partially redundant. I speculate that the collapsed, inviable pollen is *gsl1 gsl5*. Since some *GSL1 gsl5* pollen grains, but no *gsl1-1 GSL5* pollen grains, are collapsed, *GSL5* may be the more important of the two genes in pollen grain maturation, provided that *gsl1-1* encodes a functional knock-out.

Aberrant pollen grains from all mutant lines were also scored using the SEM (**Table 6.2**). In this assay, any obvious aberrances were counted, including pollen grains with bulges and abnormally large pollen grains, which were found to be misshapen and to have unusual pore structures. Thus, the presence of aberrances other than the collapsed morphology observed in my light/fluorescent microscopy assay would be reflected by a higher percentage of total aberrant pollen grains compared to collapsed pollen grains. By this assay, the percentages of total aberrant pollen grains were similar to the percentages of collapsed pollen grains for all genotypes except one: a much higher number of aberrant pollen grains were produced by the *gsl1-1/+ gsl5-2/gsl5-3* plants (63%). This increased

number probably reflects the abnormally large pollen grains found in this genotype, and indicates a second mutant pollen phenotype undetectable by my light/fluorescent microscopy assay. That this genotype has such a high percentage of aberrant pollen grains cannot be explained by a gametophytic deficiency in either GSL, since half of its pollen would be *GSL1 gsl5*, and the *gsl5* homozygotes which produce pollen only of this haplotype produce only a low percentage of aberrant pollen grains. Thus, in addition to a gametophytic role for *GSL1* and *GSL5* in pollen development, there exists a second role as well. In this role, there is again redundancy between *GSL1* and *GSL5*, and if the *gsl1-1* allele produces a complete functional knock-out, then *GSL5* may again be the more important of the two genes.

SEM showed differences in the severity of mutant pollen phenotypes between the different genotypes. The collapsed pollen grains produced by the *gsl1-1/gsl1-1 gsl5/+* mutant lines (**Fig. 6.6D**) were more anomolous that those of the single *gsl5* mutants (**Fig. 6.6C**). They were smaller, more crumpled, and almost completely lacking in any recognizable pore structure. While exine patterning was present, there were smaller spaces between reticulations. As observed with the light microscope (**Fig. 6.5I**, white arrow), collapsed pollen grains were sometimes found still attached to the tetrad (**Fig. 6.6F**). In some cases pollen grains appeared wild-type, but with a slight aberration where they may have been attached to the tetrad (**Fig. 6.6G**) - these pollen grains are probably similar to those observed in **Fig. 6.5I, no. 3**. The *gsl1-1/+ gsl5/gsl5* mutant lines produced, in addition to small, collapsed pollen grains (data not shown), many abnormally large pollen grains with an aberrant pore number and symmetry (**Fig. 6.6E**). Non-dissociated tetrads in these mutants were frequently found and even more aberrant

(**Fig. 6.6H**) than those of the *gsl1-1/gsl1-1 gsl5/+* mutant lines, the delineation between individual pollen grains barely discernable.

Pollen development and pollen callose in gsl1-1/+ gsl5-2/gsl5-3 mutant plants

In order to determine the role of *GSL1* and *GSL5* in pollen development and callose deposition, Masa Kanaoka examined cross-sections of anthers from both wild-type and mutant plants at different stages during pollen formation, staining them with toluidine blue o to visualize the cells, and with aniline blue to visualize callose under UV light. He could not discern differences between the wild-type and weaker mutants (single *gsl5* and *gsl1-1/gsl1-1 gsl5/+* mutant lines), but there were dramatic differences in the *gsl1-1/+ gsl5-2/gsl5-3* mutants (**Fig. 6.7**) (he did not analyze any *gsl1-1/+ gsl5-2/gsl5-2* mutants). At the pollen mother cell stage (**Fig. 6.7A-D**) meiosis appeared normal, and the pollen mother cells were surrounded by a callose wall. There was no apparent difference between the mutants and wild-type. At the tetrad stage, however, there was a significant difference between the wild-type (**Fig. 6.7E,F**) and the mutant (**Fig. 6.7G-J**). In the wild-type, tetrads were clearly visible, and each cell in the tetrad was surrounded by a callose wall. In the mutant, no normal tetrads were ever observed (**Fig. 6.7G,I,J**). Frequently, impaired cytokinesis following meiosis was observed (**Fig. 6.7J**). Callose walls were almost completely lacking (**Fig. 6.7H**).

It is surprising that mutants lacking callose in pollen tetrad walls still make pollen grains with a recognizable exine layer. The presence of callose in the tetrad wall has been surmised to be important for preventing the fusion of individual microspores (Waterkeyn, 1962). The work desribed in this chapter supports this hypothesis. But it

has also long been believed that tetrad wall callose directs exine patterning (Waterkeyn and Beinfait, 1970; Zhang et al., 2002). *GSL2* has been shown to be essential for exine patterning (Dong et al., 2005; Nishikawa et al., 2005). Recently, it has been discovered that mutants lacking the ability to process *GSL2*, while able to make the callose that separates the 4 meiotic products of the tetrad, cannot make the callose that surrounds the tetrad as a whole (Kanaoka, personal communication). This callose is laid down at the mother cell stage, prior to meiosis. Such mutants produce pollen with no recognizable exine layer. It is thus possible that the callose surrounding the entire tetrad is synthesized by one callose synthase, and is responsible for exine patterning, while the callose separating the individual meiotic products is made by two other callose synthases, and is important for tetrad dissociation.

I conclude that *GSL1* and *GSL5* are required for the synthesis of the callose that normally separates the microspores that form after meiosis, but not for the callose that surrounds the pollen mother cell.

Discussion

The role of callose synthase genes in plant development

The synthesis of ß-1,3-glucans has been most extensively studied in fungi, where a complex comprised of the catalytic subunit FKS1 or FKS2 and the regulatory subunit Rho1p are responsible for their synthesis (Douglas *et al.*, 1994; Schimoler-O'Rourke *et al.*, 2003). In *Arabidopsis*, a cDNA encoding the cell plate-specific, callose synthase catalytic subunit CalS1 (*GSL6*) was cloned, identified and its predicted protein found to

have sequence homology with FKS1. Based on homology to its deduced amino acid sequence, 12 putative callose synthases were found in *Arabidopsis* (Hong et *al.*, 2001). The genes encoding these proteins were annotated independently by the Stanford group (http://cellwall.stanford.edu/php/structure.php?family=gsl). The identity of one of these, *GSL5*, has been verified by dsRNAi technology (Jacobs *et al.*, 2003) and by use of mutants that interfered with the synthesis of callose (eg. Nishimura *et al.*, 2003; Østergaard *et al.*, 2002). A family of 6 putative callose synthases have been identified in barley and the identity of one of them as a callose synthase has been verified (Li *et al.*, 2003).

The challenge is to determine where and when each of these callose synthases are active, and the roles that the callose they produce have in the plant. Although callose is a normal constituent of intact, healthy plants, most of the recent attention to callose has centred on its role in disease resistance. Plants produce callose as part of their response to wounding or to pathogen attack, often forming callose plugs and papillae near the pathogen. Defense callose in *Arabidopsis* is due, at least in part, to induction above normal levels of *GSL5*; *GSL6* and *GSL11* do not appear to be involved (Jacobs *et al.*, 2003; Nishimura *et al.*, 2003).

Other studies on callose synthase have provided contradictory information about the importance of callose synthase genes in normal plant development. Hong *et al.*, 2001, have localized GSL6 to the growing cell plate where it interacts with phragmoplastin and a UDP-glucose transferase. *GSL5* transcripts were found to be expressed primarily in flowers of *Arabidopsis* (Østergaard *et al.*, 2002). However, disruption of *GLS5*, *GLS6* and *GLS11* has been reported to show no visible phenotype in

healthy plants (Nishimura *et al.*, 2003). Callose is known to play a major role in both pollen formation (Scott *et al.*, 2004), and in the cell walls of the pollen tube (Edlund *et al.*, 2004) and several *GSL* genes are preferentially expressed in anthers or in pollen (Doblin *et al.*, 2001; Østergaard *et al.*, 2002; Becker *et al.*, 2003), but the role of specific *GSL* genes in pollen development has not been reported.

I have focused our attention on two closely related genes, *AtGSL1* and *AtGSL5*. Both of the genes were expressed in all tested organs, including root, rosette leaf, stems and flowers (**Fig. 6.1**). Because *GSL1* and *GSL5* are closely related, I hypothesized that these genes may be redundant. To test whether mutations in both genes would produce a phenotype, I have obtained genetic and putative functional knockouts. For *GSL5*, I obtained a T-DNA insertion in the second exon, which results in a genetic knockout (**Fig. 6.2B**). For both *GSL1* and *GSL5*, I obtained point mutations, predicted to encode for truncated, functionally inactive proteins. The phenotypes of homozygous single mutants were compared, and crosses were made in an attempt to construct homozygous double mutants for these genes.

Both GSL1 and GSL5 have a role in sporophytic development

As long as *GSL5* was present, *GSL1* appeared to be dispensable since a homozygote for the *gsl1-1* mutation had no observable phenotype. The *GSL5* gene, on the other hand, was necessary for normal development since homozygotes for either *gsl5-2* and *gsl5-3*, and the *gsl5-2/gsl5-3* transheterozygote had smaller rosette leaves. The apparent contradiction between these results and the reported lack of such a phenotype in *GSL5* mutants by Nishimura *et al.*, 2001 and Jacobs *et al.*, 2001, may be due to different

experimental conditions. There is no reason to believe that the reduced rosette phenotype that we observed is due to any disease, although I have not grown these mutants axenically.

Plants that were *gsl1-1/gsl1-1 gsl5-2/+*, *gsl1-1/gsl1-1 gsl5-3/+*, *gsl1-1/+ gsl5-2/gsl5-2* or *gsl1-1/+ gsl5-2/gsl5-3* were produced, but all attempts to produce double homozygous mutants of the *GSL1* and *GSL5* genes by selfing these mutants failed. Both the *gsl1-1/gsl1-1 gsl5/+* lines appeared normal. Rosette leaf size was similar to that of both wild-type and *gsl1-1* single mutants, and the plants were fertile. On the other hand, plants from the *gsl1-1/+ gsl5/gsl5* lines were extremely small, with very small rosette leaves and bolts, short roots, and smaller flowers. They produced very few viable seeds. While a single allelic dose of *GSL5* in a *gsl1-1* background was sufficient for development, *GSL1* in a *gsl5-2* or *gsl5-3* background was haploinsufficient. In conclusion, these observations provide strong evidence for a role of both genes in sporophytic development, with a more substantial contribution by *GSL5*. It must be noted, however, that the *gsl1-1* allele may be weaker than *gsl5-2*, since the lesion within the *gsl5-2* mutant allele lies further toward the 5' end of the gene than the *gsl1-1* mutation. However, the latter would still exclude a highly conserved region of GSL1. Given this, and the severity of the *gsl1-1/+ gsl5/gsl5* mutant phenotypes in comparison to the *gsl5* single mutants, it is likely that the *gsl1-1* allele does encode a non-functional protein; certainly, the protein is severely impaired.

GSL1 and GSL5 are important for pollen development and fertility

I found evidence for a gametophytic role of the *GSL* genes in pollen development. Pollen fertility required at least one functional allele of either *GSL1* or *GSL5*. Both *gsl1* and *gsl5* single mutants were fertile. But when *Col-0* wild-type plants were fertilized with pollen from either of the *gsl1-1/gsl1-1 gsl5/+* mutant lines, none of the offspring inherited both mutant alleles, indicating that the pollen bearing the *gsl1 gsl5* chromosome was sterile and thus explaining the failure to obtain a *gsl1 gsl5* homozygous double mutant by selfing.

Some (15%) collapsed pollen grains were produced by both *gsl5* mutant lines, but not by *gsl1-1* single mutants. Both the *gsl1-1/gsl1-1 gsl5/+* mutant lines and the *gsl1-1/+ gsl5-2/gsl5-3* plants displayed twice as many collapsed pollen grains as the *gsl5* homozygous single mutants. These collapsed pollen grains were incapable of germination.

The collapsed, inviable pollen grain phenotype seen in the *gsl1-1/gsl1-1 gsl5/+* and *gsl1-1/+ gsl5/gsl5* double mutants may be the result of the pollen *gsl1-1 gsl5* haplotype. The expected amount of sterile pollen grains would be at least 50% if pollen bearing such a haplotype develops into a countable pollen grain. Some slightly aberrant and inviable pollen grains were observed in this assay, but not counted as collapsed, and may have been *gsl1 gsl5*. But given that I could not find 50% aberrant pollen grains for the *gsl1-1/gsl1-1 gsl5/+* mutants even under the SEM, it is possible that some *gsl1 gsl5* pollen grains may have been aborted in their development at an early stage, and therefore not observed in either microscopical assay. Alternatively, there may be *gsl1 gsl5* pollen grains which, while sterile, retain a normal morphology during their maturation. My in

vitro pollen germination assays did show some normal pollen grains which failed to produce pollen tubes, but such assays frequently do not show 100% germination even for wild-type controls.

The fact that a low number of collapsed pollen grains are found in the *gsl5* homozygotes, and not in the *gsl1-1* homozygotes, indicates that there is a low incidence for GSL1 insufficiency in a pollen haplotype where GSL5 is lacking. Provided that the *gsl1-1* allele encodes a functional knock-out, this would indicate that GSL5 plays a greater role than GSL1 in the maturation of the male gametophyte.

It should be noted that for all mutant lines, including *gsl1-1+ gsl5-2/gsl5-3*, a certain fraction of pollen grains were capable of germination. Also, pollen taken from *gsl1-1/+ gsl5-2/gsl5-3* can readily pollinate *Col-0*, but pollen taken from *Col-0* results in only limited fertilization of *gsl1-1/+ gsl5-2/gsl5-3* (data not shown). thus, the extremely limited fertility of the *gsl1-1+ gsl5-2/gsl5-3* plants is not solely due to a pollen defect.

The data indicate another and sporophytic role for both the *GSL* genes in pollen development. While the *gsl1-1/+ gsl5-2/gsl5-3* plants produced as many collapsed and inviable pollen grains as the *gsl1-1/gsl1-1 gsl5/+* plants (30%), their total number of aberrant pollen grains was much higher (63%), due to the production of many unusually large and misshapen pollen grains. But half of the pollen produced by *gsl1-1/+ gsl5-2/gsl5-3* would have the haplotype *GSL1 gsl5*. Most pollen grains of this haplotype, produced by the single *gsl5* homozygotes, are normal. Thus, the increased number of aberrant pollen grains in the *gsl1-1/+ gsl5-2/gsl5-3* cannot be explained by individual pollen haplotypes. Also, provided that the *gsl1-1* allele encodes a functionally incapable protein, the data again indicate that *GSL5* is more haplosufficient in the absence of *GSL1*

than *GSL1* is in the absence of *GSL5*. Hence, while a sporophytic role in pollen development is indicated for both genes, *GSL5* may be the more important player.

Why are GSL1 and GSL5 so important in pollen development and fertility?

Callose is known to be involved in several steps in pollen development (Heslop-Harrison, 1964; Scott et *al.*, 2004). A callose wall is laid down inside the primary wall around the pollen mother cells prior to meiosis. After meiosis, the four resulting spores are separated by a callose wall, which is laid down at cytokinesis (Otegue and Staehelin, 2004). These two callose walls are then digested at the time of release of the tetraspores. Premature dissolution of this wall causes male sterility in tobacco (Worall *et al.*, 1992). Germination of the pollen grain involves an accumulation of callose at the pore where the tube will emerge. The pollen tube has a callose wall inside of the cellulosic wall, and has a callose plug back from the tip which confines the cytoplasm to the growing tip of the pollen tube. All of these steps in which callose participates should involve one or more *GSL* genes, and a mutation that blocks any of these steps would be expected to lead to male sterility.

Light microscopy shows that 15% of mature pollen grains from the *gsl5* mutant lines, and 30% of pollen grains from the *gsl1-1/gsl1-1 gsl5/+* and *gsl1-1/+ gsl5/gsl5* mutant lines are collapsed in appearance, and inviable. These pollen grains, which are speculated to be *gsl1 gsl5* in haplotype, are smaller than normal, and shriveled. SEM shows that the exine patterning in these mutant pollen grains is present, although the distance between reticulations in the smaller pollen grains is smaller. The pores are misplaced and misshapen. But at least in the single *gsl5* and *gsl1-1/gsl1-1 gsl5/+* mutant

lines, under the light microscope, pollen morphology appears normal up until, and including, the bicellular stage (data not shown). The collapsed nature of these pollen grains may thus be due to a deficiency in GSL1 and GSL5 late in the development of the pollen grain. The role of callose at this stage of pollen development remains unknown.

My study has found a role for callose earlier in pollen development. Masa Kanoaka's data indicates that *GSL1* and *GSL5* are essential for the formation of the callose wall that separates the tetraspores, but not for the callose wall that surrounds the pollen mother cells (**Fig. 6.7**). Whereas the callose, as visualized by aniline blue staining, is present between microspores in the tetrads of wild-type plants (**Fig. 6.7F**), it is not present in the aberrant tetrads of *gsl1-1/+ gsl5-2/gsl5-3* plants (**Fig. 6.7H**) (this analysis was not done on *gsl1-1/+ gsl5-2/gsl5-2* mutants). Other *GSL* genes may be required for the synthesis of the pollen mother cell callose wall. *GSL2* or *GSL2* homologues are highly expressed in pollen (Becker *et al.*, 2003; Doblin *et al.*, 2002), and may be involved here, or in the formation of the callose wall of pollen tubes.

In the *gsl1-1/+ gsl5/gsl5* mutant lines, enlarged pollen grains were often observed, and microspores in *gsl1-1/+ gsl5-2/gsl5-3* plants were sometimes found to be enlarged and multinucleate, suggesting that cytokinesis was at least partially defective after meiosis. These large pollen grains, which have more than three pores, are found in other mutants with defective post-meiotic cyokinesis (eg. *TETRASPORE* and *STUD*) (Hülskamp *et al.*, 1997; Spielman *et al.*, 1997; Tanaka *et al.*, 2004; Yang *et al.*, 2003). It is unknown if the observed cytokinetic failure is a direct result of a lack of callose in the tetrad wall, or if *GSL1* and *GSL5* also play another role in microspore cytokinesis.

GSL1 and GSL5, and tetrad wall synthesis, may be important for the ultimate dissociation of the pollen grain tetrad. In *gsl1-1/+ gsl5/gsl5* mutant lines, undissociated tetrads were frequently found and dramatically aberrant, individual pollen grains almost indiscernable. In the *gsl1-1/gsl1-1 gsl5/+* mutant lines, while individual pollen grains could always be discerned, aberrant pollen grains were sometimes found still attached to the tetrad. In both cases, these undissociated tetrads may be the result of incomplete cytokinesis between microspores, or to another problem entirely. The callose in the tetrad walls might also act to isolate the products of meiosis in order to prevent cell cohesion and fusion (Waterkeyn, 1962; Waterkeyn and Beinfait, 1970), acting as a molecular filter to isolate developing sister spores (Heslop-Harrison, 1964; Heslop-Harrison and Mackenzie, 1967). The release of the individual cells of the tetrad as free microspores involves the degradation of the callosic wall by callase, produced by the tapetum layer of the anther (Scott et *al.*, 2004). However, tetraspore separation involves more than callose degradation, as attached tetraspores have been obtained with mutants that affect the synthesis of polygalacturonase (Rhee and Somerville, 1998), and a pollen kinesin (Yang *et al.*, 2003; Tanaka *et al.*, 2004).

The tetrad wall callose which separates the individual microspores does not appear until after meiosis, but the genetics of the tetrad wall deficiency point to a sporophytic, rather than a post-meiotic problem (**Fig. 6.8**). A tetrad of a *gsl1-1/+ gsl5-2/gsl5-3* plant has 2 pollen hapolotypes: 2 microspores are *gsl1-1 gsl5*, and 2 microspores are *GSL1 gsl5*. Its tetrads do not make any callose walls. But all of the microspores in a *gsl5* tetrad are *GSL1 gsl5*, and half of the microspores in a *gsl1-1/gsl1-1 gsl5/+* plant are *gsl1-1 gsl5*, and the tetrads in both these genotypes make complete callose walls. There

are two possibilities: tetrad wall formation is either dependent on the cumulitive genotype of all the haploid pollen grains, o the callose synthases involved in this process are laid down by the pollen mother cell prior to meiosis and activated later. Production of the tetrad wall is the most likely explanation for a 'sporophytic' role for *GSL1* and *GSL5* in pollen development; the lack of a tetrad wall is the most likely cause of the abnormally large pollen grains and severely non-dissociated tetrads seen in the *gsl1-1/+ gsl5/gsl5* mutant lines. Pollen grains in the *gsl1-1/gsl1-1 gsl5/+* mutant lines may not always dissociate because of a weaker reduction of callose in the tetrad wall, not observable by our assay.

Thus, GSL1 and GSL5 may be involved at more than one stage of pollen development, both at the cytokinetic stage, during formation of the tetrad wall, and later, following the bicellular stage. Callose is also important in pollen tube growth, as part of both the pollen tube wall, and the plugs that isolate the cytoplasm of the growing tip (Rae *et al.*, 1985; Ferguson *et al.*, 1998; Schlüpmann *et al.*, 1994; Meikle *et al.*, 1991). GSL1 and GSL5 may be responsible for the production of this callose. If so, their action is redundant. I cannot check this with my mutants as *gsl1-1 gsl5-2* and *gsl1-1 gsl5-3* pollen grains are completely inviable. I have a large library of TILLING mutants for both of these genes that harbour point mutations, which should confer more subtle phenotypes, and which may provide a role for these genes in pollen tube growth. Future investigations should also reveal other non-pollen-related roles for GSL1 and GSL5 in plant fertility, which have been indicated by this study.

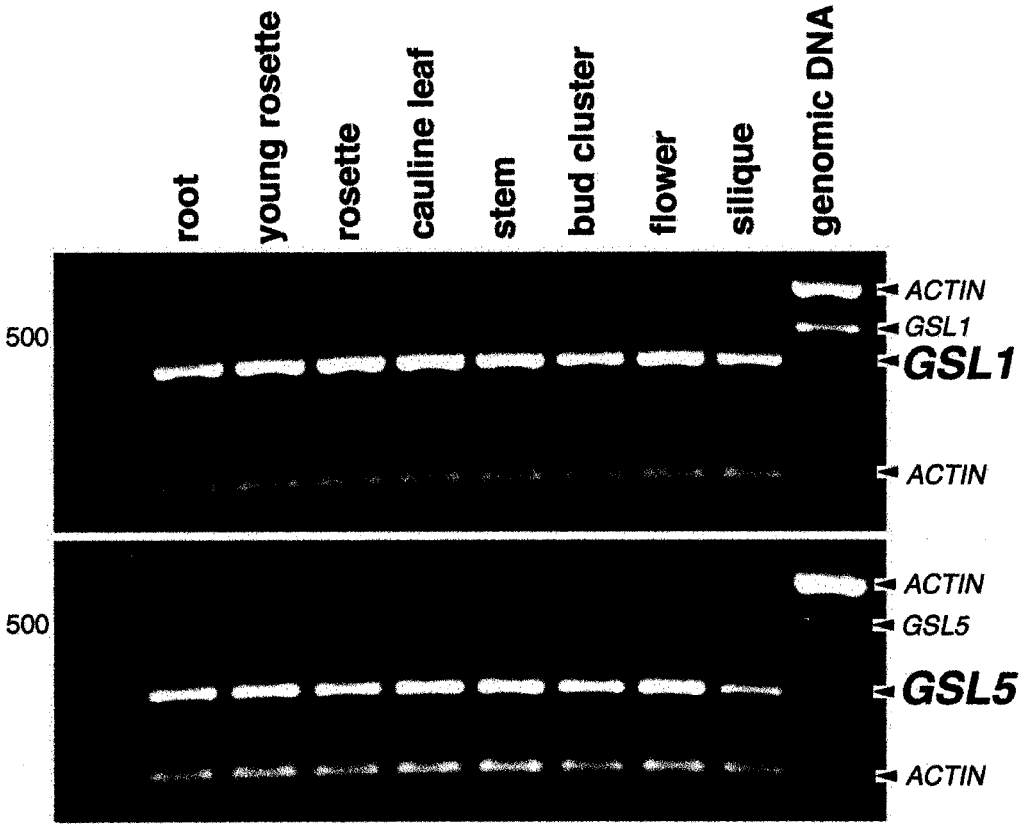

Figure 6.1. *GSL1* and *GSL5* expression in unwounded organs of *Arabidopsis*. RT-PCR analysis. All organs tested show expression of *GSL1* and *GSL5*. Expression of actin is included as a control. A control for genomic DNA is also included.

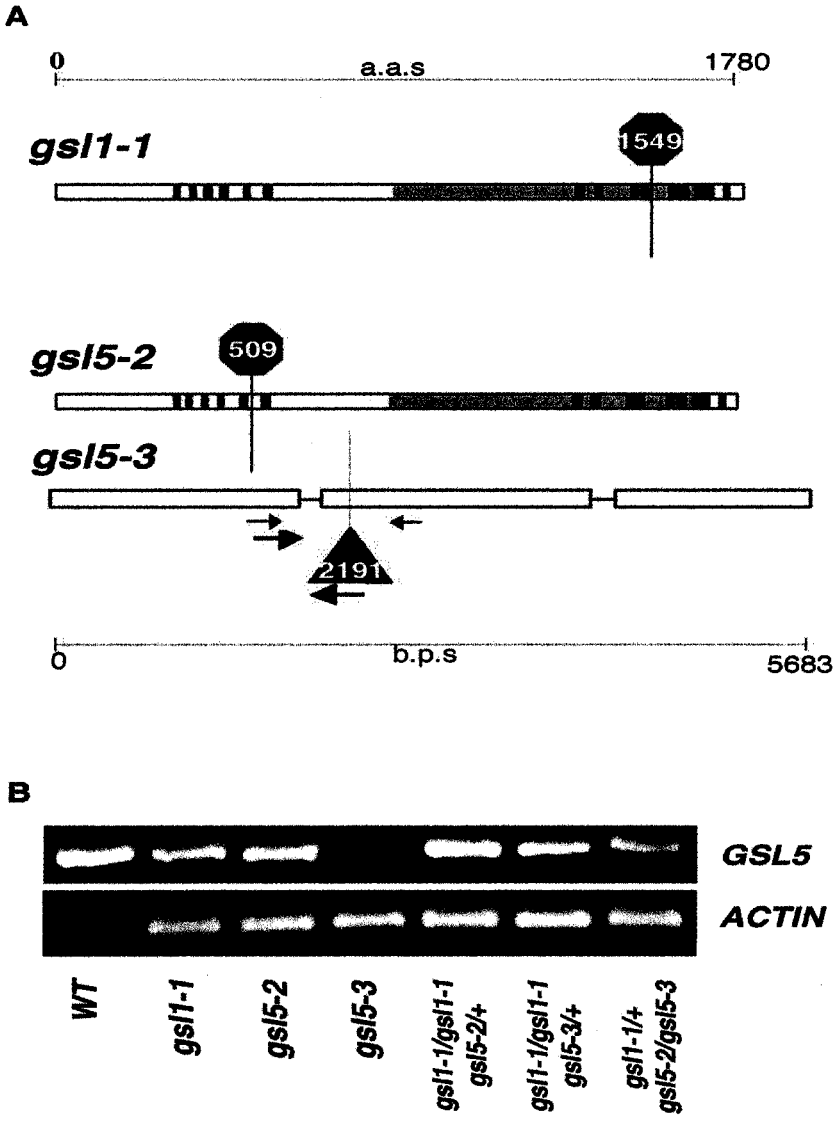

Figure 6.2. A. Putative knock-out alleles aquired for *GSL1* and *GSL5*. Mutants carrying alleles encoding for truncations in GSL1 (*gsl1-1*) and in GSL5 (*gsl5-2*) were acquired from the Seattle TILLING project. For details on how to interpret protein models, see Chapter 4; Fig. 16. The octagon represents the location of the truncation; the number is the amino acid at which the truncation occurs. *gsl5-3* carries a T-DNA insertion in *GSL5*; this was acquired from SIGnAL. The triangle represents the location of the insert; the number gives the base pair at which the insertion occurs. The gene model for *gsl5-3* also indicates the approximate location of genotyping primers. **B.** RT-PCR analysis of *GSL5* expression in mutant lines. RT-PCR was performed on RNA taken from rosette leaves only. The T-DNA insertion in *gsl5-3* completely knocked out gene expression.

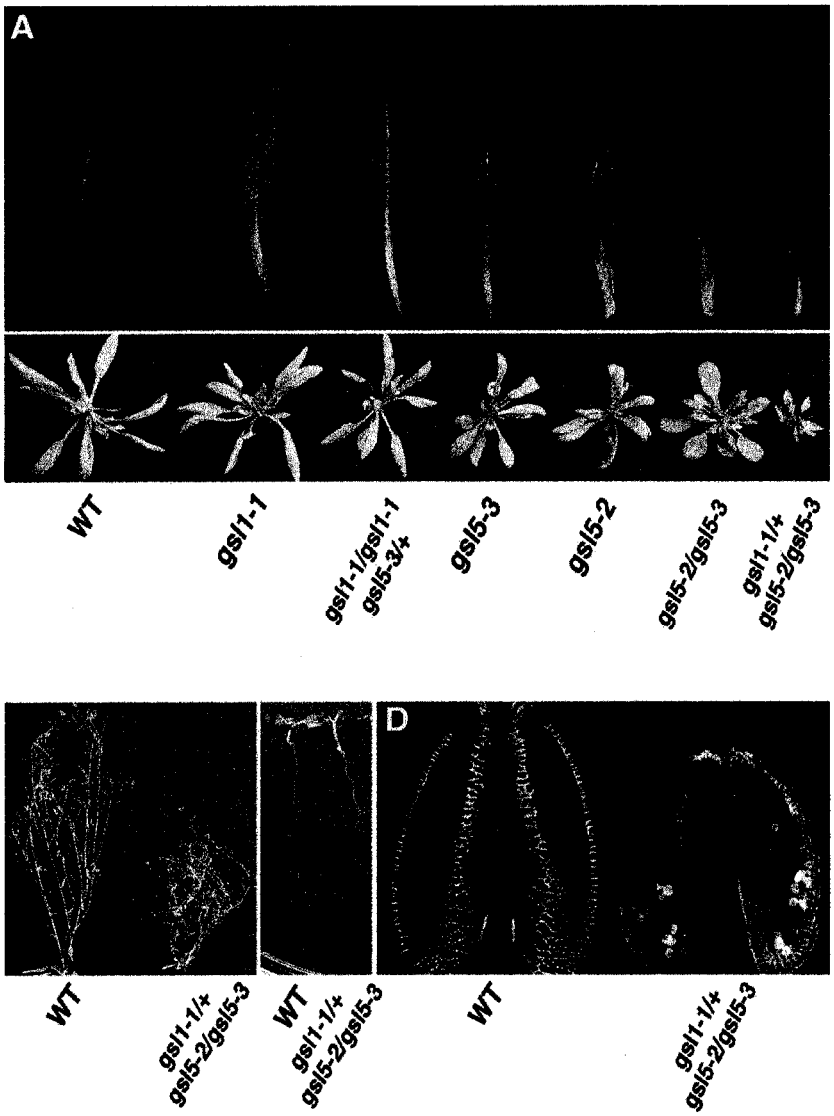

Figure 6.3. *gsl* mutant sporophytic phenotypes. **A.** Leaves and rosettes. *gsl1-1* homozygous lines showed no mutant phenotype, even when heterozygous for *gsl5* mutant alleles. *gsl5* homozygous mutants had smaller leaves, resulting in reduced rosette diameters. Trans-heterozygotes for both *gsl5* mutant alleles had a reduced leaf and rosette size, confirming the *gsl5* mutant phenotype. *gsl1-1/+ gsl5/gsl5* plants showed severe mutant phenotypes. **B-D.** Comparison of *gsl1-1/+ gsl5-2/gsl5-3* mutants with WT. Mutants had extremely short lateral bolts **(B)** and shorter roots **(C)** in comparison with wild-type. **D.** Mutants had smaller floral organs, most noticeably the anthers (anthers shown in confocal optical longitudinal section). *gsl1-1/+ gsl5/gsl5* mutant lines produced very few viable seeds.

	8 days	at bolting			open flower		6 weeks
Genotype	**primary root length (mm)**	**rosette diameter (mm)**	**#leaves**	**maximal length of largest leaf (mm)**	**pistil length (mm)**	**anther length (μm)**	**height of tallest lateral bolt (mm)**
WT	38.6±4.9	84.1±10.9	11.2±0.8	47.2±5.0	2.44±0.26	429±40	388.6±13.5
gsl1-1	36.9±13.6	80.6±8.2	12.3±0.5	47.0±4.4	2.40±0.22	398±23	335.0±44.6
gsl1-1/gsl1-1 gsl5-2/+	39.6±11.5	91.0±8.4	12.7±1.1	49.5±4.3	2.67±0.15	383±37	362.0±39.4
gsl1-1/gsl1-1 gsl5-3/+	40.8±5.4	76.2±6.8	12.8±1.0	45.1±4.8	2.66±0.33	403±38	312.0±50.7
gsl5-2	31.3±6.2	55.7±9.0	11.7±1.7	33.4±7.4	2.53±0.30	402±48	301.9±63.8
gsl5-3	36.2±7.8	62.5±9.3	12.1±1.5	37.6±6.1	2.46±0.15	346±31	355.0±102.5
gsl5-2/gsl5-3	43.9±7.5	56.5±14.2	11.3±0.5	30.3±5.0	2.75±0.32	401±19.3	
gsl1-1/+ gsl5-2/gsl5-3	17±5.3	36.8±6.0	10.8±1.1	18.2±3.3	2.15±0.18	298±37	222.5±26.3

Table 6.1. *gsl* mutant sporophytic phenotypes. Rosette measurements: numbers represent the mean diameters of 30 plants (3 plantings, 10 plants each). Root, leaf and bolt measurements: numbers represent the mean of a minimum of 10 plants, taken from a single planting. Flower measurements: numbers represent the mean of a minimum of 10 flowers taken from a minimum of 5 plants. All anthers per flower were measured. Error bars represent standard deviations. Measurements for *gsl5-2* were taken from the offspring of two homozygous lines, isolated from a thrice-outcrossed, selfed heterozygote; measurements for *gsl5-3* were taken from the offspring of one homozygous line.

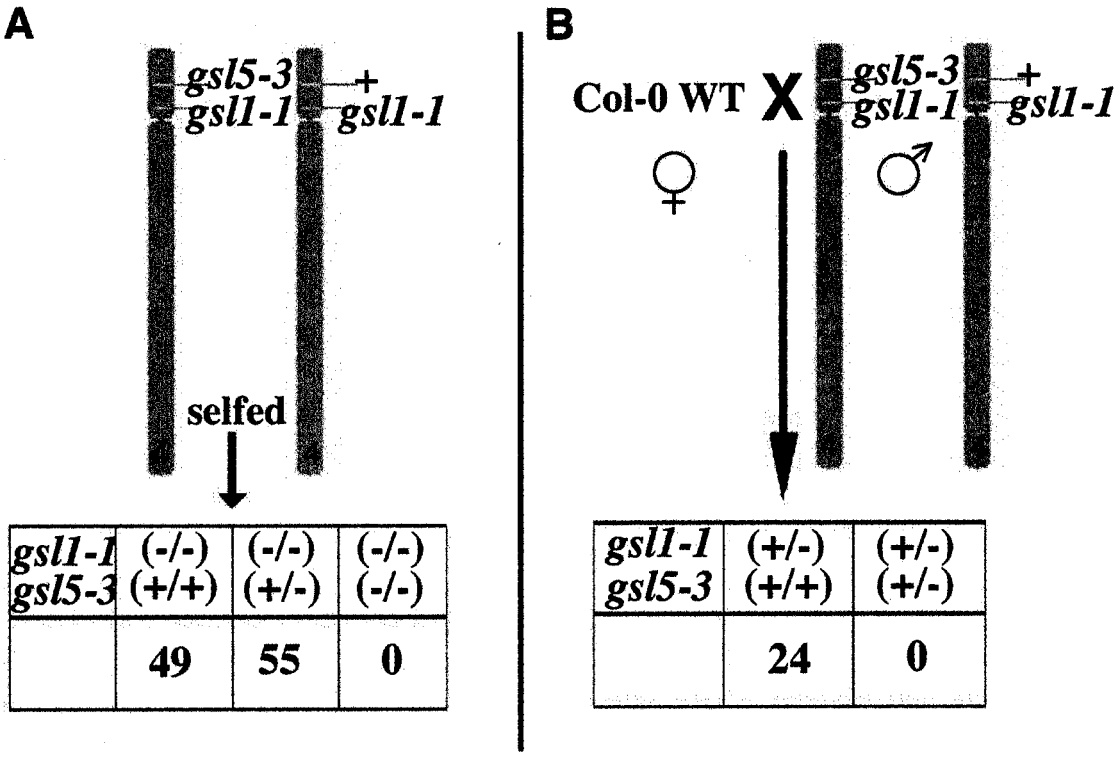

gsl1-1 gsl5-3	(-/-) (+/+)	(-/-) (+/-)	(-/-) (-/-)
	49	55	0

gsl1-1 gsl5-3	(+/-) (+/+)	(+/-) (+/-)
	24	0

Figure 6.4. The lethality of the homozygous double mutant is a male gametophytic trait. **A.** Progeny of selfed *gsl1-1/gsl1-1 gsl5-3/+* mutants. None were homozygous for both putative knock-outs. The same was found for *gsl1-1/gsl1-1 gsl5-2/+* mutants (data not shown). For the progeny of *gsl1-1/gsl1-1 gsl5-3/+*, there were also half as many heterozygotes as would be expected. **B.** Progeny of wild-type Col-0, pollinated from *gsl1-1/gsl1-1 gsl5-3/+* mutants. Transmission of the chromosome bearing both the mutation in *GSL1* and in *GSL5* through the male gametophyte was zero.

Figure 6.5. Loss-of-function in *GSL1* and *GSL5* confers aberrant pollen grain morphology and gametophytic lethality. (A,B) Confocal optical sections through **(A)** a wild-type and **(B)** a *gsl1-1/gsl1-1 gsl5-3/+* anther. Wild-type pollen grains appeared round. The mutant had a high number of collapsed pollen grains. **C-E.** Toluidine blue-stained cross-sections through a **(C)** wild-type **(D,E)** *gsl1-1/+ gsl5-2/gsl5-3* anther. **C,D.** The mutant had both collapsed (black arrow-head) and abnormally large (black arrows) pollen grains. The large pollen grains typically had an unusual number of pores (four pores can be counted in the large pollen grain on the right). **E.** Microspores were sometimes observed to be large and multi-nucleate (black arrow). **F.** Light microscopy of a whole-mounted *gls1-1/gls1-1 gls5-3/+* flower, free pollen grains. Many pollen grains had a collapsed appearance. Under high transmission, unlike normal pollen, collapsed pollen showed an apparent lack of cellularization. Using this technique, I also observed a high number of collapsed pollen inside the anther (data not shown). **G.** Alexander (cytoplasmic) staining of *gsl1-1/gsl1-1 gsl5-3/+* pollen grains. The collapsed pollen had reduced amounts of cytoplasm. **H.** Whole-mounted *gsl1-1/gsl1-1 gsl5-2/+* pollen grains. Occasionally, mutant pollen grains failed to dissociate from the tetrad. **I-K.** Fluorescent microscopy of whole-mounted, aniline-blue stained pollen grains from *gsl1-1/gsl1-1 gsl5-3/+* plants. **I.** Free pollen grains on germination medium. **J,K.** Pollen grains on the pistil of a squashed flower from a *gsl1-1/gs1-1 gsl5-3/+* plant. Normal pollen grains could generate a pollen tube and callose plug **(I no. 1 and J)** while collapsed pollen grains could not **(I no. 2 and K)**. Some pollen grains had only minor aberrances, but still had problems with germination **(I no. 3)**. Non-dissociated mutant pollen grains were again observed **(I, white arrow)**. Pictures are overlays of the same specimen under excitation (EX): 330-380/ dichroic mirror (DM): 400/ barrier filter (BA): 420 and either (L) EX: 532-587/ DM: 595/ BA: 608-683 or (M,N) transmitted light. Magnification bars: 10 μ.

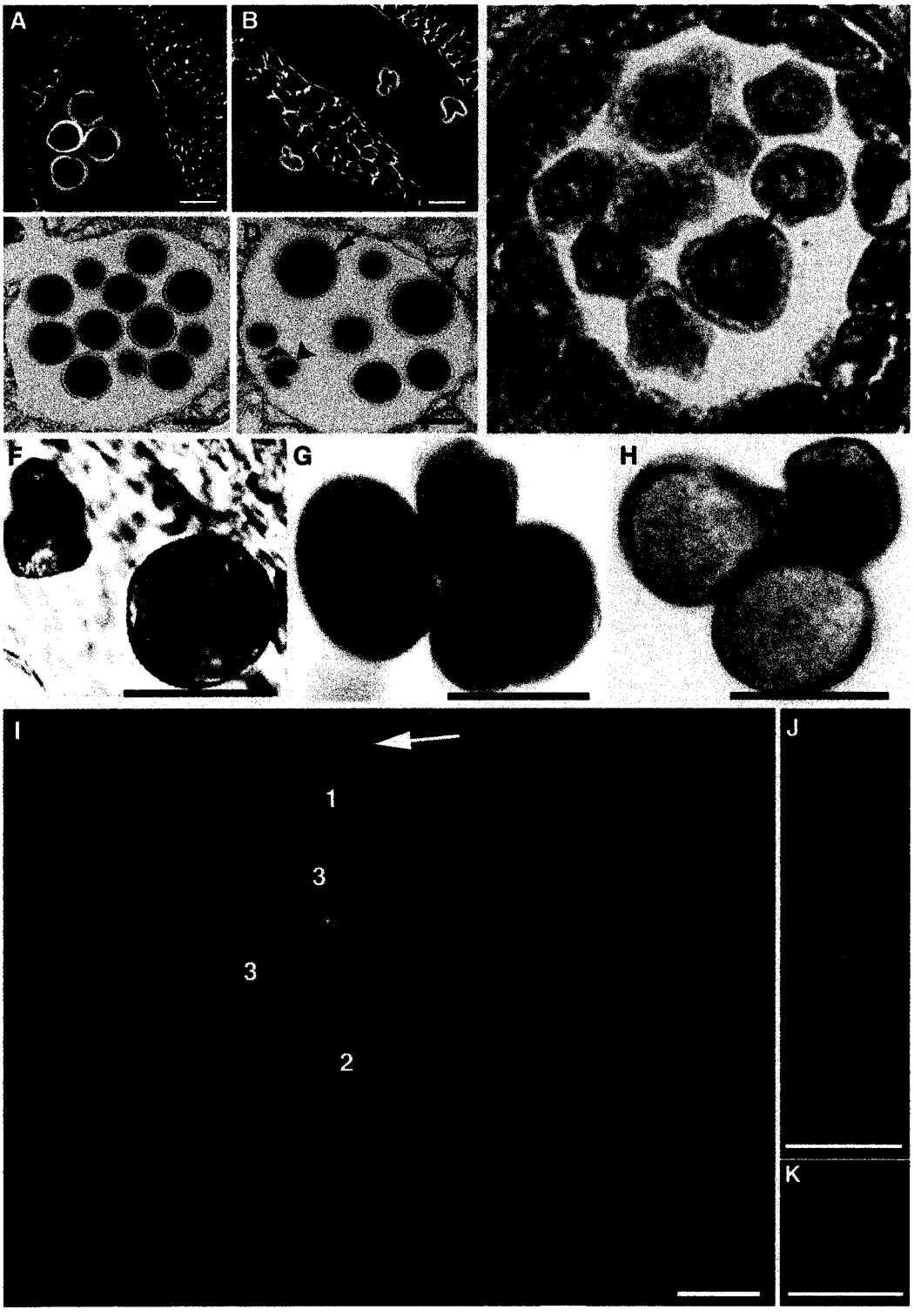
A
B
F
G
H
I
1
3
3
2
J
K

Genotype	% collapsed pollen grains	% total aberrant pollen grains
WT	0	0
gsl1-1	0	0
gsl5-2	14	6
gsl5-3	15	14
gsl5-2/gsl5-3	8	
gsl1-1/gsl1-1 gsl5-2/+	27	29
gsl1-1/gsl1-1 gsl5-3/+	26	38
gsl1-1/+ gsl5-2/gsl5-3	34	63

Table 6.2. Percentages of collapsed and total aberrant pollen grains in single and double mutants. Collapsed pollen grains counted under the light microscope, total number of aberrant pollen grains counted under the SEM. *gsl1-1/gsl1-1 gsl5-2/+*, *gsl1-1/gsl1-1 gsl5-3/+* and *gsl1-1/+ gsl5-2/gsl5-3* mutants produced a high and similar number of collapsed pollen compared to single mutants. But *gsl1-1/+ gsl5-2/gsl5-3* plants produced the highest number of total aberrant pollen. A minimum of 300 pollen grains per genotype were counted. Pollen grains were counted as collapsed if they were small and optically dense under transmitted light (picture not shown), or dramatically different in their fluorescent signature (**Fig. 22I, no. 2**). Pollen grains were counted as aberrant if they had any obvious visual defects under the SEM. For all pollen grain observations, and for all genotypes, pollen grains were collected from a minimum of 5 flowers from a minimum of 5 plants. Pollen grains from *gsl1-1/+ gsl5-2/gsl5-2* were not counted.

Figure 6.6. Mutant pollen grains have an exine layer, and the severity of their phenotype varies with genotype. SEM pictures of pollen grains. **A.** Wild-type and **B.** *gsl1-1*. These plants produce no aberrant pollen. **C.** *gsl5-2*. Both *gsl5* homozygous mutants produce a small number of aberrant pollen. **D.** *gsl1-1/gsl1-1 gsl5-3/+*. The aberrant pollen grains of the double mutants were typically more severely deformed than those of the single *gsl5* mutants. The elongated shape of the pollen grains was severely compromised, and recognizable pores were absent. While they had an exine layer, the spaces between the reticulations were smaller. These pollen grains are probably similar to that shown in **Fig. 6.5I, no. 2**. **E.** *gsl1-1/+ gsl5-2/gsl5-3*. This genotype produced pollen grains very similar to those shown in Figure 7D, as well as abnormally large pollen grains. These large pollen grains displayed a normal exine patterning. Their aberrant pore structure was easily seen under the SEM. **F.** *gsl1-1/gsl1-1 gsl5-3/+*. As with the light microscope, we sometimes detected non-dissociated, aberrant pollen grains in the double mutant. This was not typically observed in the single *gsl5* mutants. These pollen grains are similar to those found in **Fig. 6.5I**, white arrow. **G.** Sometimes, pollen grains appeared wild-type, but with a slight aberration where they may have been attached to the tetrad. This pollen grain may be similar to **Fig. 6.5I, no. 3**. **H.** *gsl1-1/+ gsl5-2/gsl5-3*. Frequently, these pollen grains showed a severe inability to dissociate. In some tetrads, individual pollen grains could barely be recognized. Magnification bars: 10 μ.

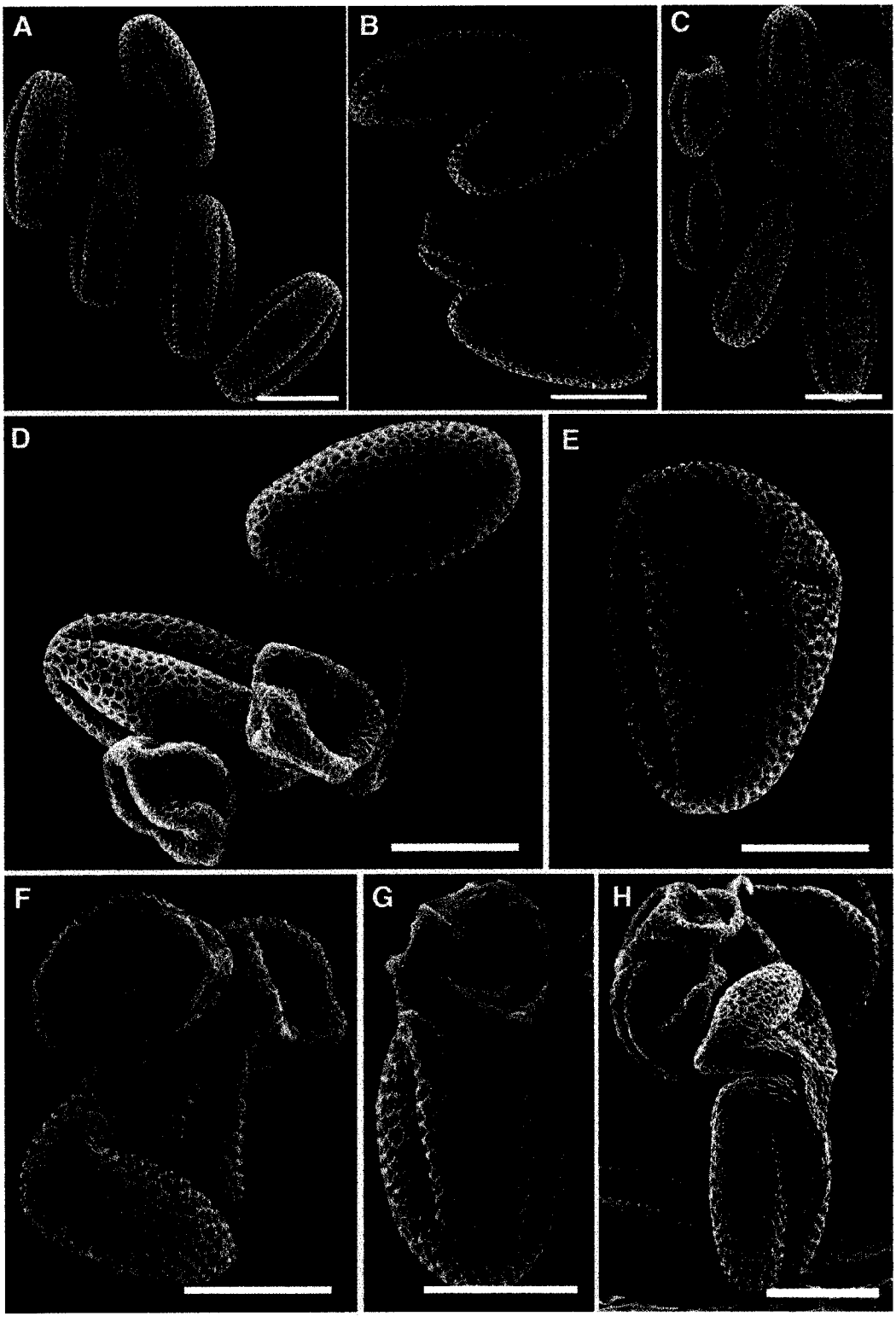
A
B
C
D
E
F
G
H

Figure 6.7. *gsl1-1/+ gsl5-2/gsl5-3* mutant plants lack a pollen tetrad callose wall. Toluidine blue and aniline blue stained sections of anthers from wild-type and *gsl1-1/+ gsl5-2/gsl5-3* mutant plants. **A,C,E,G,I,J.** light microscopy. **B,D,F,H.** UV illumination of the same figure on the direct left. **A-D.** Pollen mother cells during meiosis from (**A,B**) wild-type and (**C,D**) mutants. Meiosis appeared normal in both wild-type (**A**) and mutants (**C**). A callose wall surrounded each of the pollen mother cells in both wild-type (**B**) and mutants (**D**). **E-J.** Tetrads from (**E,F**) wild-type and (**G-J**) mutants. In wild-type plants, tetrads were clearly visible, the individual microspores clearly delineated (**E**). In the mutant, the microspores of developing tetrads were incompletely separated (**G,I,J**). In wild-type plants, each microspore of the tetrad was delineated by a callose wall (**F**). This callose was missing in mutants (**H**). (**I**) is the same picture as (**G**), but with an overlay showing what may be the outline of a whole, abnormally large tetrad (black line), the nuclei of indiviual microspores (white lines, dotted where questionable), and incomplete walls between the microspores (black dotted lines). (**J**) shows incomplete cytokinesis between two microspores (black arrowhead). This section was not stained with aniline blue in order to achieve a darker toluidine blue stain. Magnification bars: 10 μ.

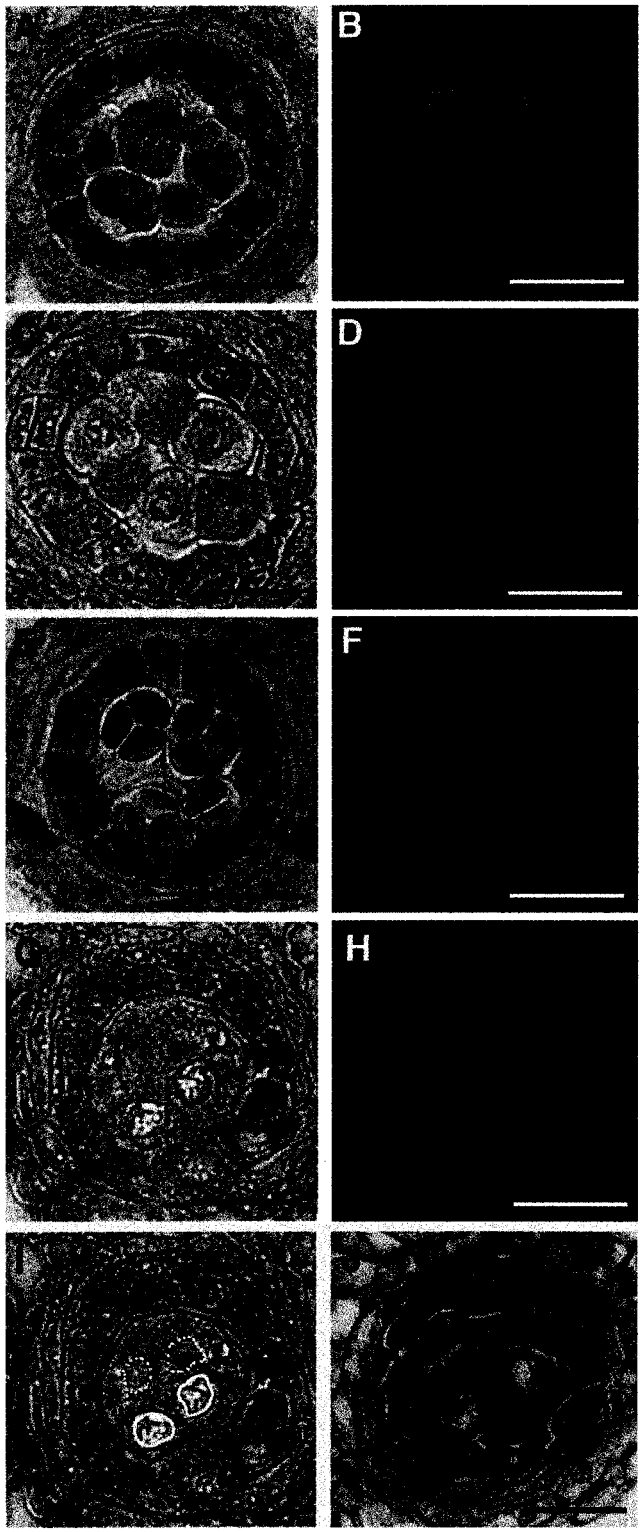
B
D
F
H

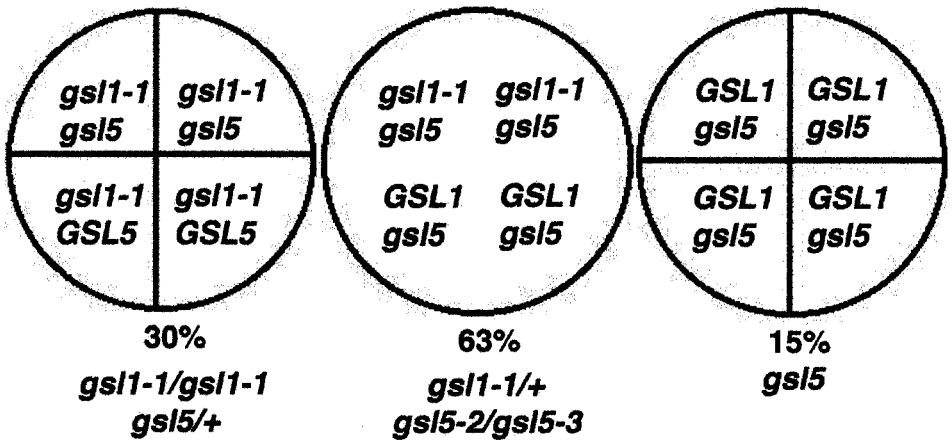

Figure 6.8. A summary of the pollen data for the *gsl5* single mutants, the *gsl1-1/gsl1-1 gsl5/+* mutants, and the *gsl1-1/+ gsl5-2/gsl5-3* mutant. The black line represents the callose wall surrounding the pollen mother cell, and the tetrad wall dividing the 4 microspores. The predicted haplotypes are shown for each microspore. The percentage of aberrant pollen grains is also shown.

CHAPTER 7 - GENERAL DISCUSSION, FUTURE WORK

Symplastic domains - studies using LYCH

I have found symplastic domains in the *Arabidopsis* root meristem that exclude the fluorescent dye, Lucifer Yellow. LYCH unloads from the phloem a at a distance from the root tip that corresponds with root hair formation. It moves readily both transversely into the endodermis and cortex and also proximally in these cell layers. Movement into the epidermis occurs at a low level; movement into the inner stele, the quiescent center and the root cap is completely restricted (Chapter 2).

Development requires that the movement of morphogenetic compounds through PD be limited, so that the compounds can affect one set of cells without affecting other cells (Ehlers et al., 1999). One very common example of a developmental process believed to require a differential cellular hormone distribution is the gravitropic response. When a root is gravitropically stimulated, auxin gradients across the root are thought to be responsible for causing differential rates of growth and hence curvature towards the gravity vector (Masson, 1995).

Auxin, a tryptophan derivative, is a very small molecule. I believe that the restrictions in movement to LYCH in the root meristem reflect symplastic domains that also restrict the free intercellular diffusion of auxin. Auxin moves from the shoot down towards the root meristem in the stele. Upon reaching the tip, it moves laterally into and basipetally through the outer tissues. It is believed that auxin redistribution during gravitropism occurs in the epidermis (Swarup et al., 2005). Auxin transport is regulated

by efflux carriers encoded by the *PIN* genes (Blilou et al., 2004). AtPIN2 has been found to be very important for proper auxin localization and gravitropic growth. This protein undergoes redistribution during gravitropic stimulus, and is thought to be responsible for the resultant auxin gradient from one side of the root to the other (Abas et al., 2006). I believe that the SEL of PD in epidermal cells restricts the diffusion of auxin out of these cells, in order to help maintain the auxin gradients set up by *AtPIN2*.

Callose and intercellular communication

I investigated the idea that these symplastic domains are essential for auxin redistribution and gravitropism. It has often been shown that callose accumulates at the two ends of the plasmodesmata, apparently as a ring that constricts the PD opening at each end (Radford et al., 1998). It is thought that this callose may be important in decreasing PD SEL (Shulz, 1999). I hypothesized that by inhibiting callose synthesis, I could increase the SEL of epidermal PD, resulting in a disruption of proper auxin localization and a lack of gravitropic response.

I found that chlorpromazine (CPZ) was an effective callose synthesis inhibitor in the *Arabidopsis* root meristem. In support of my hypothesis, at a CPZ concentration that completely inhibited PD callose synthesis in the meristem, LYCH was free to diffuse into all tissues, indicating a loss of symplastic domains, and the gravitropic response was also impaired. I am still in the process of determining what effects, if any, CPZ has on auxin movement in *Arabidopsis* root mersitems. I have obtained transgenic lines carrying three tandem copies of VENUS, a YFP variant, under control of the *DR5rev* auxin-responsive

promoter (Heisler et al., 2005). Confocal microscopy will be used to visualize the localization of auxin and how it is affected by CPZ treatment.

GFP vs LYCH movement in Arabidopsis root tips

My studies showing restrictions of movement to LYCH in the *Arabidopsis* root meristem seemed to contradict studies showing the unimpaired, intercellular movement of GFP between the same tissues. It is true that the concept of a symplastic domain is 'molecule specific', meaning that the location and extent of symplastic domains can differ, depending upon the molecules involved. But the ability of a molecule to passively diffuse through a PD would be governed solely by the SEL of that PD. If both LYCH and GFP move by passive diffusion, then LYCH, the smaller molecule, should be able to move through the same PDs as GFP.

How molecules move through PD is, however, not a well understood process. GFP fusions with LEAFY, a floral identity protein, have been shown to diffuse through PD between the L1 and underlying layers of the shoot apical meristem. Does this mean that all molecules smaller than this fusion protein are able to move freely through PD of these cell layers? Or are some proteins actively excluded? And if so, is it possible that GFP can move passively through PD in the *Arabidopsis* root meristem that are able to actively exclude other molecules such as LYCH? Conversely, is it possible that there are PD in the root meristem that GFP can move through actively and in a specific manner?

There is evidence not just to support the passive diffusion of some molecules through PD, but also the targeted movement of some molecules. In these cases, some molecules are believed to actively interact with the PD to enable their specific passage. It

is unlikely, though not impossible, that GFP, a protein that is not endogenous to plants, would have the ability to do this. SHR::GFP fusion proteins move out of the stele and into the endodermis (Nakajima et al., 2001; Sena et al., 2004). But smaller 36 kDa fusions made with GFP and a small portion of the ubiquitin protein, when expressed under the control of the *AtSUC2* promoter, cannot move out of the phloem (Stadler et al., 2005). An alternative explanation is that there is more than one kind of PD in *Arabidopsis* root meristems. I have shown with grafting experiments that the movement of GFP out of the stele is actually quite slow. Perhaps the rapid movement of LYCH into the endodermis and cortex is through one kind of PD, and the slower movement of GFP throughout the entire root meristem is through another kind of PD that either excludes LYCH or else also permits it to move very slowly.

I have also shown that GFP RNA is able to move between all cells of the root meristem. While it is unknown whether both GFP protein and its RNA are moving, there is the possibility that the GFP fluorescence reported to be seen throughout the root meristems of *AtSUC2::GFP* plants, and also observed in my studies of wild-type roots grafted to *AtSUC2::GFP* transgenic shoots is due entirely to GFP mRNA movement between PD and subsequent translation in root meristem cells. If this is true, the SEL of PD in the root meristem, believed to be 27 kDa, may in fact be quite a bit smaller, especially if the GFP mRNA has a way of being 'threaded' through the PD.

When using GFP to look at gene expression patterns in the *Arabidopsis* root, it is common practice to fuse promoters of interest with GFP carrying an endoplasmic-reticulum (ER) localization signal (Lee et al., 2005). In such cases, GFP does not move from cell to cell. It is believed that the GFP cannot move intercellularly because it is

sequestered by the ER. Such localization signals target proteins, not mRNA. If it is really GFP mRNA movement that is ultimately responsible for the GFP fluorescence observed throught the root meristem of *AtSUC2::GFP* plants, then the same fluorescence should also be seen throughout the meristem in *AtSUC2::GFP-er* plants, since mRNA movement would not be affected by such a signal. It is possible, however, that the ER localization signal, which is an additional 78 base pairs, makes the mRNA larger than a certain cut-off point in size for movement through PD. Alternatively, the presence of an ER localization signal on an mRNA may target it for occlusion from intercellular trafficking through PD.

It is puzzling that when expressed under the control of the *Sultr1;1* promoter, GFP is found in the lateral root cap of root tips, but does not move into the endodermis or stele (Takahashi et al., 2000). If all PD in the root meristem permit the free diffusion of the protein or the mRNA, then movement should occur out of the lateral root cap and throughout the organ. It is unknown by what mechanism a promoter such as that for *AtSUC2* might be able to target a protein or mRNA molecule for PD trafficking, but this possibility should be investigated. If such a mechanism exists, it doesn't confer movement to GFP fusions such as GFP-Ubi (Stadler et al., 2005). There is the possibility that the GFP fusion proteins are less fluorescent, and thus not detectable in other tissues. Using confocal microscopy, I have observed a highly reduced fluorescence in these fusions (data not shown). Alternatively, while the *AtSUC2* promoter may confer movement of mRNA or protein, there may still be a cut-off size for such movement. *GFP-Ubi* has over 200 base pairs more than GFP only; the fusion protein is 36 kDa and the Stokes radius is significantly larger. If a small mRNA, smaller than or equal to the

size of GFP mRNA and that doesn't normally move throughout the root meristem is put under the control of the *AtSUC2* promoter, does it gain the ability to move? And if so, do other companion cell-specific genes have promoters that do this? And why? That is, do the companion cells provide sink tissues with mRNA or proteins required for growth, and thus have a way of tagging them for movement through PD in these tissues?

Callose synthase and PD callose - mutant analyses

More work needs to be done in determining a role for callose in intercellular communication. As yet, no *GSL* gene has been conclusively shown to be involved in the production of callose associated with PD in roots, or with the control of the SEL in PDs. Future studies would provide both information on how plants form and regulate their PD, and the importance of PD regulation on intercellular trafficking and plant development.

Analysis should continue of the effects of single, double and triple *GSL* mutants on the movement of LYCH into cells in the root tip. Will any of these mutants cause the loss of boundaries between the symplastic domains? Will any cause a shift in the boundaries? Is there any correlation between changes in callose in the root, and especially callose associated with plasmodesmata and changes in symplastic domains?

A second approach would be to see if any of the *GSL* mutants affect the movement of GFP. The mutant line *gsl3-2* shows a dramatic restriction in the movement of GFP from the phloem into cells of the root tip, indicating a loss of intercellular communication. Other mutant lines may demonstrate increased intercellular communication. Studies of Stadler et al., 2005 have shown that in wild-type roots while GFP can move from the sieve cells into cells of the root tip, if GFP is fused to another

protein so as to increase its size, the movement is either totally blocked, or greatly restricted. By grafting the GFP-producing scions to mutant stocks, mutants could be screened for increased ability of these larger GFP-protein fusions to move out of the phloem and from cell to cell in the root tip.

GSL3 and intercellular communication

So far, preliminary phenotyping has shown *GSL3* to be the most likely candidate for a PD callose synthase. The TILLING mutant line *gsl3-2* has a mutation which confers a single amino acid change in a highly conserved region of the protein, and which segregates with a mutant root phenotype of excessive lateral branching and loss of cellular connectivity.

Work on GSL3 is not yet completed, and phenotyping should not continue until this mutant has been genetically rescued. Genetic rescue is crucial for verifying that the mutation of interest is causing any observed developmental defects. This is especially crucial for the TILLING mutants, which even after several outcrosses will still have some background mutations. An advantage of having an extensive library of T-DNA and TILLING mutants is that there a good chance of finding more than one mutant line per gene displaying a mutant phenotype. As demonstrated by *gsl5-2/gsl5-3* and *gsl3-1/gsl3-2*, trans-heterozygotes between mutant lines can be used as a quick and elegant way to verify mutational effects. This is valuable in situations such as this one where genetic rescue using wild-type constructs is especially difficult due to large gene size (callose synthases are the largest genes in the *Arabidopsis* genome). For *GSL3*, a search should be continuted for other gain-of-function mutant alleles that can be used for trans-

heterozygote verification of observed phenotypes. Alternatively, genetic rescue could be re-attempted using the 23 kB fragment from the F22D22 BAC that contains a wild-type allele for *GSL3* (described in chapter 5). It is unknown why previous *Agrobacterium* transformations were unsuccessful, but a vector system other than pGREEN should be used.

I have two hypotheses about the lack of root intercellular communication in the *gsl3-2* mutants. Callose synthesis is either upregulated, leading to increased PD closure, or callose synthesis is deregulated in such a way as to affect PD formation between cells. A role for callose in PD formation has never been shown, although callose is found at the phragmoplast during cell division (Hong et al., 2001), where and when PD would be formed. Once genetic rescue has been completed, PD callose in these mutants needs to be observed directly. Fluorescent antibody labeling of callose was attemped as described in chapter two, but results were inconclusive. Changes in callose levels may be too subtle to observe with such a method. Transmission electron microscopy (TEM) should be used along with colloidal gold antibodies to callose in order to both look at levels of callose deposition as well as its localization to PD. TEM should also give information about numbers and localization of PD, and may be useful for detecting any changes in PD structure.

Effects of the mutation on auxin distribution should be observed using reporter genes such as YFP, GFP and GUS, driven by the auxin-responsive promoter *DR5*. Effects on cellular identity should also be assessed by using cell-specific markers. *En7* and *Co2* are independent endodermis and cortex specific transcripts (Heidstra, 2004). By fusing their promoters with reporter genes, information can be gained about cell identity

in the mutants. In some of the mutants, epidermal cells resemble cortical cells in size and shape. Do these cells also express *Co2*? In other mutants, there is no recognizable endodermal layer. Is *En7* expression also lacking?

gsl3-1, a putative knock-out for *GSL3* has no phenotype. I believe that the mutant phenotype seen in the *gsl3-2* mutants is due to a gain-of-function mutation. Presumably, knocking out *GSL3* has no effect because the gene is redundant with one or more callose synthases. *GSL3* resides in a phylogenetic cluster with *GSL6,9* and *12* (chapter 4). *GSL9* is not expressed in roots. I have already made a double mutant between *GSL3* and *GSL6*, which shows no mutant phenotype. I have a putative knock-out mutant for *GSL12*. A triple knock-out of *GSL3*, *GSL6* and *GSL12* is likely to show an effect, and should be constructed.

GSL1 and GSL5

Multiple roles for *GSL1* and *GSL5* have been found in plant development. The two genes, which are within a few centimorgans of each other on the same chromosome are redundant, although *GSL5* appears to be the more important of the two genes. A knock-out for *GSL1* has no mutant phenotype; knock-outs for *GSL5* have smaller sized rosette leaves. Plants with no functional *GSL5* allele, and only one functional *GSL1* allele, are extremely dwarfed and have extremely reduced fertility . Such a haplo-insufficiency indicates dosage is very important in the role that these callose synthases play in organ size.

gsl1/+ gsl5/gsl5 plants, while almost completely infertile, did make pollen grains approximately one third of which appeared wild-type, and which could germinate. Pollen

from these plants could be used to successfully fertilize wild-type *Col-0* plants, but reverse crosses were unsuccessful. The infertility of these plants is thus due in part to a sporophytic problem.

At least one copy of either *GSL1* or *GSL5* was found to be required for the development of a functional pollen grain. Developing pollen grains with neither gene in their haplotype did not progress beyond the bicellular stage of development, and collapse. The gametophytic lethality of pollen grains bearing mutant alleles for both genes is likely the reason that double knock-outs for *GSL1* and *GSL5* could not be generated.

These genes also play a role in cytokinesis between meiotic products of pollen mother cells. The most severe mutants, with *gsl1/+ gsl5/gsl5* genotypes, produced many aberrantly large pollen grains with unusual pore structures, indicative of pollen post-meiotic cytokinesis defects (Hülskamp et al., 1997; Speilman et al., 1997). This problem cannot be caused by individual pollen haplotypes, since none of the other mutant genotypes, including *gsl1/gsl1 gsl5/+* showed pollen with this phenotype.

Pollen grains from the *gsl1/+ gsl5/gsl5* plants showed frequent problems with dissociation from the tetrad. Plants of this genotype had pre-meiotic mother cells surrounded by a callose wall, but a complete lack of callose dividing the individual microspores of the tetrad following meiosis. Again, this lack of callose was found only in this particular genotype. Callose at this stage is thus the result either of either the mother cell's genotype, if the genes are expressed pre-meiotically, or of the collective genotype of the tetrad, if the genes are expressed post-meiotically. Until now, the idea that callose in the tetrad walls might act to isolate products of meiosis and prevent cell cohesion and fusion was only a theory (Waterkeyn, 1962; Waterkeyn and Beinfait, 1970;

Heslop-Harrison, 1964; Heslop-Harrison and Mackenzie, 1967). The idea that this portion of the tetrad wall is not dependent on genes expressed by the individual microspores is a new one.

All mutant pollen grain phenotypes from the *gsl1/+ gsl5/gsl5*, whether collapsed, non-dissociated or aberrantly large, demonstrated the presence of an exine layer. This is a surprising result, since it had previously been thought that callose in the tetrad wall was essential for formation of the exine layer (Paxon-Sowders et al., 1997). GSL2 has recently been found to be important for exine patterning (Nishikawa et al., 2005; Dong et al., 2005). We now know that mutants of KOMPEITO, an *Arabidopsis* Rhomboid homolog (Kanaoka et al., 2005), fail to process GSL2. As a result, the mutants fail to make callose surrounding the pollen mother cell and resultant tetrad, although they still make callose between the microspores. Pollen grains end up dissociating, but lacking an exine layer (Kanaoka, personal communication). Combined with my results, the data suggests that deposition of callose in the pollen tetrad wall is an intricate process involving multiple callose synthases, and that tetrad wall callose plays multiple roles depending on where or when it is synthesized. Callose on the outer wall is synthesized by GSL2, and is involved in exine formation; callose between the individual microspores is synthesized by GSL1 and GSL5, and is necessary for dissociation of the individual pollen grains.

Work on *GSL1* and *GSL5* has led to a number of interesting insights into the callose synthase family. For example, it was hypothesized that each GSL might serve a separate function in plant development. I now know that in at least the case of GSL1 and GSL5, callose synthases can serve multiple functions in plant development. While I have

found a specific role for these genes in post-meiotic cytokinesis, tetrad wall formation and pollen grain dissociation, I still don't know their sporophytic role in organ size. Are they involved in cell division, as is known for *GSL6* (Hong et al., 2001) and as I suspect for *GSL3*? Or are they involved in cell elongation? While mutant pollen grains for these genes have exine patterning, the spaces between reticulations are smaller, hinting at problems with expansion. I also don't know why *gsl1/gsl1 gsl5/+* plants are mostly infertile, nor do I know why pollen grains lacking both *GSL1* and *GSL5* collapse beyond the bicellular stage.

Other roles for callose in plant development

The mutant library I have amassed for 9 of the 12 callose synthases can be used to determine other roles for these genes in plant development. Preliminary phenotyping has revealed at least a couple of other interesting single mutants: . *gsl10-1*, a TILLING mutant, showed gametophytic lethality, and *gsl7-1*, a putative knock-out, segregated with a mutant phenotype of slightly smaller, rounder flowers. I have other mutant lines for *GSL7* and *GSL10* that can be used in trans-heterozygous combination with these mutations; in this way, I can easily verify the genetic nature of these mutant phenotypes (a TILLING line for *GSL7* carries the loss of an intron splicing site, and I have an exonic T-DNA insertion line, SALK_143945, for *GSL10*). Work on these mutants should be continued.

Work on *GSL1* and *GSL5* has revealed that there is genetic redundancy in this family of genes. This is likely why so few mutants of interest were found from screening

single mutant lines. Double and triple mutants will undoubtably need to be generated with respect to phylogenetic relationships, in order to fully understand the role that each of these callose synthases is playing in plant development.

REFERENCES

Abas L, Benjamins R, Malencia N, Paclorek T, Wisniewska, Moulinier-Anzola JC, Sieberer T, Friml J, Luschnig C (2006) Intracellular trafficking and proteolysis of the *Arabidopsis* auxin-efflux facilitator PIN2 are involved in root gravitropism. Nature Cell Biol 8: 249-256

Alexander MP (1969) Differential staining of aborted and nonaborted pollen. Stain Tech 44: 117-122

Alonso JM, Stepanova AN, Leisse TJ, Kim CJ, Chen H, Shinn P, Stevenson DK, Zimmerman J, Barajas P, Cheuk R, Gadrinab C, Heller C, Jeske A, Koesema E, Meyers CC, Parker H, Prednis L, Ansari Y, Choy N, Deen H, Geralt M, Hazari N, Hom E, Karnes M, Mulholland C, Ndubaku R, Schmidt I, Guzman P, Aguilar-Henonin L, Schmid M, Weigel D, Carter DE, Marchand T, Risseeuw E, Brogden D, Zeko A, Crosby WL, Berry CC, and Ecker JR (2003) Genome-wide insertional mutagenesis of *Arabidopsis thaliana*. Science 301: 653-657

Baluska F, Šamaj J, Hlavacka A, Kendrick-Jones J, Volkmann D (2004) Actin-dependent fluid-phase endocytosis in inner cortex cells of maize root apices. J Exp Bot 55: 463-473

Bayer E, Thomas CL, Maule AJ (2004) Plasmodesmata in *Arabidopsis thaliana* suspension cells. Protoplasma 223: 93-102

Becker, J.D., Boavida, J.C., Carneiro, J., Haury, M. and Feijó, J.A. 2003. Transcriptional profiling of *Arabidopsis* tissues reveals the unique characteristics of the pollen transcriptome. Plant Physiol 133: 713-725.

Benfey PN, Linstead PJ, Roberts K, Schiefelbein JW, Hauser MT, Aeschbacher RA (1993) Root development in *Arabidopsis*: four mutants with dramatically altered root morphogenesis. Development 119: 57-70

Benhamou N (1992) Ultrastructural detection of β-1→3-glucans in tobacco root tissue infected by *Phytophthora parasitica* var *nicotianae* using a gold-complexed tobacco β-1→3-glucanase. Physiol Mol Plant Pathol 41: 351-370

Berleth T, Jurgens G (1993) the role of the *monopteros* gene in organising the basal body region of the *Arabidopsis* embryo. Development 118: 575-587

Billou B, Xu J, Wildwater M, Willemsen V, Paponov I, Friml J, Heldstra R, Aida M, Palme K, Scheres B (2005) The PIN auxin efflux facilitator network controls growth and patterning in *Arabidopsis* roots. Nature 433: 39-44

Birnbaum K, Shasha DE, Wang JY, Jung JW, Lambert GM, Galbraith DW, Benfey PN (2003) A gene expression map of the *Arabidopsis* root. Science 302: 1956-1960

Blilou I, Xu J, Wildwater M, Willemsen V, Paponov I, Friml J, Heidstra R, Aida M, Palme K, Scheres B (2005) The PIN auxin efflux facilitator network controls growth and patterning in *Arabidopsis* roots. Nature 433: 39-44

Botha CEJ, Cross RHM (2000) Towards reconciliation of structure with function in plasmodesmata – who is the gatekeeper? Micron 31: 713-721

Braselton, J.P., Wilkinson, M.J. and Clulow, S.A. 1996. Feulgen staining of intact plant tissues for confocal microscopy. Biotech & Histochem 71: 84-87.

Bret-Harte MS, Silk WK (1994) Nonvascular, symplastic diffusion of sucrose cannot satisfy the carbon demands of growth in the primary root tip of *Zea mays* L. Plant Physiol 105: 19-33

Brown I, Trethowan J, Kerry M, Mansfield J, Bolwell GP (1998) Localization of components of the oxidative cross-linking of glycoproteins of callose synthesis in papillae formed during the interaction between non-pathogenic strains of *Xanthomonas campestris* and French bean mesophyll cells. Plant J 15: 333-343

Burton RA, Wilson SM, Hrmova M, Harvey AJ, Shirley NJ, Medhurst A, Stone BA, Newbigin EJ, Bacic A, Fincher GB (2006) Cellulose synthase-like *CslF* genes mediate the synthesis of cell wall (1,3;1,4)-β-D-glucans. Science 311: 1940-1942.

Chen R, Guan C, Boonsirichai K, Masson PH (2002) Complex physiological and molecular processes underlying root gravitropism. Plant Mol Biol 49: 305-17

Chiu, W., Niwa, Y., Zeng, W., Hirano, T., Kobayashi, H. and Sheen, J. (1996) Engineered GFP as a vital reporter in plants. Curr. Biol. 6:325-330

Chu G, Vollrath D, Davis RW (1986) Separation of large DNA molecules by contour-clamped homogeneous electric fields. Science 234: 1582-1585

Cleland RE, unpublished data

Cleland RE, Fujiwara T, Lucas WJ (1994) Plasmodesmal-mediated cell-to-cell transport in wheat roots is modulated by anaerobic stress. Protoplasma 178: 81-85

Complainville A, Brocard L, Roberts I, Dax E, Sever N, Sauer N, Kondorosi A, Wolf S, Oparka K, Crespi M (2003) Nodule initiation involves the creation of a new symplastic field in specific root cells of *Medicago* species. Plant Cell 15: 2778-2791

Crameri, A. (1996) Improved green fluorescent protein by molecular evolution using DNA shuffling. Nature Biotechnol 14:315-319

Cui X, Shin H, Song C, Laosinchai W, Amano Y, Brown Jr RM (2001) A putative plant homolog of the yeast beta-1,3-glucan synthase subunit *FKS1* from cotton (*Gossypium hirsutum* L.) fibers. Planta 213: 223-230

Delmer DP (1999) Cellulose biosynthesis: exciting times for a difficult field of study. Annu Rev Plant Physiol Plant Mol Biol 50: 245-276

Delmer DP, Volokita M, Solomon M, Fritz U, Delphendahl W, Herth W (1993) A monoclonal antibody recognizes a 65 kDa higher plant membrane polypeptide which undergoes cation-dependent association with callose synthase in vitro and co-localizes with the site of high callose deposition in vivo. Protoplasma 176: 33-42

Derrick PM, Barker H, Oparka KJ (1990) Effect of virus infection on symplastic transport of fluorescent tracers in *Nicotiana clevelandii* leaf epidermis. Planta 181: 555-559

Dhugga KS (2001) Building the wall: genes and enzyme complexes for polysaccharide synthases. Curr Opin Plant Biol 4: 488-493

Ding B, Kwon M-0, Warnberg L (1996) Evidence that actin filaments are involved in controlling the permeability of plasmodesmata in tobacco mesophyll. Plant J 10: 157-164

Ding B, Turgeon R, Parthasarathy MV (1992) Substructure of freeze-substituted plasmodesmata. Protoplasma 169:28-41

Doblin, M.S., De Melis, L., Newbigin, E., Bacic, A., Read, S.M. (2001) Pollen tubes of *Nicotiana alata* express two genes from different beta-glucan synthase families. Plant Physiol 125: 2040-2052.

Dong X, Hong Z, Sivaramakrishnian M, Mahfouz M, Verma DPS (2005) Callose synthase (CalS5) is required for exine formation during microgametogenesis and for pollen viability in *Arabidopsis*. Plant J 42: 315-328

Donofrio, N.M. and Delaney, T.P. 2001. Abnormal callose response phenotype and hypersusceptibility to Peronospoara parasitica in defence-compromised *arabidopsis nim1-1* and salicylate hydroxylase-expressing plants. Mol Plant Microbe Interact 14: 439-450.

Douglas, C.M., Foor, F., Marrinan, J.A., Morin, N., Nielsen, J.B., Dahl, A.M., Mazur, P., Baginsky, W., Li, W., El-Sherbeini, M., Clemas, J.A., Mandala, S.M., Frommer, B.R. and Kurtz, M.B. 1994. The Saccharomyces cerevisiae *FKS1 (ETG1)* gene encodes an integral membrane protein which is a subunit of 1,3-beta-D-glucan synthase. Proc Natl Acad Sci USA 91: 12907-12911.

Duckett CM, Oparka KJ, Prior L, Dolan L, Roberts K (1994) Dye-coupling in the root epidermis of *Arabidopsis* is progressively reduced during development. Development 120: 3247-3255

Edlund, A., Swanson, R. and Preuss, D. 2004. Pollen and stigma structure and function: The role of diversity in pollination. Plant Cell Suppl 16: 84-97.

Ehlers K, Binding H, Kollman R (1999) The formation of symplastic domains by plugging of plasmodesmata: a general event in plant morphogenesis? Protoplasma 209: 181-192

Enns LC, Kanaoka MM, Torii KU, Comai L, Okada K, Cleland RE (2005) Two callose synthases, GSL1 and GSL5, play an essential and redundant role in plant and pollen development and in fertility. Plant Mol Biol 58: 333-349

Erwee MG, Goodwin PB (1984) Characterization of the *Egeria densa* leaf symplast: response to plasmolysis, depolasmolysis and to aromatic amino acids. Protoplasma 122: 162-168

Erwee MG, Goodwin PB (1985) Symplast domains in extrastelar tissues of *Egeria densa* Planch. Planta 163: 9-19

Falquet, L., Pagni, M., Bucher, P., Hulo, N., Sigrist, C.J., Hofmann, K. and Bairoch, A. 2002. The PROSITE database, its status in 2002. Nucleic Acids Res 30: 235-238.

Fei, H. and Sawhney, V.K. 2001. Ultrastructural characterization of *male sterile 33* (*ms33*) mutant in *Arabidopsis* affected in pollen desiccation and maturation. Can J Bot 79: 118-129.

Ferguson, C., Teeri, T.T., Siika-aho, M., Read, S.M. and Bacic, A. 1998. Location of cellulose and callose in pollen tubes and grains of *Nicotiana tabacum*. Planta 206: 452-460.

Fischer DB, Oparka KJ (1996) Post-phloem transport: principles and problems. J Exp Bot 47: 1141-1154

Ghoshroy S, Lartey R, Sheng J, Citovsky V (1997) Transport of proteins and nucleic acids through plasmodesmata. Annu Rev Plant Physiol Plant Mol Biol 48: 27-50.

Gisel A, Barella S, Hempel FD, Zambryski PC. (1999) Temporal and spatial regulation of symplastic trafficking during development in Arabidopsis thaliana apices. Development 126: 1879-1889

Gisel A, Hempel FD, Barella S, Zambryski PC (2002) Leaf-to-shoot apex movement of symplastic tracer is restricted coincident with flowering in *Arabidopsis*. Proc Nat Acad Sci US 99: 1713-1717

Goodwin PB (1983) Molecular size limit for movement in the symplast of the *Elodea* leaf. Planta 157: 124-130

Goodwin PB, Cantril LC (1999) Use and limitations of fluorochromes for plasmodesmal research. In: Plasmodesmata. Structure, function, role in cell communication, van Bel AJE, van Kesteren WJP eds. Springer, Berlin. Pp. 67-84

Hadfi K, Speth V, Neuhaus G (1998) Auxin-induced developmental patterns in *Brassica juncea* embryos. Development 125: 879-887

Harriman RW, Shao A-P, Wasserman BP (1992) Inhibition and ultraviolet-induced chemical modification of UDP-glucose: (1,3)-β-glucan (callose) synthase by chlorpromazine. Plant Physiol 100: 1927-1933.

Haseloff, J., Siemering, K.R., Prasher, D.C., and Hodge, S. (1997) Removal of a cryptic intron and subcellular localization of green fluorescent protein are required to mark transgenic *Arabidopsis* plants brightly. PNAS 94:2122-2127.

Heidstra R, Welch D, Scheres B (2004) Mosaic analyses using marked activation and deletion clones dissect Arabidopsis SCARECROW action in asymmetric cell division. Gen Dev 18:1964-1969

Heisler MG, Ohno C, Das P, Sieber P, Reddy GV, Long JA, Meyerowitz E (2005) Patterns of auxin transport and gene expression during primordium development revealed by live imaging of the *Arabidopsis* influorescence meristem. Current Biology 15: 1899-1911

Heslop-Harrison, J. 1964. Cell walls, cell membranes, and protoplasmic connections during meiosis and pollen development. In: H.F. Linskens (Ed.), Pollen Physiology and Fertilization, North-Holland Publishing Company, Amsterdam, pp. 39-47.

Heslop-Harrison, J. and Mackenzie, A. 1967. Autoradiography of soluble [2-^{14}C]thymidine derivatives during meiosis and microsporogenesis in *Lilium* anthers. J. Cell Sci 2: 387-400.

Hobbie L, Estelle M (1995) The *axr4* auxin-resistant mutants of *Arabidopsis thaliana* define a gene important for root gravitropism and lateral root initiation. Plant J 7: 211-220

Holdaway-Clark TL (2005) Regulation of plasmodesmal conductance. In: Plasmodesmata. Annu Plant Rev, Vol 18, Oparka KJ, ed. Blackwell, Oxford. Pp 279-297

Holdaway-Clark TL, Walker NA, Hepler PK, Overall RL (2000) Physiological elevations in cytoplasmic free calcium by cold or ion injection result in transient closure of higher plant plasmodesmata. Planta 210: 329-335

Hong Z, Delauney AJ, Verma DPS (2001) A cell plate-specific callose synthase and its interactions with phragmoplastin. Plant Cell 13: 755-768

Hosey MM, Lazdunski M (1988) Calcium channels: molecular pharmacology, structure and regulation. J Memb Biol 104: 81-105

Hughes JE, Gunning BES (1980) Glutaraldehyde-induced deposition of callose. Can J Bot 58: 250-258

Hülskamp M., Parekh, N.S., Grini, P., Schneitz, K., Zimmerman, I., Lolle, S.J. and Pruitt, R.E. 1997. The *STUD* gene is required for male-specific cytokinesis after telophase II of meiosis in *Arabidopsis thaliana*. Dev Biol 187: 114-124.

Iglesias VA, Meins Jr F (2000) Movement of plant viruses is delayed by a β-1-3-glucanase-deficient mutant showing a reduced plasmodesmatal size exclusion limit and enhanced callose deposition. Plant J 21: 157-166

Imlau A, Truernit E, Sauer N (1999) Cell-to-cell and long-distance trafficking of the green fluorescent protein in the phloem and symplastic unloading of the protein into sink tissues. Plant Cell 11: 309-322

Ishikawa H, Evans ML (1993) The role of the distal elongation zone in the response of maize roots to auxin and gravity. Plant Physiol 102: 1203-1210

Itaya A, Liang G, Woo Y-M, Nelson RS, Ding B (2000) Nonspecific intercellular protein trafficking probed by green-fluorescent protein in plants. Protoplasma 213: 165-175

Jackson, D (2005) Transcription factor movement through plasmodesmata. In: Plasmodesmata, Annu Plant Rev 18, Oparka KJ, ed. Blackwell, Oxford. Pp113-134

Jackson D, Veit B, Hake S (1994) Expression of maize *KNOTTED1* related homeobox genes in the shoot apical meristem predicts patterns of morphogenesis in the vegetative shoot. Development 128: 13-23

Jacobs, AK, Lipka, V, Burton, RA, Panstruga, R, Strizhov, N, Schulze-Lefert, P and Fincher, GB (2003) An *Arabidopsis* callose synthase, GSL5, is required for wound and papillary callose formation. Plant Cell 15: 2503-2513

Jaffe MJ, Leopold AC (1984) Callose deposition during gravitropism of *Zea mays* and *Pisum sativum* and its inhibition by 2-deoxy-D-glucose. Planta 161: 20-26

Kanaoka MM, unpublished data

Kanaoka MM, Urban S, Freeman M, Okada K (2005) An *Arabidopsis* Rhomboid homolog is an intramembrane protease in plants. FEBS Lett. 579: 5723-5728

Kauss H (1996) Callose synthesis. In: Membranes: specialized functions in plants, ed. Smalwood M, Knox JP, Bowles DJ. pp 77-92. Bios Scientific Publ: Oxford

Kim I, Hempel FD, Sha K, Pfluger J, Zambryski PC (2002) Identification of a developmental transition in plasmodesmatal function during embryogenesis in *Arabidopsis thaliana.* Development 129: 1261-1272

Kim J-Y, Rim Y, Wang J, Jackson D (2005) A novel cell-to-cell trafficking assay indicates that the KNOX homeodomain is necessary and sufficient for intercellular protein and mRNA trafficking. Genes& Development 19: 788-793

Klee, JH (1987) The effects of overproduction of two Agrobacterium tumefaciens T-DNA auxin biosynthetic gene products in transgenic petunia plants. Genes Dev 1: 86-96

Kobayashi K, Kim I, Cho E, Zambryski P (2005) Plasmodesmata and plant morphogenesis. In: Plasmodesmata. Annu Plant Rev, Vol 18, Oparka KH, ed. Blackwell, Oxford. Pp 90-11

Kragler F, Monzer J, Xoconostle-Cázares B, Lucas WJ (2000) Peptide antagonists of the plasmodesmal macromolecular trafficking pathway. EBMO J 19: 2856-2868

Lee J-Y, Colinas, J, Wang JY, Mace D, Ohler U, Benfey PN (2005) Transcriptional and posttranscriptional regulation of transcription factor expression in *Arabidopsis* roots PNAS 103:6055-6060

Li H, Bacic A, Read SM (1999) Role of a callose synthesis zymogen in regulating wall deposition in pollen tubes of *Nicotiana alata.* Planta 208: 528-538

Li J, Burton RA, Harvey AJ, Hrmova M, Wardak AZ, Stone BA, Fincher GB (2003) Biochemical evidence linking a putative callose synthase gene with (1-3)-β-D-glucan biosynthesis in barley. Plant Mol Biol 53: 213-225

Liarzi O, Epel BL (2005) Development of a quantitative tool for measuring changes in the coefficient of conductivity of plasmodesmata induced by development, biotic, and abiotic signals. Protoplasma 225: 67-76

Liepman AH, Wilkerson CF, Keegstra K (2005) Expression of cellulose synthase-like (*Csl*) genes in insect cells reveals that *CslA* family members encode mannan synthases. Proc Natl Acad Sci USA 102: 2221-2226

Liu CM, Xu ZH, Chua NH (1993) Auxin polar transport is essential for the establishment of bilateral symmetry during early plant embryogenesis. Plant Cell 5: 621-630

Lucas WJ, Lee J-Y (2004) Plasmodesmata as a supracellular control network in plants. Nature Reviews Mol Cell Biol 5: 712-726

Lucas WJ, Ding B, van der Schoot C (1993) Plasmodesmata and the supercellular nature of plants. Now Phytol 125: 435-476

Malamy JE, Benfey PN (1997) Down and out in *Arabidopsis*: the formation of lateral roots. Trends Plant Sci 2: 390-396

Masson PH (1995) Root gravitropism. BioEssays 17: 119-127

Mayer, U. and Jurgens, G. 2004. Cytokinesis: lines of division taking shape. Curr Opinion Plant Biol 7: 599-604.

McCormack BA, Gregory AC, Kerry ME, Smith C, Bolwell GP (1997) Purification of an elicitor-induced glucan synthase (callose synthase) from suspension cultures of French bean: purification and immunolocation of a probable M(r)-65,000 subunit of the enzyme. Planta 203: 196-203

McCormick, S. 1993. Male gametophyte development. Plant Cell 5: 1265-1275.

Meikle, P.J. Bonig, I., Hoogenraad, N.J., Clarke, A.E., and Stone, B.A. (1991) The location of (1→3)-β-glucans in the walls of pollen tubes of *Nicotiana alata* using a (1→3)-β-glucan-specific monoclonal antibody. Planta 185: 1-8

Morris DA, Friml J, Zazímalová E (2004) The transport of auxin. In: Plant hormones. Biosynthesis, signal transduction, action! Davies PJ, ed. Kluwer, Dordrecht. Pp. 437-470

Nakajima K, Sena G, Newy T, Benfey PN (2001) Intercellular movement of the putative transcription factor SHR in root patterning. Nature 413: 307-311

Nelson RS (2005) Movement of viruses to and through plasmodesmata. In: Plasmodesmata. Annu Plant Rev, Vol 18, Oparka KJ, ed. Blackwell, Oxford. Pp 188-211

Ng PC, Henikoff S (2003) SIFT: predicting amino acid changes that affect protein fuction. Nucleic Acids Res 31: 3812-3814

Nishikawa S, Zinkl GM, Swanson RJ, Maruyama D, Preuss D (2005) Callose (beta-1,3 glucan) is essential for *Arabidopsis* pollen wall patterning, but not tube growth. BMC Plant Biol 5: 22-30

Nishimura, M.T., Stein, M., Hou, B.H., Vogel, J.P., Edwards, H. and Somerville, S.C. 2003. Loss of a callose synthase results in salicylic acid-dependent disease resistance. Science 301: 969-972

O'Driscoll D, Wilson G, Steer MW (1991) Lucifer yellow and fluorescein isothiocyanate uptake by cells of *Morinda citrifolia* in suspension cultures is not confinded to the endocytic pathway. J Cell Sci 100: 237-241

Olesen P, Robards AW (1990) The neck region of plasmodesmata: general architecture and some functional aspects. In: Robards AW, Lucas WJ, Pitts JD, Jongsma HJ, Spray DC (eds) Parallels in cell to cell junctions in plants and animals. Springer, Berlin. Pp 145-170

Oparka KJ, Prior DAM (1992) Direct evidence for pressure-generated closure of plasmodesmata. Plant J 2: 741-750

Oparka KJ, Duckett CM, Prior DAM, Fischer DB (1994) Real-time imaging of phloem unlaoding in the root tip of *Arabidopsis*. Plant J 6: 759-766

Oparka KJ, Roberts AG, Boevink P, Santa Cruz S, Roberts I, Pradel KS, Imlau A, Kotlizky G, Sauer N, Epel B (1999) Simple, but not branched, plasmodesmata allow the nonspecific trafficking of proteins in developing tobacco leaves. Cell 97: 743-754

Oparka KJ, Robinson D, Prior DAM, Derrick P, Wright KM (1988) Uptake of Lucifer Yellow CH into intact barley roots: evidence for fluid-phase endocytosis. Planta 176: 541-547

Ormenese S, Havelange A, Bernier G, van der Schoot C (2002) The shoot apical meristem of *Sinapis alba* L expands its central symplastic field during the floral transition. Planta 215: 67-78

Østergaard, L., Petersen, M., Mattsson, O. and Mundy, J. 2002. An *Arabidopsis* callose synthase. Plant Mol Biol 49, 559-566.

Østergaard, L. and Yanofsky, M.F. 2004. Establishing gene function by mutagenesis in *Arabidopsis thaliana*. Plant J 39: 682-696.

Otegui, M.S. and Staehelin, A. 2004. Electron tomographic analysis of post-meiotic cytokinesis during pollen development in *Arabidopsis thaliana*. Planta 218: 501-515.

Ottenschläger I, Wolff P, Wolverton C, Bhalerao RP, Sandberg G, Ishikawa H, Evans M, Palme K (2003) Gravity-regulated differential auxin transport from columella to lateral root cap cells. Proc Nat Acad Sci USA 100: 2987-2991

Overall, R.L. and Blackman, L.M. 1996. A model of the macromolecular structure of plasmodesmata. Trends Plant Sci 1: 307-311.

Paxon-Sowders DM, Owen HA, Makaroff CA (1997) A comparative ultrastructural analysis of exine pattern development in wild-type *Arabidopsis* and a mutant defective in pattern formation. Protoplasma 198: 53-65

Pear JR, Kawagoe Y, Schreckengost WE, Delmer DP. 1996. Higher plants contain homologs of the bacterial celA genes encoding the catalytic subunit of cellulose synthase. Proc Natl Acad Sci USA 93: 12637-12642.

Radford JE, Vesk M, Overall RL (1998) Callose deposition at plasmodesmata. Protoplasma 201: 30-37

Radford JE, White RG (2001) Effects of tissue-preparation-induced callose synthesis on estimates of plasmodesma size exclusion limits. Protoplasma 216: 47-55

Rae, A.L., Harris, P.J., Bacic, A. and Clarke, A.E. 1985. Composition of the cell walls of *Nicotiana alata* Link et Otto pollen tubes. Planta 166: 128-133.

Rinne PLH, van der Schoot (1998) Symplastic fields in the tunica of the shoot apical meristem coordinate morphogenetic events. Development 125: 1477-1485

Rinne PLH, Kaikuranta PM, van der Schoot C (2001) The shoot apical meristem restores its symplastic organization during chilling-induced release from dormancy. Plant J 26: 249-264

Rinne PLH, van den Boogaard R, Mensink MGJ, Kopperud C, Kormelink R, Goldbach R, van der Schoot C (2005) Tobacco plants respond to the constitutive expression of the tosporvirus movement proteint NS_M with a heat-reversible sealing of plasmodesmata that impairs development. Plant J 43: 688-707

Roberts AG, Oparka KJ (2003) Plasmodesmata and the control of symplastic transport. Plant Cell Environ 26: 103-124

Rost, B. 1996a. Methods in Enzymology 266: 525-539.

Rost, B., Fariselli, P. and Casadio, R. 1996b. Prot Science 7: 1704-1718.

Ruan Y-L, Llewellyn DJ, Furbank RT (2001) The control of single-celled cotton fiber elongation by developmentally reversible gating of plasmodesmata and coordinated expression of sucrose and K^+ transporters and expansin. Plant Cell 13: 47-60

Ruegger M, Dewey E, Hobbie L, Brown D, Bernasconi P, Turner J, Muday G, Estelle M (1997) Reduced naphthylphthalamic acid binding in the *tir3* mutant of *Arabidopsis* is associated with a reduction in polar auxin transport and diverse morphological defects. Plant Cell 9: 745-757

Ryu, J., Han, K., Park, J., Choi, S.Y. (2003) Enhanced uptake of a heterologous protein with an HIV-1 Tat protein transduction domains (PTD) at both termini. Mol Cells 16:385-391

Sabatini S, Beis D, Wolkenfelt H, Murfett J, Guilfoyle T, Malamy J, Benfey P, Leyser O, Bechtold N, Weisbeek P, Scheres B (1999) An auxin-dependent distal organizer of pattern and polarity in the *Arabidopsis* root. Cell 99: 463-472

Sagi G, Katz A, Guenoune-Gelbart D, Epel BL (2005) Class 1 reversibly glycosylated polypeptides are plasmodesmal-associated proteins delivered to plasmodesmata via the Golgi apparatus. Plant Cell 17: 1788-1800

Schimoler-O'Rourke, R., Renault, S., Mo, W. and Selitrennikoff, C.P. 2003. *Neurospora crassa* FKS protein binds to the (1,3)beta-glucan synthase substrate, UDP-glucose. Curr Microbiol 46: 408-412

Schlüpmann, H., Bacic, A. and Read, S.M. 1994. Uridine diphosphate glucose metabolism and callose synthesis in cultured pollen tubes of *Nicotiana alata* Link et Otto. Plant Physiol 105: 659-670

Schulz A (1999) Physiological control of plasmodesmal gating. In: Plasmodesmata. Structure, Function, Role in Communication, van Bel AJE, van Kesteren WJP eds. Springer, Berlin. Pp 173-204

Schulz A (2005) Role of plasmodesmata in solute loading and unloading. In: Plasmodesmata. Annu Plant Rev Vol 18, Oparka KJ, ed. Blackwell, Oxford. Pp135-161

Scott, R.J., Spielman, M. and Dickinson, H.G. 2004. Stamen structure and function. Plant Cell 16 Suppl: S46-S60

Sena G, Jung JW, Benfey PN (2004) A broad competence to respond to SHORT ROOT revealed by tissue-specific ectopic expression. Development 131: 2817-2826

Sessions A, Yanofsky MF, Weigel D (2000) Cell-cell signaling and movement by the floral transcription factors LEAFY and APETALA1. Science 289: 779-782

Sheen, J., Hwang, S., Niwa, Y., Kobayashi, H., and Galbraith, D.W. (1995) Green-fluoresceent protein as a new vital marker in plant cells. Plant J 8:777-784.

Shpak ED, Berthiaume CT, Hill EJ, Torii KU (2004) Synergistic interaction of three ERECTA-family receptor-like kinases controls *Arabidopsis* organ growth and flower development by promoting cell proliferation. Development 131: 1491-1501

Shulz A (1999) Physiological control of plasmodesmal gating. In: Plasmodesmata. Structure, Function, Role in Communication. van Bel AJE, van Kesteren WJP eds. Springer, Berlin. pp 173-204

Sivaguru M, Fujiwara T, Samaj J, Baluska F, Zang Z, Osawa H, Maeda T, Mori T, Volkmann D, Matsumoto H (2000) Aluminum-induced 1→3-β-D-glucan inhibits cell-to-cell trafficking of molecules through plasmodesmata. A new mechanism of aluminum toxicity in plants. Plant Physiol 124: 991-1005

Smith LG, Greene B, Veit B, Hake S (1992) A dominant mutation in the maize homeobox gene, *Knotted-1*, causes its ectopic expression in leaf cells with altered fates. Development 116: 21-30

Spielman, M., Preuss, D., Li, F.-L., Browne, W.E., Scott, R.J. and Dickinson, H.G. 1997. *TETRASPORE* is required for male meiotic cytokinesis in *Arabidopsis thaliana.* Development 124: 2645-2657.

Stadler R, Wright KM, Lauterbach C, Amon G, Gahrtz M, Feuerstein A, Oparka KJ, Sauer N (2005) Expession of GFP-fusions in Arabidopsis companion cells reveals non-specific protein trafficking into sieve elements and identifies a novel post-phloem domain in roots. Plant J 41: 319-331

Stone BA, Clark AE. (1992) Chemistry and Biology of (1-3)-ß-glucans. La Trobe Univ Press: Victoria, Australia. 803 pp.

Swarup R, Kramer EM, Perry P, Knox K, Ottoline Leyser HM, Haseloff J, Beemster GTS, Bhalerao R, Bennet MJ (2005) Root gravitropism requires lateral root cap and epidermal cells for transport and response to a mobile auxin signal. Nature Cell Biol 7: 1057-1065

Takahashi, H., Watanabe-Takahashi, A., Smith, F.W., Blake-Kalff, M., Hawkesford, M.J., and Saito, K. (2000) The roles of three functional sulphate transporters involved in uptake and translocation of sulphate in *Arabidopsis thaliana.* Plant J 23:171-182

Tanaka, H., Ishikawa, M., Kitamura, S., Takahashi, Y., Soyano, T., Machida, C. and Machida, Y. 2004. The *AtNACK1/HINKEL* and *STUD/TETRASPORE/AtNACK2* genes, which encode functionally redundant kinesins, are essential for cytokinesis in *Arabidopsis*. Genes to Cells 9: 1199-1211

Terry BR, Robards AW (1987) Hydrodynamic radius alone governs the mobility of molecules through plasmodesmata. Planta 171:145-157

Terry BR, Matthews EK, Haseloff J (1995) Molecular characterization of recombinant green fluorescent protein by fluorescent correlation microscopy. Biochem Biophys Res Commun 217: 21-27

Till, B.J., Reynolds, S.H., Greene, E.A., Codomo, C.A., Enns, L.C., Johnson, J.E., Burtner, C., Odden, A.R., Young, K., Taylor, N.E., Henikoff, J.G., Comai, L. and Henikoff, S. 2003a. Large-scale discovery of induced point mutations with high-throughput TILLING. Genome Res 13: 524-530

Till, B.J., Colbert, T., Tompa, R., Enns, L., Codomo, C., Johnson, J., Reynolds, S.H., Henikoff, J.G., Greene, E.A., Steine, M.N., Comai, L. and Henikoff, S. 2003b. High-throughput TILLING for functional genomics. In: E. Grotewald (Ed.), Plant Functional Genomics: Methods and Protocols, Humana Press, Totowa, NJ, pp. 205-220.

Timpte C, Lincoln C, Pickett, FB, Turner J, Estelle M (1995) The AXR1 and AUX1 genes of Arabidopsis function in separate auxin-response pathways. Plant J 8: 561-569

Torii KU, Mitsukawa N, Oosumi T, Matsuura Y, Yokoyama R, Whittier RF Komeda Y (1996) The *Arabidopsis ERECTA* gene encodes a putative receptor protein kinase with extracellular leucine-rich repeats. Plant Cell 8: 735-746

Tucker EB (1982) Translocation in the staminal hairs of *Setcreasea purpurea*. 1. A study of cell ultrastructure and cell-to-cell passage of molecular probes. Protoplasma 113: 193-201

Turnbull, C.G.N., Booker, J.P. and Leyser, H.M.O. 2002. Micrografting techniques for testing long-distance signalling in *Arabidopsis*. Plant Journal 32: 255-262.

Turner, A., Wells, B. and Roberts, K. 1994. Plasmodesmata of maize root tips: structure and composition. J Cell Sci 107: 3351-3361.

van Bel AJE, Ehlers K (2005) Electrical signaling via plasmodesmata. In: Plasmodesmata, Annu Plant Rev Vol 18, Oparka KJ, ed. Blackwell, Oxford. Pp 263-278

van der Schoot C, van Bel AJE (1990) Mapping membrane potential differences and dye coupling in internodal tissues of tomato (*Solanum lycopersicum* L). Planta 182: 9-21

Verma, D.P.S. 2001. Cytokinesis and building of the cell plate in plants. Annu Rev Plant Physiol Plant Mol Biol 52: 751-784.

Verma, D.P., and Hong, Z. (2001) Plant callose synthase complexes. Plant Mol Biol 47: 693-701.

Waigmann E, Lucas WJ, Citovsky V, Zambryski P (1994) Direct functional assay for tobacco mosaic virus cell-to-cell movement protein and identification of a domain involved in increasing plasmodesmal permeability. Proc Natl Acad Sci USA 91: 1433-1437

Waterkeyn, L. 1962. Les parois microsporocytaires de nature callosique chez *Hellborus* et *Tradescantia.* Cellule 62: 225-255.

Waterkeyn, L. and Beinfait, A. 1970. On a possible function of the callosic special wall in *Ipomoea purpurea* (L.) Roth. Grana 10: 13-20.

Wolf S, Deom CM, Beachy RN, Lucas WJ (1989) Movement protein of tobacco mosaic virus modifies plasmodesmatal size exclusion limit. Science 246: 377-379

Worall, D., Hird, D.L., Hodge, R., Paul, W., Draper, J. and Scott, R. 1992. Premature dissolution of the microsporocyte callose wall causes male sterility in transgenic tobacco. Plant Cell 4: 759-771.

Wright KM, Oparka KJ (1996) The fluorescent probe HPTS as a phloem-mobile, symplastic tracer: an evaluation using confocal laser scanning microscopy. J Exp Bot 47: 439-445

Wu X, Dinneny JR, Crawford KM, Rhee Y, Citovsky V, Zambryski PC, Weigel D (2003) Modes of intercellular transcription factor movement in *the Arabidopsis* apex. Development 130: 3735-3745

Wyner CL, Hernández-Ábalos JM, Doonon JH (2001) Microinjection reveals cell-to-cell movement of green fluorescent protein in cells of maize coleoptiles. Planta 212: 692-695

Xoconostle-Cazares B, Xiang Y, Ruiz-Medrano R, Wang H-L, Monzer J, Yoo B-C, McFarland KC, Franceschi VR, Lucas WJ (1999) Plant paralog to viral movement protein that potentiates transport of mRNA into the phloem. Science 283: 94-98

Yang, C-Y., Spielman, M., Coles, J.P., Li, Y., Ghelani, S., Bourdon, V., Brown, R.C., Lemmon, B.E., Scott, R.J. and Dickinson, H.G. 2003. *TETRASPORE* encodes a kinesin required for male meiotic cytokinesis in *Arabidopsis*. Plant J 34: 229-240.

Yang RL, Evans ML, Moore R (1990) Microsurgical removal of epidermal and cortical cells: evidence that the gravitropic signal moves through the outer layers in the primary root of maize. Planta 180: 530-536

Zhang C, Guinel FC, Moffatt BA (2002) A comparitive ultrastructural study of pollen development in *Arabidopsis thaliana* ecotype Columbia and male-sterile mutant *Apt1-3*. Protoplasma 219: 59-71

Zhu T, Lucas WJ, Rost TL (1998a) Directional cell-to-cell communication in the *Arabidopsis* root apical meristem. I. An ultrastructural and functional analysis. Protoplasma 203: 35-47.

Zhu T, O'Quinn RL, Lucas WJ, Rost TL (1998b) Directional cell-to-cell communication in the *Arabidopsis* root apical meristem. II. Dynamics of plasmodesmatal formation. Protoplasma 204: 84-93

CURRICULUM VITAE

LINDA C. ENNS

Education

1998 - present	-Ph.C., Department of Biology, University of Washington, Seattle, WA.
1996 - 1998	-M.Sc., Department of Biology, Carleton University, Ottawa, ON.
1989 - 1995	-B.Sc. Hon., Department of Biology, Carleton University, Ottawa, ON.

Publications

Enns LC, Kanaoka MM, Torii K, Comai L. Okada K, Cleland RE. (2005) Two callose synthases, GSL1 and GSL5, play an essential and redundant role in plant and pollen development and in fertility. Plant Mol Biol 58:333-349.

Enns LC, McCully ME and Canny MJ. (2006) Branch roots of young maize seedlings, their production, growth and phloem supply from the primary root. Functional Plant Biology (In Press)

Enns LC and Cleland RE (2006) A Role of Callose in Delineating Symplastic Domains in the *Arabidopsis* root tip (in preparation)

Enns LC and Cleland RE (2006) A reexamination of GFP intercellular movement in the *Arabidopsis* root tip (in preparation).

Till BJ, Reynolds SH, Weil C, Springer N, Burtner C, Young K, Bowers E, Codomo CA, **Enns LC**, Odden AR, Greene EA, Comai L, Henikoff S. (2004) Discovery of induced point mutations in maize genes by TILLING. Plant Biol. 4:12.

Comai L, Young K, Till BJ, Reynolds SH, Greene EA, Codomo CA, **Enns LC**, Johnson JE, Burtner C, Odden AR, Henikoff S. (2004) Efficient discovery of DNA polymorphisms in natural populations by Ecotilling. Plant J. 37:778-86.

Till BJ, Colbert T, Tompa R, **Enns LC**, Codomo CA, Johnson JE, Reynolds SH, Henikoff JG, Greene EA, Steine MN, Comai L, Henikoff S. (2003) High-throughput TILLING for functional genomics. Methods Mol Biol. 236:205-20.

Greene EA, Codomo CA, Taylor NE, Henikoff JG, Till BJ, Reynolds SH, **Enns LC**, Burtner C, Johnson JE, Odden AR, Comai L, Henikoff S. (2003) Spectrum of chemically induced mutations from a large-scale reverse-genetic screen in Arabidopsis. Genetics 164:731-40.

Till BJ, Reynolds SH, Greene EA, Codomo CA, **Enns LC**, Johnson JE, Burtner C, Odden AR, Young K, Taylor NE, Henikoff JG, Comai L, Henikoff S. (2003) Large-scale discovery of induced point mutations with high-throughput TILLING. Genome Res. 13:524-30.

Enns, L.C., M.J. Canny, and M.E. McCully. (1999) An investigation of the role of solutes in the xylem sap and in the xylem parenchyma as the source of root pressure. Protoplasma. 211:183-197.

Enns, L.C., M.E. McCully, and M.J. Canny. (1998) Solute concentrations in xylem sap along vessels of maize primary roots at high root pressure. Journal of Experimental Botany. 49:1539-1544.

Grants awarded

02-15-03 to 01-31-06 - NSF award IBN-026173 - $217,711.
Callose synthases: what do they do in the *Arabidopsis* root?

Courses lectured

winter quarter, 2006 -Biology 220 - Plant Form and Function, University of Washington

fall quarter, 2005 -Biology 161 - Introduction to Cellular and Molecular Biology, University of Washington

Conference presentations

July 2005 -American Society of Plant Biology (ASPB). Annual meeting. Seattle, WA.

June 2005 -International Arabidopsis conference. Annual meeting. Madison, WI. Two callose synthases, GSL1 and GSL5, play an essential and redundant role in plant and pollen development and in fertility. (poster)

July 2004 -ASPB. Annual meeting. Lake Buena Vista, FL. Callose synthase and plant development. (poster)

July 2003 -ASPB. Annual meeting. Honolulu, HI. Callose and plant development. (poster)

July 2002 -ASPB. Annual meeting. Denver, CO. The role of callose in root intercellular communication and plant development. (poster)

July 2001 -Society for Developmental Biology (SDB). Annual meeting. Seattle, WA.
The role of callose in root gravitropism. (poster)

July 1998 -Canadian Society of Plant Physiologists (CSPP). Annual meeting. Montreal, Quebec. Root pressure is not produced by the osmotic pressure of solutes in the xylem sap. (oral presentation)

Aug. 1997 -American SPP/ CSPP. Joint annual meeting, with the participation of the Japanese SPP and the Australian SPP. Vancouver, B.C. Root pressure and the ion concentrations in xylem vessels and parenchyma. (poster)

Feb. 1997 -Proceedings of the Fifty-second Annual Northeastern Corn Improvement Conference. Ottawa, ON. Source-sink relations in a maize seedling: the parallel between patterns of sieve tube number and branch root number in the primary root of *Zea mays.* (oral presentation)

Dec. 1995 -CSPP. Eastern regional meeting. Toronto, ON. Branch root development related to phloem anatomy in the primary root of *Zea mays.* (oral presentation)

June 1994 -Canadian Federation of Biological Societies (CFBS). Montreal, Quebec.

Early and prolific branching of the basal region of corn seedling roots: is it a survival mechanism unaffected by environmental cues? (poster)

Synergistic activities

2001-2003 -Technician and Production Efficiency Manager, Arabidopsis TILLING Project, Seattle
2000-2001 -Teaching assistant, Biology Lab (Bio203), University of Washington
1999-2001 -Teaching assistant, Plant Physiology Lab (Bot372), University of Washington
1998 -Teaching assistant, Biology Lab (Bio100), Carleton University
1994-1997 -Teaching assistant, Plant Form and Function Lab (Bio202), Carleton University

Honours and professional activities

2002-present -Member, American Society of Plant Biology
1999-2000 -Member, American Society for Gravitational and Space Biology (ASGSB)
1998-2000 -Plant Molecular Integration and Function fellowship (PMIF)
1998 -Senate Medal for Outstanding Academic Achievement, Carleton University
1998 -Honourable mention, President's Award for oral contribution, Canadian Society of Plant Physiologists (CSPP)
1998 -Teaching fellowship, Carleton University
1997 -Teaching fellowship, Carleton University
1989-1990 -Canada Science Scholarship
1989-1990 -Mercy Neal Southam Entrance Scholarship, Carleton University

Collaborators & Other Affiliations

1. Collaborators: R. E. Cleland, K. Torii and L. Comai, U. of Washington, Seattle; M. Kanaoka and K. Okada, Kyoto U., Japan; N. Sauer, University of Erlangen, Germany; F. Baluska, U. of Bonn, Germany; M.E. McCully and M.J. Canny, Carleton U, Ottawa.
2. Graduate advisors: R. E. Cleland, K. Torii, L. Comai, E. Van Volkenburgh, U. of Washington; M.E. McCully, M.J. Canny, J.J. Cheetham, Carleton U